

Doctoral thesis

Observational Predictions  
of Generalized Galilean Genesis

Sakine Nishi

Department of Physics, Rikkyo University  
15RA002B



# Abstract

Inflation is a very successful scenario for the early universe. However, even an inflationary universe has a singularity in the past, and the alternative scenarios motivated by this problem have been discussed. In this thesis, we focus on one of the alternative scenarios called Galilean genesis. This scenario has the fascinating feature that the universe starts expanding from approximately Minkowski space-time. If this model gives the same observational prediction as that of inflation and solves the problems that inflation solves, we have to discuss how one can distinguish the two models. Thus, in this thesis, we discuss two aspects of primordial gravitational waves generated in the genesis phase. One is the gravitation and solution of GWs during the genesis-reheating transformation and, after that, the radiation-dominated universe. The other is the possibility of the various spectrum of GWs by extending the existing genesis models. The genesis models we discuss in this thesis are described in the Horndeski theory, which is the generalized scalar-tensor theory having up to second derivative terms.

For the phase transition and the reheating, we figure out the spectrum in some cases and discuss the range of the frequency of the detector, which can catch the gravitational waves. As a result, we can find the spectrum for genesis by using the detector, which can detect at a higher frequency than we project now. For the low-frequency region, we can not find the gravitational waves because the amplitude cannot grow in Minkowski space-time.

For the various spectrum of gravitational waves, we study the extension of the existing model. The generalized Galilean genesis model has one constant parameter, and then we additionally introduce a parameter. In the previous study, we can find the various spectrum only for scalar perturbation by introducing one parameter. However, by extending the model, we can find the spectrum of gravitational waves and scalar perturbation are varying by two parameters. This result implies that whatever observational result we find, it can be explained by this Galilean genesis model. In this model, we can distinguish between the models with the consistency relation.



# Contents

<b>Introduction</b>	<b>3</b>
<b>Acknowledgements</b>	<b>5</b>
<b>I Review of Cosmology</b>	<b>7</b>
<b>1 Standard Big Bang Cosmology</b>	<b>9</b>
1.1 Expanding Universe and the Hubble law . . . . .	9
1.2 Big bang model . . . . .	10
1.3 Metric . . . . .	11
1.4 Field equations . . . . .	12
1.5 Horizons . . . . .	15
<b>2 Inflation</b>	<b>17</b>
2.1 Problems . . . . .	18
2.2 Slow-roll inflation . . . . .	20
2.3 K-inflation . . . . .	24
2.4 G-inflation . . . . .	25
<b>3 Modified Gravity</b>	<b>27</b>
3.1 $f(R)$ theory . . . . .	27
3.2 Brans-Dicke theory . . . . .	28
3.3 Kinetic gravity braiding . . . . .	29
3.4 Galileon theory . . . . .	31
3.5 Horndeski theory . . . . .	33
3.6 GLPV theory . . . . .	35
3.7 Conclusions in this chapter . . . . .	36
<b>4 Cosmological perturbations</b>	<b>37</b>
4.1 Perturbations . . . . .	37

4.2	Matter perturbation . . . . .	40
4.3	Gauge . . . . .	41
4.4	Cosmological perturbations in General Relativity . . . . .	42
4.5	Cosmological perturbations in Horndeski Theory . . . . .	43
4.6	Power spectrum . . . . .	44
<b>5</b>	<b>Some topics in Modern Cosmology</b>	<b>53</b>
5.1	Curvaton field . . . . .	53
5.2	Reheating of the universe . . . . .	54
5.3	Alternative scenarios to inflation . . . . .	58
<b>II</b>	<b>Galilean Genesis</b>	<b>63</b>
<b>6</b>	<b>Generalized Galilean genesis</b>	<b>65</b>
6.1	Generalized genesis solutions . . . . .	66
6.2	Background evolution . . . . .	68
6.3	Primordial perturbations . . . . .	74
6.4	Curvaton . . . . .	78
6.5	Conclusions in this chapter . . . . .	79
<b>7</b>	<b>Reheating and primordial gravitational waves in GGG</b>	<b>81</b>
7.1	Gravitational particle production . . . . .	82
7.2	The spectrum of primordial gravitational waves . . . . .	87
7.3	Examples . . . . .	91
7.4	Conclusions in this chapter . . . . .	96
<b>8</b>	<b>Scale-invariant perturbations</b>	<b>99</b>
8.1	A new Lagrangian for Galilean Genesis . . . . .	100
8.2	Problems . . . . .	102
8.3	Power Spectra . . . . .	105
8.4	An example . . . . .	110
8.5	Conclusions in this chapter . . . . .	111
	<b>Conclusions</b>	<b>113</b>

# Introduction

How our Universe started may be one of the interesting subjects not only for researchers but also for everyone. The Big Bang cosmology is the well-known scenario of the universe, and then the inflationary scenario was proposed to solve the problems of the big bang. Nowadays the standard cosmological scenario of the primordial universe is inflation, however, this scenario has the problem that the universe has a singularity at the initial time.

Motivated by this problem, there are many alternative scenarios. In this thesis, we focus on the specific model called Galilean genesis [1]. Though the scenario which has accelerating expansion is called inflation, we call inflation for the model that the expansion law is the approximately de-Sitter expansion to distinguish between the inflation and its alternatives.

In this way, there exist many models of the early universe, and our interest is to find which scenario was caused. To consider this, what we often do is to check the instabilities in the model, to compare to the observation and so on. There is the possibility the problems appeared by this research can be avoided by extending the model.

For the scalar perturbation, WMAP and Planck satellites are the famous detector. They observe the cosmic microwave background (CMB) and the temperature of Universe, and we can find many cosmological parameters. For the gravitational waves, there are famous detectors such as LIGO, Virgo, DECIGO, and KAGRA. The event may be fresh in our memory that the direct detection was achieved and reported in February 2016. The gravitational waves generated from binary black hole can be detected in present days, and we expect the detection of primordial gravitational waves in the future.

This thesis is based on my work during doctoral course [2] and [3]. The main topic of these study is gravitational waves generated during genesis phase. The information we already have to compare the models are the flat spectrum in inflation and blue spectrum in alternative scenarios. The contents of this thesis are as follows.

In part 1, we introduce some basic topics of cosmology. First, we introduce the discovery of expanding universe such as Hubble law and how to explain the physical values in cosmology. As our goal is to discuss the alternative scenario to inflation by using modified gravity theory, we will introduce the models of inflation and some modified theories. Then finally we introduce some cosmological topics we will discuss in Galilean genesis in part 2.

In part 2, we discuss some topics for Galilean genesis. First, we introduce the generalized model of the Galilean genesis [4]. Then we will discuss the gravitational reheating in generalized Galilean genesis, and compare the shape of the power spectrum [2]. Moreover, then we discuss farther modification of generalized Galilean genesis to get the various spectrum of the scalar perturbation and gravitational waves [3]. Then finally, we conclude the discussion of this thesis.

## Conventions

Indices for space	$a, b, c, \dots = 1, 2, 3$
Indices for spece-time	$\alpha, \beta, \gamma, \dots = 0, 1, 2, 3$
Unit	$c = 1, \hbar = 1$
Signeture	$(-, +, +, +)$
Christoffel symbol	$\Gamma_{\mu\nu}^{\rho} = \frac{1}{2}g^{\rho\sigma}(g_{\mu\rho,\nu} + g_{\rho\nu,\mu} - g_{\mu\nu,\rho})$
Riemann tensor	$R^{\rho}_{\mu\nu\sigma} = -\partial_{\mu}\Gamma^{\rho}_{\nu\sigma} + \partial_{\nu}\Gamma^{\rho}_{\mu\sigma} - \Gamma^{\kappa}_{\nu\sigma}\Gamma^{\rho}_{\mu\kappa} + \Gamma^{\kappa}_{\mu\sigma}\Gamma^{\rho}_{\nu\kappa}$
Ricci tensor	$R_{\mu\nu} = g^{\rho\sigma}R_{\rho\mu\sigma\nu}$
Ricci scalar	$R = g^{\mu\nu}R_{\mu\nu}$
Einstein tensor	$G_{\mu\nu} = R_{\mu\nu} - \frac{1}{2}g_{\mu\nu}R$
Gravitational constant	$G = G_{\text{Newton}} = \frac{M_{\text{Pl}}^{-2}}{8\pi}$



# Acknowledgements

First of all, I would like to thank my supervisor, Tsutomu Kobayashi. I have learned many things from him since I was an undergraduate student. And I would like to thank all the members of the group of theoretical physics at Rikkyo University and all the people who have discussed with me. It is a very fortunate for me to be able to study and discuss together in a very active group. I also would like to thank my family and friends. The works I wrote in this thesis were supported in part by the JSPS Research Fellowships for Young Scientists No. 15J04044.



Part I

Review of Cosmology



# Chapter 1

## Standard Big Bang Cosmology

Inflation is the most standard scenario for explaining the evolution of the early universe. In this thesis, our goal is to discuss the alternative scenario to inflation and to compare the scenarios. Thus let us introduce the basic materials of cosmology in this section, and review the history of cosmology from discovering the expanding universe to developing the inflationary scenario.

### 1.1 Expanding Universe and the Hubble law

The fact that the Universe is expanding is known very well. The man who found this is Edwin Hubble [5]. Vesto M. Slipher found that the spectrum of most galaxies was redshifted, and this suggests the galaxies are moving far away. Meanwhile, many models for the universe were discussed as a solution of general relativity (GR). Then in 1929, Hubble found the law from the observation shown as fig.1.1, and the law is described as

$$v = Hr, \tag{1.1.1}$$

where  $v$  is the velocity of the galaxy,  $H$  is called the Hubble parameter explained in the following section, and  $r$  is the distance from here to the galaxy. Defining  $a(t)$  as the representation of length between observers, the Hubble parameter is defined by the scale factor  $a(t)$ ,

$$H(t) \equiv \frac{\dot{a}}{a}. \tag{1.1.2}$$

According to the observational results, many galaxies go away, and those far from us moves faster than that is near here. Eq.(1.1.1) shows the velocity of the galaxy, and we can find the fact that the universe expands.

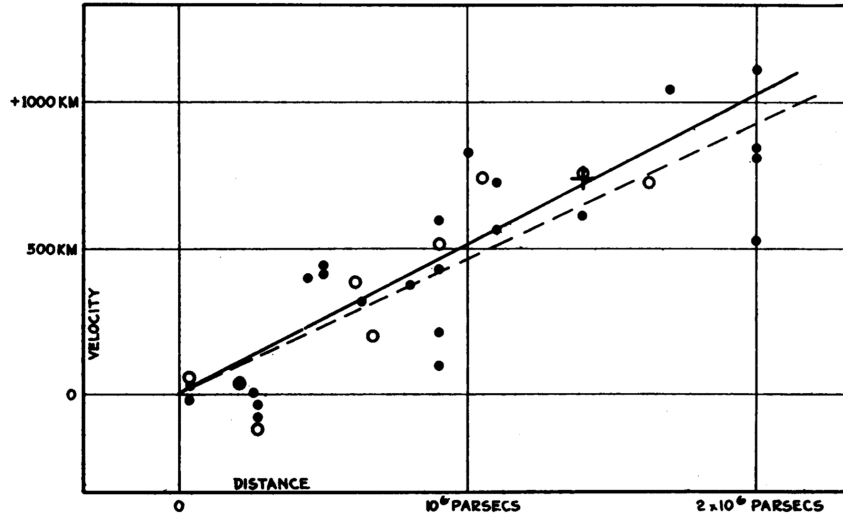


Figure 1.1: The relation of velocity and distance for nebulae. The black points have the relation of proportion shown as the line. After combining these points into groups as the circles, the relation is shown as the dashed line. This figure is cited from [5].

## 1.2 Big bang model

As the universe is expanding, we can consider easily the universe begins from the hot and high-density state. Such a scenario the universe started from the hot universe is called the big bang. However, before we obtain the evidence of big bang theory, the influential theories were explaining the evolution of the universe such as the steady-state theory or big bang theory. In Steady-state theory, the energy density is unvarying although universe expands. The temperature at present is calculated, and the observation founded it for radio astronomy. Arno A. Penzias and Robert W. Wilson tried to remove the noise by improving observation equipment, and they found big bang theory explains the noise. The noise has the spectrum of the black body at the temperature of 3K, and this number is accord to what calculated by researchers who studied big bang theory. This is called cosmic microwave background (CMB). The equipment for CMB is currently developed, and now we have the temperature of the universe by the result of COBE and Planck (fig.1.2)

$$T_0 \sim 2.7 \text{ K.} \quad (1.2.1)$$

Also, there was the problem that the total amount of light elements in the universe was much larger than that can be generated with stars. However, calculating the amount of light elements produced by Big Bang nucleosynthesis, we found it is same to the obser-

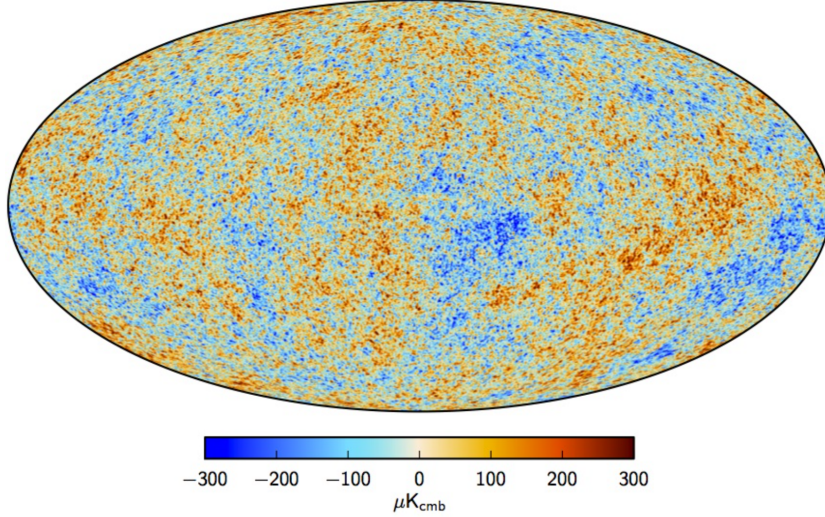


Figure 1.2: The CMB map of Planck [6]. The noise of temperature characterized by  $K_{cmb}$  is mapped with color coding.

vation. In this way, big bang theory became standard. However, there is some unsolved point such as flatness and horizon problem and so on. We will review these problems in the later section.

### 1.3 Metric

From now let us introduce many expressions to discuss some cosmological topic. As we treat the evolution of space-time, we would like to introduce the metric at first. Generally we describe the line element as

$$ds^2 = g_{\mu\nu} dx^\mu dx^\nu, \quad (1.3.1)$$

which can be divided by time and space as

$$ds^2 = g_{00} dt^2 + g_{0i} dx^0 dx^i + g_{ij} dx^i dx^j. \quad (1.3.2)$$

Seeing the large scale from the fundamental observer with the proper time  $x^0 = ct$ , we can assume the universe is isotropic and homogeneous and we can set

$$g_{00} = 1, \quad (1.3.3)$$

$$g_{0i} = 0. \quad (1.3.4)$$

The distance between two observer  $dl(t_0)$  changes with  $a(t)$  as

$$dl(t) = a(t)dl(t_0), \quad (1.3.5)$$

where  $a(t)$  is called scale factor. Similarly,  $g_{ij}$  is given as

$$g_{ij} = a^2(t)\gamma_{ij}, \quad (1.3.6)$$

where  $\gamma_{ij}$  shows the metric of 3 dimensional space. Therefore we have

$$ds^2 = -dt^2 + a^2(t)\gamma_{ij}dx^i dx^j. \quad (1.3.7)$$

This is called Friedmann-Lemaître-Robertson-Walker (FLRW) metric. Note that we often use the conformal time defined by

$$d\eta = \frac{dt}{a(t)}. \quad (1.3.8)$$

In polar coordinate system, it can be written as

$$ds^2 = -dt^2 + a^2(t) [dr^2 + r^2(d\theta^2 + \sin^2 \theta d\phi^2)]. \quad (1.3.9)$$

Then, introducing curvature  $K$ , the metric is given by

$$ds^2 = -dt^2 + a^2(t) \left[ \frac{dr^2}{1 - Kr} + r^2(d\theta^2 + \sin^2 \theta d\phi^2) \right]. \quad (1.3.10)$$

## 1.4 Field equations

It is known that our universe evolves throughout some eras such as radiation dominant phase or matter dominant phase. The description of the evolution depends on how the equation of state is shown. Let us we discuss the evolution of the universe in each epoch with solving the field equations. First, we introduce the FLRW metric with curvature

$$ds^2 = -dt^2 + a^2(t) \left[ \frac{dr^2}{1 - Kr} + r^2(d\theta^2 + \sin^2 \theta d\phi^2) \right]. \quad (1.4.1)$$

Applying this metric to the Einstein equation with cosmological constant  $\Lambda$ , we obtain

$$R_{\mu\nu} - \frac{1}{2}g_{\mu\nu}R + g_{\mu\nu}\Lambda = 8\pi GT_{\mu\nu}, \quad (1.4.2)$$

where  $T_{\mu\nu}$  is the energy momentum tensor which is given as

$$T_{\mu\nu} = \begin{pmatrix} \rho & 0 & 0 & 0 \\ 0 & p & 0 & 0 \\ 0 & 0 & p & 0 \\ 0 & 0 & 0 & p \end{pmatrix}. \quad (1.4.3)$$



Then we can find

$$\left(\frac{\dot{a}}{a}\right)^2 = \frac{8\pi G}{3}\rho - \frac{K}{a^2} + \frac{\Lambda}{3}, \quad (1.4.4)$$

$$\frac{\ddot{a}}{a} = -\frac{4\pi G}{3}(\rho + 3p) + \frac{\Lambda}{3}, \quad (1.4.5)$$

where  $\rho$  is the energy density, and  $p$  is the pressure. These equations are derived from Einstein equations and called Friedmann equation eq.(1.4.4) and acceleration equation eq.(1.4.5). The energy momentum tensor  $T_{\mu\nu}$  is subject to the conservation law as

$$T_{\mu\nu}{}^{;\nu} = 0, \quad (1.4.6)$$

from which we obtain

$$\dot{\rho} + 3\frac{\dot{a}}{a}(\rho + p) = 0. \quad (1.4.7)$$

If the equation of state is written as

$$p = w\rho, \quad (1.4.8)$$

where  $w$  is a constant parameter depending on what is dominant in the era we are considering, we can solve eq.(1.4.7) as

$$\rho = a^{-3(w+1)}. \quad (1.4.9)$$

To consider the rate of the energy, we introduce the density parameter  $\Omega_a$  for energy density whose component is characterized by  $a$

$$\Omega_{a0} = \frac{\rho_{a0}}{\rho_{c0}}, \quad (1.4.10)$$

where  $\rho_{c0}$  is the critical energy density,

$$\rho_{c0} = \frac{3H_0^2}{8\pi G}. \quad (1.4.11)$$

The critical energy density is given by eq.(1.4.4) with taking  $K = 0$ ,  $\Lambda = 0$  and present time  $t = t_0$ . For  $K$  and  $\Lambda$  the density parameter is given as

$$\Omega_{K0} = \frac{K}{H_0^2}, \quad (1.4.12)$$

$$\Omega_{\Lambda0} = \frac{\Lambda}{3H_0^2}, \quad (1.4.13)$$

where we set the scale factor at present time  $a_0 = 1$ . The total energy density  $\rho_{tot}$  is written as

$$\rho_{tot} = \sum \rho_a. \quad (1.4.14)$$

Although various components is supposed, we assume  $\rho_{tot}$  has radiation  $\rho_r$ , matter  $\rho_m$ , and dark energy  $\rho_d$  from now on. The general equation for scale factor is given as

$$\frac{da}{dt} = \left[ H_0^2 \left\{ \frac{\Omega_{r0}}{a^2} + \frac{\Omega_{m0}}{a} + \Omega_{d0} a^2 \exp \left[ 3 \int (1+w) a^{-1} da \right] \right\} \right]^{1/2}, \quad (1.4.15)$$

Practically, the evolution of scale factor for present era can be find by fixing these parameters by observation. Let us solve the equations by assuming the case that the components except one can be negligible.

### 1.4.1 Radiation dominant phase

In the radiation dominant phase, coefficient  $w$  in the equation of state is

$$w = \frac{1}{3}, \quad (1.4.16)$$

Thus, the equation for the scale factor  $a(t)$  in radiation dominant phase is given as

$$\dot{a}(t) = \frac{H_0^2 \Omega_{r0}}{a^2}. \quad (1.4.17)$$

The solution of this equation is

$$a(t) = a(t_i) \left( 2H_0 \Omega_{r0}^{1/2} (t - t_i) \right)^{1/2}, \quad (1.4.18)$$

where  $t_i$  is the end of the inflation and we assume the integral constant can be negligible.

### 1.4.2 Matter dominant phase

During the matter dominant phase  $w$  is given as

$$w = 0. \quad (1.4.19)$$

Therefore, we can find the equation for the scale factor  $a(t)$  in matter dominant phase as

$$\dot{a}(t) = \frac{H_0^2 \Omega_{m0}}{a}. \quad (1.4.20)$$

Thus the solution is

$$a(t) = a(t_r) \left( \frac{3}{2} H_0 \Omega_{m0}^{1/2} (t - t_r) \right)^{3/2}, \quad (1.4.21)$$

where  $t_r$  is the start of the matter dominant phase and we assume the integral constant can be negligible.

### 1.4.3 Dark energy

In the case that  $\Omega_d$  is dominant, we do not have information for  $w$  because we do not know what the dark energy is. The equation for scale factor is given as

$$\dot{a}(t) = H_0^2 \Omega_d a^2 \exp \left[ 3 \int (1+w) a^{-1} da \right]. \quad (1.4.22)$$

If this dark energy is cosmological constant, the parameter for the equation of state is

$$w = -1. \quad (1.4.23)$$

To make the accelerating expansion of the universe, the condition for  $w$  is

$$w < -\frac{1}{3}. \quad (1.4.24)$$

## 1.5 Horizons

To discuss the following topics, we have to introduce the definitions of length and horizon in cosmology. Let us consider the length that the light runs from  $t = t_0$  to  $t = t_1$ . Light goes on the null geodesic line  $ds = 0$  and from the isotropy we have

$$l_e = \int_{t_0}^{t_1} \frac{1}{a(t)} dt. \quad (1.5.1)$$

This length is measured in comoving coordinate, and  $l_e$  extend with scale factor  $a(t)$ . We introduce the length  $l_h$  as

$$l_h = a(t) l_e, \quad (1.5.2)$$

Considering the path of light for the past, the region which has causal relation characterized by

$$l_p = a(t) \int_{t_{ini}}^{t_0} \frac{1}{a(t)} dt, \quad (1.5.3)$$

where we take  $t = t_{ini}$  as the birth of the universe and  $t = t_0$  as the present time. We call this  $l_p$  particle horizon. Conversely, the causal relation for future is shown by

$$l_e = a(t) \int_{t_0}^{t_\infty} \frac{1}{a(t)} dt, \quad (1.5.4)$$

and it is called event horizon. These expressions so far are for the distance for space. Then let us consider the distance for time especially the age of the universe. Taking  $t_0$  as the initial time of big bang and  $t$  as the present time, we obtain

$$t_{age} = t_0 - t = \int_t^{t_0} dt = \int_a^1 \frac{da}{aH}, \quad (1.5.5)$$

where we take the scale factor at the present time as  $a(t) = 1$ . This can be calculated roughly and described as inverse of the Hubble parameter

$$t_{age} \sim H_0^{-1}. \quad (1.5.6)$$

Precisely, applying the solution of eq.(1.4.15) with determining  $\Omega_a$  from observation, we can find the age of universe.

$$t_{age} \sim 13.8 \text{ Gyr}. \quad (1.5.7)$$

## Chapter 2

# Inflation

In this section, we introduce some models of inflation. Inflation needs accelerating expansion, so we have

$$\ddot{a} > 0. \tag{2.0.1}$$

Let us review some typical models of inflation. From now on we assume  $K = 0$  and  $\Lambda = 0$  in eq.(1.4.4) and eq.(1.4.5), and we use

$$\left(\frac{\dot{a}}{a}\right)^2 = \frac{8\pi G}{3}\rho, \tag{2.0.2}$$

$$\frac{\ddot{a}}{a} = -\frac{4\pi G}{3}(\rho + 3p). \tag{2.0.3}$$

Inflation is known as the scenario which can solve these problems of the big bang. There are many models of inflation, and we will discuss the specific models in the later section. Basically, in inflationary phase the expansion law is approximated by de Sitter expansion as

$$a(t) = a(t_i)e^{H(t-t_i)}, \tag{2.0.4}$$

$$H \equiv \frac{\dot{a}}{a} = \text{const}, \tag{2.0.5}$$

where  $t = t_i$  is the initial time of inflation. How long the inflationary phase continued is characterized by e-folding number shown as

$$N = \log \frac{a_f}{a_i} = \int H dt. \tag{2.0.6}$$

Let us review how inflation could solve the problems and derive the e-folding number  $N$  which is needed to do that.

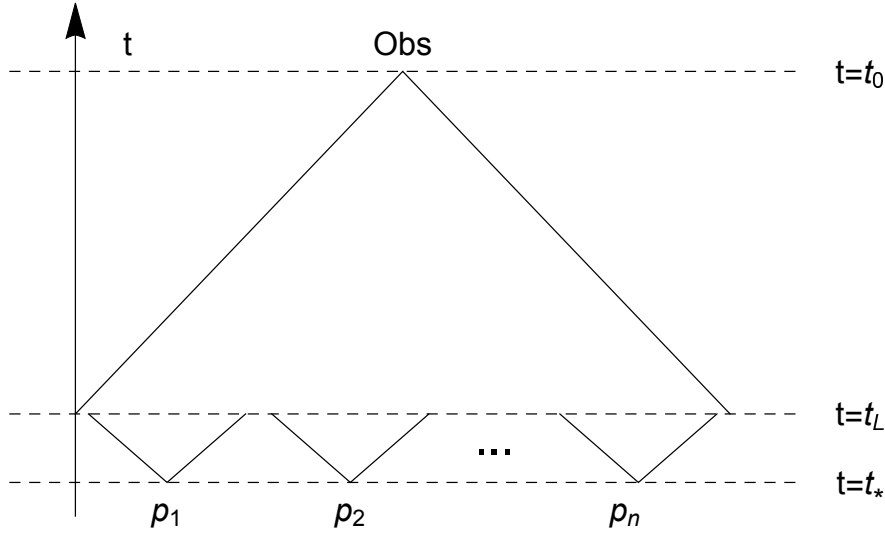


Figure 2.1: The schematic picture of the horizon problem.  $t_0$  is the present time,  $t_L$  is the last scattering time and  $t_*$  is the start of radiation dominant phase. *Obs* is the observer seeing the CMB, he or she observe particle horizon scale. The event horizon is smaller than the particle horizon.

## 2.1 Problems

Before the introduction of many models of inflationary scenario, we have to know what are the problems for Big Bang scenario. In this section, let us discuss the problems by inflationary scenario. Following discussion is the review of [7, 8].

### 2.1.1 Horizon problem

In introduction we referred to CMB observation. Figure 1.2 is the observational result of CMB from Planck2015 [6]. As we can see in this figure, the structure of CMB has isotropy and small fluctuation. It is natural to consider that this structure was initially the quantum fluctuation and it was expanded by the evolution of the universe. However, in big bang scenario, we can not explain the figure of CMB. The event horizon from the beginning of big bang to the last scattering is smaller than the particle horizon shown in fig.2.1. In big bang scenario, CMB structure has to show some regions which have different temperature because the regions do not have causality each other. This problem is called horizon problem. The structure shown as CMB is explained by the expansion of

Inflationary phase, and thus let us consider this problem. The event horizon is given as

$$l_e = a(t_L) \int_{t_L}^{t_*} \frac{1}{a(t)} dt, \quad (2.1.1)$$

where we take  $t_L$  is the time of last scattering, and  $t_*$  is the end of inflation. As the expansion in inflation is given in eq.(2.0.4), the particle horizon is

$$l_p = a(t) \int_{t_0}^{t_\infty} \frac{1}{a(t)} dt. \quad (2.1.2)$$

To obtain the CMB structure we need  $l_e > l_p$ , after some calculations we can find the e-folding number needed to solve this problem. For the event horizon, we have

$$\begin{aligned} l_e &= a(t_L) \int_{t_L}^{t_*} \frac{1}{a(t_*) \exp[H_{inf}(t - t_*)]} dt \\ &= \frac{a(t_L)}{a(t_*) H_{inf}} (e^N - 1) \\ &\simeq \frac{a(t_L)}{a(t_*) H_{inf}} e^N. \end{aligned} \quad (2.1.3)$$

For particle horizon, by using eq.(1.4.15) we obtain

$$l_e \simeq \frac{a(t_L)}{a_0 H_0} \quad (2.1.4)$$

Thus we find

$$e^N > \frac{a_* H_{inf}}{a_0 H_0}. \quad (2.1.5)$$

Then, applying the observational results, we can estimate the number of  $N$  as

$$N > 62. \quad (2.1.6)$$

### 2.1.2 Flatness problem

For the number of curvature  $K$ , some observation suggests  $|\Omega_K| < 1$ . In addition, CMB suggests the most optimum number is  $\Omega_K = 0$ . However, this is at present. If we seek the exact value,  $K$  becomes too high precision. Considering inflationary scenario solves this problem because  $\Omega_K$  becomes negligible during the inflationary era in any  $K$ . Let us focus on the density parameter  $\Omega_\rho$  and  $\Omega_K$ . From the Friedmann equation, we need the condition

$$\Omega_\rho > \Omega_K. \quad (2.1.7)$$

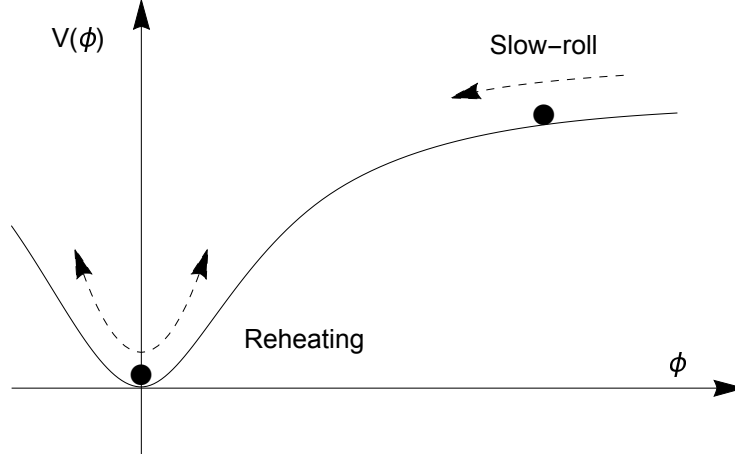


Figure 2.2: Schematic picture of inflationary scenario. The inflaton rolls down on its potential, and after that the inflaton oscillates at the bottom of the potential.

In inflation, recalling  $a_f = a_i e^N$  and  $H = \text{const.}$ , we can anticipate easily that this problem can be solved because  $\Omega_K$  is written as

$$\Omega_K = \frac{K}{a^2 H^2}. \quad (2.1.8)$$

After some calculations we can find the e-folding number needed to solve this problem. If the energy density at the beginning of radiation dominant phase is  $\rho_r = [2 \times 10^{16} \text{GeV}]^4$ , we have

$$N > 62. \quad (2.1.9)$$

## 2.2 Slow-roll inflation

Constructing the model of inflationary scenario, we define the Lagrangian as

$$\mathcal{L}_{tot} = \mathcal{L}_{GR} + \mathcal{L}_{inf}. \quad (2.2.1)$$

The models of inflationary scenario is shown by the gravitational field  $g_{\mu\nu}$  and a scalar field  $\phi$  called inflaton, and its Lagrangian is shown as

$$\mathcal{L}_{GR} = \frac{R}{16\pi G}, \quad (2.2.2)$$

$$\mathcal{L}_{inf} = -\frac{1}{2}(\partial\phi)^2 - V(\phi), \quad (2.2.3)$$



where  $V(\phi)$  is the potential of the inflaton. From this we obtain energy density  $\rho$ , pressure  $p$  and the field equation for  $\phi$  as

$$\rho = \frac{1}{2}\dot{\phi}^2 + V(\phi), \quad (2.2.4)$$

$$p = \frac{1}{2}\dot{\phi}^2 - V(\phi), \quad (2.2.5)$$

$$\ddot{\phi} + 3H\dot{\phi} + V_\phi = 0, \quad (2.2.6)$$

where “ $\dot{\phi}$ ” is the derivative of  $\phi$ . For the slow-roll inflation, we consider the scenario that the inflaton rolls down on its potential as fig.2.2. Then at the end of inflation, the inflaton oscillates at the bottom of the potential and decay into the other field. The oscillation and decay make high temperature, and it called reheating we will discuss in sec.5.2 . To construct the slow-roll inflation we assume

$$\dot{\phi}^2 \ll V, \quad (2.2.7)$$

$$|\ddot{\phi}| \ll 3H|\dot{\phi}|. \quad (2.2.8)$$

Thus we have

$$3H\dot{\phi} + V_\phi = 0. \quad (2.2.9)$$

From these equations, we can find the conditions for the potential

$$\left(\frac{V_\phi}{V}\right)^2 \ll 24\pi G \quad (2.2.10)$$

$$\frac{V_{\phi\phi}}{V} \ll 24\pi G \quad (2.2.11)$$

When we discuss the model of inflation, we often use slow-roll parameters [9] as follows. The slow-roll parameters are explained by derivative of potential  $V(\phi)$

$$\epsilon_V = \frac{1}{8\pi G} \left(\frac{V_\phi}{V}\right)^2, \quad (2.2.12)$$

$$\eta_V = \frac{1}{8\pi G} \frac{V_{\phi\phi}}{V}, \quad (2.2.13)$$

or written by Hubble parameter  $H(t)$

$$\epsilon_H = -\frac{\dot{H}}{H^2} = \frac{3\dot{\phi}}{2V + \dot{\phi}^2}, \quad (2.2.14)$$

$$\eta_H = -\frac{1}{2} \frac{\ddot{H}}{H\dot{H}} = -\frac{\ddot{\phi}}{H\dot{\phi}}. \quad (2.2.15)$$

To consider the slow-roll approximation, we need the absolute numbers of these parameters are much smaller than 1. In this inflationary scenario, the end of inflation quits when the slow-roll parameter becomes larger than 1. Then let us consider some specific models of slow-roll inflation.

### 2.2.1 Large-field inflation

The Large-field inflation (chaotic inflation) is proposed by A. D. Linde [10]. In this model the potential of the inflaton is given as

$$V(\phi) = V_0\phi^n, \quad (2.2.16)$$

where  $n$  is the number and  $V_0$  is the constant. In this model, the slow-roll parameter is given as

$$\epsilon_V = \frac{n^2}{8\pi G\phi^2}. \quad (2.2.17)$$

Thus the inflation in this model quit when the parameter becomes  $\epsilon > 1$  after the scalar field rolling down its potential. For example, now we consider the case of

$$V(\phi) = \frac{1}{2}m^2\phi^2, \quad (2.2.18)$$

where  $m$  is the mass of inflaton. As the second derivative of time for inflaton  $\phi$  written as

$$\ddot{\phi} = \frac{d\dot{\phi}}{dt} = \dot{\phi} \frac{d\dot{\phi}}{d\phi}, \quad (2.2.19)$$

the field equations eq.(2.0.2) and eq.(2.2.6) without the approximations derive the equation

$$\frac{d\dot{\phi}}{d\phi} = -\frac{\sqrt{12\pi G}(\dot{\phi}^2 + m^2\phi^2)^{1/2} + m^2\phi^2}{\dot{\phi}}. \quad (2.2.20)$$

Therefore we can figure out this relation in fig.2.3. As this  $d\dot{\phi}/d\phi$  attracts to the state of

$$\frac{d\dot{\phi}}{d\phi} \simeq 0, \quad (2.2.21)$$

we obtain from eq.(2.2.20)

$$\dot{\phi} = -\frac{m}{\sqrt{12\pi G}}. \quad (2.2.22)$$

Thus we find the solutions as

$$\phi(t) = \phi_i - \frac{m}{\sqrt{12\pi G}}(t - t_i), \quad (2.2.23)$$

$$a(t) = a_i \exp \left[ \sqrt{\frac{4\pi G}{3}} m \phi_i (t - t_i) - \frac{m^2}{6} (t - t_i)^2 \right], \quad (2.2.24)$$

where  $t = t_i$  is the initial time of inflation. Therefore, to make the e-folding number larger than  $N = 60$ , we take

$$\phi_i \gtrsim G^{-\frac{1}{2}}. \quad (2.2.25)$$

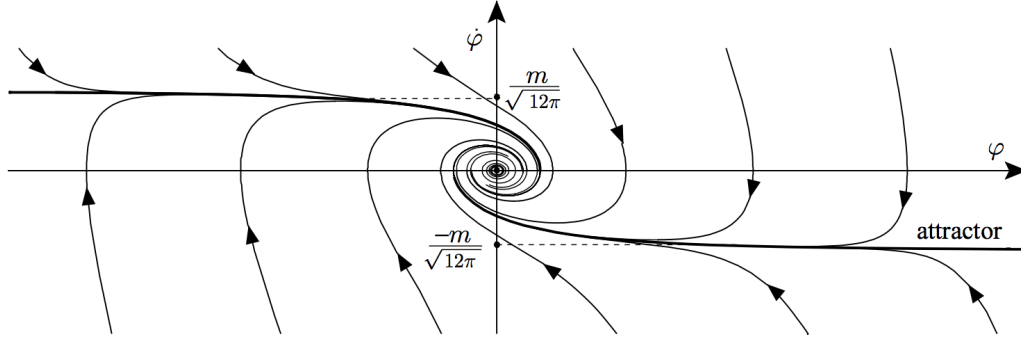


Figure 2.3: The phase space in large-scale inflation. The state attracts to the thick line. This figure is cited from [11] with the unit  $G = 1$ .

### 2.2.2 Small-field inflation

In this model the potential of the inflaton is typically written as

$$V(\phi) = V_0 \left[ 1 - \left( \frac{\phi}{\mu} \right)^n \right], \quad (2.2.26)$$

where  $\mu$  has the mass scale. Now we consider the example as

$$V(\phi) = \frac{\lambda}{4} (\phi^2 - v^2)^2, \quad (2.2.27)$$

where the vacuum state is at  $\phi = \pm v$ . Solving the equations, we can find the solution for  $a(t)$

$$a(t) = a_i \exp \left[ \sqrt{\frac{4\pi G}{3}} m \phi_i (t - t_i) - \frac{m^2}{6} (t - t_i)^2 \right], \quad (2.2.28)$$

where  $t = t_i$  is the initial time of inflation. In this model, the slow-roll parameter is given as

$$\epsilon_V = \frac{n^2 \phi^{-2}}{8\pi G} \left[ 1 - \left( \frac{\mu}{\phi} \right)^n \right]^{-2}. \quad (2.2.29)$$

To satisfy  $\epsilon_V \ll 1$ , we obtain  $\phi < \mu$  and  $G^{-\frac{1}{2}} < \phi$ . Thus we find the inflation occurs if  $\mu > G^{-\frac{1}{2}}$ .

### 2.2.3 Starobinsky inflation

The inflation models we reviewed up to now have the kinetic energy and the various potential of the inflaton in GR. However, there are many models inflation generated in modified gravity. Starobinsky inflation is a kind of these models [12]. In this model, the Lagrangian of GR is extended as

$$\mathcal{L} = R + \alpha R^2, \quad (2.2.30)$$

where  $\alpha$  is the parameter. Such model is included in  $f(R)$  gravity in sec.3.1. In this model, the field equations are

$$-(1 + 2\alpha R)\dot{H} = \alpha\ddot{R} - \alpha\dot{R}H, \quad (2.2.31)$$

$$3(1 + 2\alpha R)H^2 = \frac{1}{2}\alpha R^2 - 6\alpha H\dot{R}. \quad (2.2.32)$$

As the slow-roll parameters during inflation are much smaller than 1, we can find the solutions as

$$H \simeq H - \frac{1}{12\alpha}(t - t_i), \quad (2.2.33)$$

$$a \simeq a_i \exp[H_i(t - t_i) - \frac{1}{72\alpha}(t - t_i)^2], \quad (2.2.34)$$

$$R \simeq 12H^2 - \frac{1}{6\alpha^2}. \quad (2.2.35)$$

In this model, the slow-roll parameter is given as

$$\epsilon_H = 0 \quad (2.2.36)$$

## 2.3 K-inflation

In the inflation models we reviewed so far, inflation is caused by the inflaton rolling down its potential. In K-inflation, there are no potential and inflaton driven by kinetic energy. This is studied in [13] and [14]. The Lagrangian and detail are shown in sec.2.3. This model is not a modified gravity but the subclass of Galileon theory we will review in the later section. In this case, we have

$$\mathcal{L} = K(\phi, X), \quad (2.3.1)$$

where  $K(\phi, X)$  is arbitrary function of  $\phi$  and  $X$ .  $X$  is the kinetic term of scalar field  $\phi$  as

$$X = -\frac{1}{2}g^{\mu\nu}\partial_\mu\phi\partial_\nu\phi. \quad (2.3.2)$$

The models which have such like this Lagrangian are called K-essence [13] or K-inflation [14]. In this model, the energy momentum tensor  $T_{\mu\nu}$  is

$$T_{\mu\nu} = K_X \partial_\mu \phi \partial_\nu \phi - g_{\mu\nu} K, \quad (2.3.3)$$

and thus the energy density  $\rho$  and the pressure  $p$  are

$$\rho = 2XK_X - K, \quad (2.3.4)$$

$$p = K. \quad (2.3.5)$$

Thus we can find the parameter of the equation of state  $w$

$$w = \frac{p}{\rho} = \frac{K}{2XK_X - K}. \quad (2.3.6)$$

## 2.4 G-inflation

G-inflation is first discussed in [15] and generalized in [16]. In this inflation model, we discuss general model of inflation which is described in Horndeki theory [17, 18] which we will review in sec.3.5. In that paper, we calculate under the assumption that the state of universe attracts to the de-Sitter expansion. The inflationary models written by one scalar field and gravitational field are included in this model.



## Chapter 3

# Modified Gravity

In this section, we introduce some modified gravity theories. General relativity is very beautiful and successful theory. However, there are some problems we can not explain the phenomena in cosmology. We have not understood what dark energy and dark matter are and how these come from yet. To find the answer to the questions we have two methods, introducing some new fields or modifying the gravitational theory. Now we focus on the latter method. Nowadays many modified gravity theories are discussed. The later section in this thesis, we use generalized Galilean theory. This contains some theories of modified gravity. Thus, now we introduce some theories and understand the features of them. There are many kinds of modified gravity theory, and now we will show some of them.

### 3.1 $f(R)$ theory

$f(R)$  theory is investigated by Hans A. Buchdahl [19] and the action is written as

$$S_{ein} = \frac{1}{16\pi G} \int d^4x \sqrt{-g} f(R) + S_{matter}. \quad (3.1.1)$$

In this theory, we consider the extended Lagrangian

$$\mathcal{L}_{f(R)} = f(R), \quad (3.1.2)$$

where  $f(R)$  is the function of  $R$ . The field equations are given by

$$f'(R)R_{\mu\nu} - \frac{1}{2}f(R)g_{\mu\nu} - \nabla_\mu \nabla_\nu f'(R) + g_{\mu\nu} \dot{f}'(R) = 8\pi G T_{\mu\nu}. \quad (3.1.3)$$

In FLRW metric, we obtain

$$3f'(R)H^2 = \frac{1}{2}(f'(R)R - f(R)) - 3H\dot{f}'(R) \quad (3.1.4)$$

$$-2f'(R)\dot{H} = \ddot{f}'(R) - H\dot{f}'(R) \quad (3.1.5)$$

Now let us consider the case of

$$f(R) = R + \alpha R^n. \quad (3.1.6)$$

If we take  $n = 2$ , we can find that Starobinski inflation we discussed in sec.(2.2.3) is included in this theory. In this case, eq.(3.1.4) becomes

$$3(1 + n\alpha R^{n-1})H^2 = \frac{1}{2}(n-1)\alpha R^n - 3n(n-1)\alpha H R^{n-2} \dot{R}, \quad (3.1.7)$$

and we need  $1 + n\alpha R^{n-1} \gg 1$  to make the accelerating expansion of the universe. Thus we obtain

$$H^2 \simeq \frac{n-1}{6n} \left( R - 6nH \frac{\dot{R}}{R} \right). \quad (3.1.8)$$

## 3.2 Brans-Dicke theory

Brans-Dicke theory (BD theory) is given by C. Brans and R. H. Dicke [20]. The action is given as

$$\mathcal{S}_{BD} = \frac{1}{16\pi G} \int d^4x \left[ \phi R - \frac{\omega_{BD}(\phi)}{\phi} \nabla_\mu \phi \nabla^\mu \phi - U(\phi) \right], \quad (3.2.1)$$

where  $\omega_{BD}$  is the constant in the original version. However, we discuss  $\omega_{BD}$  as the function of the scalar field in many of the BD theories.

It is known that this theory has the relation to  $f(R)$  theory [19, 21]. Let us introduce new scalar field and consider the Lagrangian

$$\mathcal{L} = f(\psi) + f_\psi(R - \psi), \quad (3.2.2)$$

where  $f_\psi = \frac{\partial f}{\partial \psi}$ . Taking the variation with  $\psi$ , we obtain

$$f_{\psi\psi}(R - \psi) = 0. \quad (3.2.3)$$

Because of  $f_{\psi\psi} \neq 0$ , we find

$$\psi = R. \quad (3.2.4)$$

If we take  $\phi = f_\psi$ , the Lagrangian eq.(3.2.2) is equal to the Lagrangian of the  $f(R)$  theory eq.(3.1.2). Moreover, eq.(3.2.2) becomes

$$\begin{aligned} \mathcal{L} &= f_\psi R - f_\psi \psi + f(\psi) \\ &= \phi R - U(\phi), \end{aligned} \quad (3.2.5)$$

$$U(\phi) = \phi \psi(\phi) - f(\psi(\phi)). \quad (3.2.6)$$



The Lagrangian eq.(3.2.5) is eq.(3.2.1) with  $\omega_{BD} = 0$ .

Moreover, by using the conformal transformation

$$g_{\mu\nu} \rightarrow \hat{g}_{\mu\nu} = \Omega^2 g_{\mu\nu}, \quad (3.2.7)$$

let us see that  $f(R)$  theory and BD theory can be described in Einstein frame. Under this transformation, the action of  $f(R)$  theory eq.(3.2.5) changes as

$$\begin{aligned} S &= \int dx^4 \sqrt{-g} \left[ \frac{1}{16\pi G} f_R R - U \right] \\ &\rightarrow \int dx^4 \sqrt{-\tilde{g}} \left[ \frac{1}{16\pi G} f_R \Omega^{-2} (\tilde{R} + 6\Box(\ln \Omega) - 6\tilde{g}^{\mu\nu} \partial_\mu(\ln \Omega) \partial_\nu(\ln \Omega)) - \Omega^{-4} U \right] \end{aligned} \quad (3.2.8)$$

where

$$U = \frac{f_R R - f}{16\pi G}. \quad (3.2.9)$$

If we choose  $\Omega^2 = f_R (> 0)$  and define

$$\kappa\phi \equiv \sqrt{\frac{3}{2}} \ln f_R, \quad (3.2.10)$$

we obtain

$$S = \int dx^4 \sqrt{-\tilde{g}} \left[ \frac{1}{16\pi G} \tilde{R} - \frac{1}{2} \tilde{g}^{\mu\nu} \partial_\mu \phi \partial_\nu \phi - V(\phi) \right] \quad (3.2.11)$$

$$V(\phi) = \frac{f_R R - f}{2\kappa^2 f_R^2}. \quad (3.2.12)$$

Therefore, we can find these theories are included in scalar-tensor theory.

### 3.3 Kinetic gravity braiding

In this case, the action is written as

$$\mathcal{L} = K(\phi, X) - G(\phi, X) \Box \phi, \quad (3.3.1)$$

where  $K(\phi, X), G(\phi, X)$  are arbitrary functions. We call this model Kinetic gravity braiding [22]. We assume the metric

$$ds^2 = -dt^2 + a^2(t) dx^2. \quad (3.3.2)$$

The field equation for scalar field is

$$P_\phi - \nabla_\mu J^\mu = 0, \quad (3.3.3)$$

where we have

$$P_\phi = K_\phi - [(\nabla^\mu \phi) \nabla_\mu] G_\phi, \quad (3.3.4)$$

$$J^\mu = (\mathcal{L}_X - 2G_\phi) \nabla_\mu \phi - G_X \nabla_\mu X, \quad (3.3.5)$$

where  $P_\phi = \partial_\phi P$  and the pressure  $P$

$$P = K - [(\nabla^\mu \phi) \nabla_\mu] G. \quad (3.3.6)$$

The energy momentum tensor is given as

$$T_{\mu\nu} \equiv \frac{2}{\sqrt{-g}} \frac{\delta \mathcal{S}_\phi}{\delta g^{\mu\nu}} = \mathcal{L}_X \nabla_\mu \phi \nabla_\nu \phi - g_{\mu\nu} P - \nabla_\mu G \nabla_\nu \phi - \nabla_\nu G \nabla_\mu \phi. \quad (3.3.7)$$

Thus the energy density  $\rho$  and the pressure  $p$  is

$$\rho = \dot{\phi} J + 2X G_\phi - K, \quad (3.3.8)$$

$$p = K - 2X G_\phi - 2X G_X \ddot{\phi}. \quad (3.3.9)$$

Assuming the scalar field depends on time  $\phi = \phi(t)$ , only the component for  $J^0$  in eq.(3.3.5) is remaining. Thus the equation for scalar field is reduced to

$$\dot{J} + 3HJ = P_\phi, \quad (3.3.10)$$

$$J \equiv J^0 = (K_X - 2G_\phi + 3H\dot{\phi}G_X)\dot{\phi}, \quad (3.3.11)$$

Focusing on energy density in eq.(3.3.8), we have

$$\rho = 2X(K_X - G_\phi) - K + 6\dot{\phi}HXG_X, \quad (3.3.12)$$

and we can find  $\rho$  includes the Hubble parameter  $H$ . As we may already find from eq.(2.3.4), the energy density in k-essence does not have the Hubble parameter  $H$ . In such case, we can find Hubble parameter from energy density, however, in this case, energy density  $\rho$  and Hubble parameter  $H$  are corresponding to each other. This feature is called as kinetic gravity braiding. Introducing the parameter  $\kappa$  as the rate of kinetic braiding

$$\kappa = XG_X, \quad (3.3.13)$$

we can rewrite  $\rho$  with replacing the term which do not have  $\kappa$  to  $\mathcal{E}$  as

$$\rho = \mathcal{E} + 6\dot{\phi}H\kappa. \quad (3.3.14)$$

Thus the Hubble parameter  $H$  is

$$H^2 = 2\dot{\phi}H\kappa + \frac{1}{3}\mathcal{E}, \quad (3.3.15)$$

and we can solve the equation

$$H = \kappa\dot{\phi} + \sigma\sqrt{(\kappa\dot{\phi})^2 + \frac{1}{3}\mathcal{E}}, \quad (3.3.16)$$

where we take  $\sigma = \pm 1$ . This suggests us one energy state has two ways of the evolution of universe. Then let us consider the evolution of the universe. Assuming this model is invariant under the transformation for  $\phi$

$$\phi \rightarrow \phi + c, \quad (3.3.17)$$

we can find  $P_\phi = 0$  from eq.(3.3.10)

$$\dot{J} + 3HJ = 0. \quad (3.3.18)$$

Solving this equation, we obtain

$$J = \frac{\text{const.}}{a^3} = (K_X - 2G_\phi + 3H\dot{\phi}G_X)\dot{\phi}. \quad (3.3.19)$$

This suggests that the state becomes  $J \rightarrow 0$  as the universe expands. The state such as  $J = 0$ , in this case, is called an attractor.

### 3.4 Galileon theory

The Galileon theory was constructed by A. Nicolis, R. Rattazzi and E. Trincherini [23]. This section is a review of [24, 25, 26]. As its name is "Galileon", this model have Galilean shift symmetry

$$\partial_\mu\phi \rightarrow \partial_\mu\phi + b_\mu, \quad (3.4.1)$$

where  $\phi$  is the scalar field. First, let us consider the Lagrangian of the original Galileon theory in flat space-time. Now we assume the Lagrangian as  $\mathcal{L}(\phi, \partial_\mu\phi, \partial_\mu\partial_\nu\phi)$ , and in this case the Euler Lagrange equation is written as

$$\frac{\partial\mathcal{L}}{\partial\phi} - \partial_\mu\frac{\partial\mathcal{L}}{\partial\phi_\mu} + \partial_\mu\partial_\nu\frac{\partial\mathcal{L}}{\partial\phi_{\mu\nu}} = 0, \quad (3.4.2)$$

where we define,

$$\phi_\mu \equiv \partial_\mu\phi, \quad \phi_{\mu\nu} \equiv \partial_\mu\partial_\nu\phi. \quad (3.4.3)$$

The Lagrangian in  $D$  dimension is given as

$$\mathcal{L}_n = \mathcal{T}_{(2n)}^{\mu_1 \dots \mu_n \nu_1 \dots \nu_n} \phi_{\mu_1 \nu_1} \phi_{\mu_n \nu_n}, \quad (3.4.4)$$

where  $(2n)$  is the number of indices which  $\mathcal{T}$  has, and we define

$$\mathcal{T}_{(2n)}^{\mu_1 \dots \mu_n \nu_1 \dots \nu_n} \phi_{\mu_1 \nu_1} \equiv \mathcal{A}_{2(n+1)}^{\mu_1 \dots \mu_{n+1} \nu_1 \dots \nu_{n+1}} \phi_{\mu_{n+1}} \phi_{\nu_{n+1}}, \quad (3.4.5)$$

$$\mathcal{A}_{(2m)}^{\mu_1 \dots \mu_m \nu_1 \dots \nu_m} \equiv \frac{1}{(D-m)!} \epsilon^{\mu_1 \dots \mu_m \rho_1 \dots \rho_m} \epsilon^{\nu_1 \dots \nu_m}_{\rho_1 \dots \rho_m}. \quad (3.4.6)$$

The Levi-Civita tensor is given as

$$\epsilon^{\mu_1 \dots \mu_m} \equiv -\frac{1}{\sqrt{-g}} \delta_1^{[\mu_1} \delta_2^{\mu_2} \dots \delta_m^{\mu_m]}. \quad (3.4.7)$$

Deriving the field equation from this Lagrangian, we have no higher derivative terms of  $\phi$  because these terms are canceled. For example, the Lagrangian in 4 dimensional flat space-time has four Lagrangians as

$$\mathcal{L}_2 = -\phi_\mu \phi^\mu, \quad (3.4.8)$$

$$\mathcal{L}_3 = \phi^\mu \phi^\nu \phi_{\mu\nu} - \phi^\mu \phi_\mu \square \phi, \quad (3.4.9)$$

$$\mathcal{L}_4 = -(\square \phi)^2 (\phi_\mu \phi^\mu) + 2(\square \phi) \phi_\mu \phi^{\mu\nu} \phi_\nu + (\phi_{\mu\nu} \phi^{\mu\nu}) - 2\phi_\mu \phi^{\mu\nu} \phi_{\nu\rho} \phi^\rho, \quad (3.4.10)$$

$$\begin{aligned} \mathcal{L}_5 = & -(\square \phi)^3 \phi_\mu \phi^\mu + 3(\square \phi)^2 \phi_\mu \phi^{\mu\nu} \phi_\nu + 3(\square \phi) \phi_{\mu\nu} \phi^{\mu\nu} \phi_\rho \phi^\rho \\ & - 6(\square \phi) \phi_\mu \phi^{\mu\nu} \phi_{\nu\rho} \phi^\rho - 2(\phi_\mu{}^\nu \phi_\nu{}^\rho \phi_\rho{}^\mu) (\phi_\lambda \phi^\lambda) \\ & - 3(\phi_{\mu\nu} \phi^{\mu\nu}) (\phi_\rho \phi^{\rho\lambda} \phi_\lambda) + 6(\phi_\mu \phi^{\mu\nu} \phi_{\nu\rho} \phi^{\rho\lambda} \phi_\lambda). \end{aligned} \quad (3.4.11)$$

So far we have considered the Lagrangian in the flat space-time. In the curved space-time, we use

$$\phi_\mu \equiv \nabla_\mu \phi, \quad \phi_{\mu\nu} \equiv \nabla_\mu \nabla_\nu \phi. \quad (3.4.12)$$

Thus the Galilean shift symmetry is broken in curved space-time. This alteration generates the third or higher derivatives terms for the field equation of  $\mathcal{L}_4$  and  $\mathcal{L}_5$ . For the equation of motion  $\sum \mathcal{E}_i = 0$ , we obtain  $\mathcal{E}_4$  for  $\mathcal{L}_4$  as

$$\begin{aligned} \mathcal{E}_4 = & -\frac{1}{2} (\phi_\mu \phi^\mu) (\phi_\mu{}^\mu{}^\rho - \phi_{\mu\rho}{}^{\mu\rho}) + \frac{1}{2} \phi^\mu \phi^\nu (2\phi_{\mu\rho\nu}{}^\rho - \phi_{\mu\nu\rho}{}^\rho - \phi_\rho{}^\rho{}_{\mu\nu}) \\ & + \frac{5}{2} (\square \phi) \phi^\mu (\phi_{\mu\nu}{}^\nu - \phi_\nu{}^\mu{}_\mu) - 3\phi_\mu \phi^{\mu\nu} (\phi_\rho{}^\rho{}_\nu - \phi_{\nu\rho}{}^\rho) \\ & - 2\phi^\mu \phi^{\nu\rho} (\phi_{\nu\rho\mu} - \phi_{\mu\nu\rho}) + (\square \phi)^3 + 2(\phi_\mu{}^\nu \phi_\nu{}^\rho \phi_\rho{}^\mu) - 3(\square \phi) (\phi_{\mu\nu} \phi^{\mu\nu}). \end{aligned} \quad (3.4.13)$$

By integrating by parts, we can remove the higher derivative terms of  $\phi$ . Thus  $\mathcal{E}_4$  has

$$\begin{aligned} \mathcal{E}_4 \supset & +\frac{1}{4} \phi_\mu \phi^\mu \phi_\nu \nabla^\nu R - \frac{1}{2} \phi_\mu \phi_\nu \phi_\rho \nabla^\rho R^{\mu\nu} - \frac{5}{2} \square \phi \phi_\mu R^{\mu\nu} \phi_\nu \\ & + 2\phi_\mu \phi^{\mu\nu} R_{\nu\rho} \phi^\rho + \frac{1}{2} \phi_\mu \phi^\mu \phi_{\nu\rho} R^{\nu\rho} + 2\phi_\mu \phi_\nu \phi_{\rho\sigma} R_{\mu\rho\nu\sigma}, \end{aligned} \quad (3.4.14)$$

and we find the higher derivative terms of metric. To remove these terms, we introduce  $\mathcal{L}_4^{\text{nonmin}}$

$$\mathcal{L}_4^{\text{nonmin}} = (\phi_\mu \phi^\mu)(\phi_\nu G^{\nu\lambda} \phi_\lambda). \quad (3.4.15)$$

Thus we have

$$\mathcal{L}_4 + \mathcal{L}_4^{\text{nonmin}} = (\phi_\mu \phi^\mu) \left[ 2(\square\phi)^2 - 2(\phi_{\mu\nu} \phi^{\mu\nu}) - \frac{1}{2}(\phi_\mu \phi^\mu)R \right]. \quad (3.4.16)$$

In the same way, we introduce  $\mathcal{L}_5^{\text{nonmin}}$  for  $\mathcal{L}_5$

$$\mathcal{L}_5^{\text{nonmin}} = (\phi_\mu \phi^\mu)(\phi_\nu G^{\nu\lambda} \phi_\lambda). \quad (3.4.17)$$

and we have the total Lagrangian for  $\mathcal{L}_5$  as

$$\mathcal{L}_5 + \mathcal{L}_5^{\text{nonmin}} = (\phi_\mu \phi^\mu) \left[ (\square\phi)^3 - 3\square\phi(\phi_{\mu\nu} \phi^{\mu\nu}) + 2(\phi_\mu{}^\nu \phi_\nu{}^\lambda \phi_\lambda{}^\mu) - 6(\phi_\mu \phi^{\mu\nu} G_{\nu\lambda} \phi^\lambda) \right]. \quad (3.4.18)$$

### 3.5 Horndeski theory

As we discussed so far, many modified gravity theories exist. Later we discuss some topics of galilean genesis, and we use Horndeski theory. Horndeski theory is known as the most generalized scalar tensor theory in which the field equations do not have more than third-time derivative terms. This theory is investigated by Horndeski at 1972 [17] and widely known by recent research about generalization of the galilean theory [18] and applying the cosmological context [16]. The Lagrangian is written as

$$\begin{aligned} S_{\text{Hor}} &= \int d^4x \sqrt{-g} (\mathcal{L}_2 + \mathcal{L}_3 + \mathcal{L}_4 + \mathcal{L}_5), \\ \mathcal{L}_2 &= G_2(\phi, X), \\ \mathcal{L}_3 &= -G_3(\phi, X) \square\phi, \\ \mathcal{L}_4 &= G_4(\phi, X)R + G_{4X} [(\square\phi)^2 - (\nabla_\mu \nabla_\nu \phi)^2], \\ \mathcal{L}_5 &= G_5(\phi, X)G^{\mu\nu} \nabla_\mu \nabla_\nu \phi - \frac{1}{6}G_{5X} [(\square\phi)^3 - 3\square\phi(\nabla_\mu \nabla_\nu \phi)^2 + 2(\nabla_\mu \nabla_\nu \phi)^3], \end{aligned} \quad (3.5.1)$$

where  $(\nabla_\mu \nabla_\nu \phi)^2 = \nabla_\mu \nabla^\nu \phi \nabla_\nu \nabla^\mu \phi$ ,  $(\nabla_\mu \nabla_\nu \phi)^3 = \nabla_\mu \nabla^\nu \phi \nabla_\nu \nabla^\lambda \phi \nabla_\lambda \nabla^\mu \phi$ , and  $G_i(\phi, X)$  ( $i = 2, 3, 4, 5$ ) is the arbitrary function of scalar field  $\phi$  and its kinetic term  $X =: -\frac{1}{2}(\partial\phi)^2$ . We can obtain the Lagrangian we have already discussed. For example, if we take

$$\begin{aligned} G_2(\phi, X) &= G_3(\phi, X) = G_5(\phi, X) = 0, \\ G_4(\phi, X) &= \text{const.}, \end{aligned} \quad (3.5.2)$$

we can find the Lagrangian of general relativity, or we take

$$\begin{aligned} G_2(\phi, X) &= K(\phi, X), \\ G_3(\phi, X) &= G(\phi, X), \\ G_4(\phi, X) &= G_5(\phi, X) = 0, \end{aligned} \quad (3.5.3)$$

we can find the Lagrangian of kinetic gravity braiding in sec(3.3). Although this theory includes Galilean theory, we do not assume the Galilean shift symmetry eq.(3.4.1) in Horndeski theory. The field equations in Horndeski theory is derived in [16]. The Friedmann equation is

$$\sum_{i=2}^5 \mathcal{E}_i = 0, \quad (3.5.4)$$

$$\mathcal{E}_2 = 2XG_{2X} - G_2, \quad (3.5.5)$$

$$\mathcal{E}_3 = 6X\dot{\phi}HG_{3X} - 2XG_{3\phi}, \quad (3.5.6)$$

$$\mathcal{E}_4 = -6H^2G_4 + 24H^2X(G_{4X} + XG_{4XX}) - 12HX\dot{\phi}G_{4\phi X} - 6H\dot{\phi}G_{4\phi}, \quad (3.5.7)$$

$$\mathcal{E}_5 = 2H^3X\dot{\phi}(5G_{5X} + 2XG_{5XX}) - 6H^2X(3G_{5\phi} + 2XG_{5\phi X}), \quad (3.5.8)$$

The evolution equation is given as

$$\sum_{i=2}^5 \mathcal{P}_i = 0, \quad (3.5.9)$$

$$\mathcal{P}_2 = G_2, \quad (3.5.10)$$

$$\mathcal{P}_3 = -2X(G_{3\phi} + \ddot{\phi}G_{3X}), \quad (3.5.11)$$

$$\begin{aligned} \mathcal{P}_4 &= 2(3H^2 + 2\dot{H})G_4 - 12H^2XG_{4X} - 4H\dot{X}G_{4X} - 8\dot{H}XG_{4X} - 8HX\dot{X}G_{4XX} \\ &\quad + 2(\ddot{\phi} + 2H\dot{\phi})G_{4\phi} + 4XG_{4\phi\phi} + 4X(\ddot{\phi} - 2H\dot{\phi})G_{4\phi X}, \end{aligned} \quad (3.5.12)$$

$$\begin{aligned} \mathcal{P}_5 &= -2X(2H^3\dot{\phi} + 2H\dot{H}\dot{\phi} + 3H^2\ddot{\phi})G_{5X} - 4H^2X^2G_{5XX} \\ &\quad + 4HX(\dot{X} - HX)G_{5\phi X} + 2[2(HX)\dot{X} + 3H^2X]G_{5\phi} + 4HX\dot{\phi}G_{5\phi\phi}, \end{aligned} \quad (3.5.13)$$

Finally, the field equation for  $\phi$  is given by

$$\frac{1}{a^3} \frac{d}{dt}(a^3 J) = P_\phi, \quad (3.5.14)$$

where

$$J = \dot{\phi}G_{2X} + 6HXG_{3X} - 2\dot{\phi}G_{3\phi} + 6H^2\dot{\phi}(G_{4X} + 2XG_{4XX}) - 12HXXG_{4\phi X} + 2H^3X(3G_{5X} + 2XG_{5XX}) - 6H^2\dot{\phi}(G_{5\phi} + XG_{5\phi X}), \quad (3.5.15)$$

$$P_\phi = K_\phi - 2X(G_{3\phi\phi} + \ddot{\phi}G_{3\phi X}) + 6(2H^2 + \dot{H})G_{4\phi} + 6H(\dot{X} + 2HX)G_{4\phi X} - 6H^2XG_{5\phi\phi} + 2H^3X\dot{\phi}G_{5\phi X}, \quad (3.5.16)$$

### 3.6 GLPV theory

We can construct the more general class of theory. The more extended theory is discussed by Gleyzes et al. [27]. This theory can have higher time derivative terms, in spite of the Horndeski theory have no more than second order time derivative terms.

$$\begin{aligned} \mathcal{L}_{GLPV} &= \mathcal{L}_2 + \mathcal{L}_3 + \mathcal{L}_4 + \mathcal{L}_5, \\ \mathcal{L}_2 &= G_2(\phi, X), \\ \mathcal{L}_3 &= -G_3(\phi, X)\square\phi, \\ \mathcal{L}_4 &= G_4(\phi, X)R + G_{4X}[(\square\phi)^2 - (\nabla_\mu\nabla_\nu\phi)^2] + F_4(\phi, X)\epsilon^{\mu\nu\rho\sigma}\epsilon^{\mu'\nu'\rho'\sigma'}\phi_\mu\phi_{\mu'}\phi_{\nu\nu'}\phi_{\rho\rho'}, \\ \mathcal{L}_5 &= G_5(\phi, X)G^{\mu\nu}\nabla_\mu\nabla_\nu\phi - \frac{1}{6}G_{5X}[(\square\phi)^3 - 3\square\phi(\nabla_\mu\nabla_\nu\phi)^2 + 2(\nabla_\mu\nabla_\nu\phi)^3] \\ &\quad + F_5(\phi, X)\epsilon^{\mu\nu\rho\sigma}\epsilon^{\mu'\nu'\rho'\sigma'}\phi_\mu\phi_{\mu'}\phi_{\nu\nu'}\phi_{\rho\rho'}\phi_{\sigma\sigma'}, \end{aligned} \quad (3.6.1)$$

where  $F_4$  and  $F_5$  are arbitrary functions and  $\epsilon^{\mu\nu\rho\sigma}$  is the total antisymmetric Levi-Civita tensor. For this to reduce to the Horndeski theory we take

$$\begin{aligned} F_4(\phi, X) &= 0, \\ F_5(\phi, X) &= 0. \end{aligned} \quad (3.6.2)$$

Now we use ADM decomposition in which the metric is given as

$$ds^2 = -N^2dt^2 + \gamma_{ij}(dx^i + N^i dt)(dx^j + N^j dt), \quad (3.6.3)$$

where  $N$  is lapse function,  $N^i$  is shift vector and  $\gamma_{ij}$  is the spatial metric. The Lagrangian of the GLPV theory is written as

$$\begin{aligned} \mathcal{L}_2 &= A_2(t, N), \\ \mathcal{L}_3 &= A_3(t, N)K, \\ \mathcal{L}_4 &= A_4(t, N)(K^2 - K_{ij}^2) + B_4(t, N)R^{(3)}, \\ \mathcal{L}_5 &= A_5(K^3 - 3KK_{ij}^2 + 2K_{ij}^3) + B_5(t, N)K^{ij}\left(R_{ij} - \frac{1}{2}g_{ij}R^{(3)}\right), \end{aligned} \quad (3.6.4)$$

where  $K_{ij}$  is the extrinsic curvature

$$K_{ij} = \frac{1}{2N} (g_{ij} - \nabla_i N_j - \nabla_j N_i), \quad (3.6.5)$$

$A_i(t, N)$  and  $B_i(t, N)$  are arbitrary functions which have the following relations

$$\begin{aligned} A_2 &= G_2 + \sqrt{2X} \int \frac{G_{3\phi}}{2\sqrt{2X}} dX, \\ A_3 &= - \int G_{3X} \sqrt{2X} dX - 2\sqrt{2X} G_{4\phi}, \\ A_4 &= -G_4 + 2X G_{4X} - X G_{5\phi} - 4X^2 F_4, \\ A_5 &= \frac{(2X)^{3/2}}{6} G_{5X} + (2X)^{5/2} F_5, \\ B_4 &= G_4 - \sqrt{2X} \int \frac{G_{5\phi}}{4\sqrt{2X}} dX, \\ B_5 &= - \int G_{5X} \sqrt{2X} dX. \end{aligned} \quad (3.6.6)$$

For this expression, In order to reduce to the Horndeski theory, we take the conditions

$$\begin{aligned} A_4 &= -B_4 + 2X B_{4X}, \\ A_5 &= -\frac{1}{3} X B_{5X}. \end{aligned} \quad (3.6.7)$$

### 3.7 Conclusions in this chapter

In this section, we have discussed many modified theories. As we have reviewed in this chapter, many kinds of modified theories are discussed. We have introduced GLPV theory as the beyond theory of Horndeski, but there is the more expanded theory called XG3 [28]. First, we have studied relatively simple models such as  $f(R)$  theory, Brans-Dicke theory or K-essence, and after those theories, we have studied more complicated and generalized theory. In such a generalized theory, we assume some conditions or ansatz. What we have reviewed is for one scalar field and one gravitational field, but there are many models which have multi-scalar fields or gravitational fields. In part 2, although there are many generalized theories of scalar-tensor theory, we use Horndeski theory as the simple example to see the typical features of each term.



## Chapter 4

# Cosmological perturbations

In this section, we introduce cosmological perturbations. First, we discuss how the perturbation behaves in general relativity. As we use Horndeski theory in sec.3.5, we finally derive the quadratic action or equation for perturbations in Horndeski theory. This section is the review of [11].

### 4.1 Perturbations

Let us introduce gauge transformation for point  $x^\gamma$  as

$$x^\gamma \rightarrow \tilde{x}^\gamma = x^\gamma + \xi^\gamma, \quad (4.1.1)$$

and discuss some tensor value  $A_{\mu\nu}$  under this transformation. Under the transformation,  $A_{\mu\nu}$  changes to  $\tilde{A}_{\mu\nu}$  as

$$A_{\mu\nu}(x^\gamma) = {}^{(0)} A_{\mu\nu}(x^\gamma) + \delta A_{\mu\nu}, \quad (4.1.2)$$

$$\tilde{A}_{\mu\nu}(\tilde{x}^\gamma) = {}^{(0)} A_{\mu\nu}(\tilde{x}^\gamma) + \delta \tilde{A}_{\mu\nu}, \quad (4.1.3)$$

and this can be written in another expression under the transformation

$$A_{\mu\nu}(x^\gamma) \rightarrow \tilde{A}_{\mu\nu}(x^\gamma) = \frac{dx^\mu}{dx^\alpha} \frac{dx^\nu}{dx^\beta} A_{\alpha\beta}(x^\gamma). \quad (4.1.4)$$

This equation is derived from the transformation of tensor field. Applying the transformation for scalar field  $q$  and vector field  $v_\mu$ , we obtain

$$\begin{aligned}\tilde{q}(\tilde{x}^\gamma) &= q(x^\gamma) \\ &= {}^{(0)}q(x^\gamma) + \delta q,\end{aligned}\tag{4.1.5}$$

$$\begin{aligned}\tilde{v}_\mu(\tilde{x}^\gamma) &= \frac{dx^\alpha}{d\tilde{x}^\mu} v_\alpha(x^\gamma) \\ &= \frac{d(\tilde{x}^\alpha - \xi^\alpha)}{d\tilde{x}^\mu} v_\alpha(x^\gamma) \\ &\simeq v_\mu(x^\gamma) - {}^{(0)}v_\alpha(x^\gamma) \xi_\mu^\alpha \\ &= {}^{(0)}v_\mu(x^\gamma) + \delta v_\mu - {}^{(0)}v_\alpha(x^\gamma) \xi_{,\mu}^\alpha,\end{aligned}\tag{4.1.6}$$

and

$${}^{(0)}q(\tilde{x}^\gamma) = {}^{(0)}q(x^\gamma) + {}^{(0)}q_{,\alpha} \xi^\alpha,\tag{4.1.7}$$

$${}^{(0)}v_\mu(\tilde{x}^\gamma) = {}^{(0)}v_\mu(x^\gamma) + {}^{(0)}v_{\mu,\alpha} \xi^\alpha.\tag{4.1.8}$$

Therefore, we find for  $\delta q$  and  $\delta v_\mu$  as

$$\delta q \rightarrow \delta \tilde{q} = \delta q - {}^{(0)}q_{,\alpha} \xi^\alpha,\tag{4.1.9}$$

$$\delta v_\mu \rightarrow \delta \tilde{v}_\mu = \delta v_\mu - {}^{(0)}v_{\mu,\alpha} \xi^\alpha - {}^{(0)}v_\alpha \xi_{,\mu}^\alpha.\tag{4.1.10}$$

Let us apply this transformation for metric  $g_{\mu\nu}$ . Decomposing the metric into  $g_{00}, g_{0i}, g_{ij}$  and referring to the result for  $A_{\mu\nu}$ , we find

$$\delta \tilde{g}_{00} = \delta g_{00} - 2a^2 \left\{ -\frac{1}{a} (a\xi^0)' \right\},\tag{4.1.11}$$

$$\delta \tilde{g}_{0i} = \delta g_{0i} + a^2 \left\{ (\xi_s' - \xi^0)_{,i} - \xi_{\perp i,0} \right\},\tag{4.1.12}$$

$$\delta \tilde{g}_{ij} = \delta g_{ij} + a^2 (-\xi_{\perp j,i} - \xi_{\perp i,j} - 2\xi_{s,ij} - 2\mathcal{H}\delta_{ij}\xi^0),\tag{4.1.13}$$

If we set the metric including only scalar perturbations as

$$ds^2 = a(\eta)^2 \left[ -(1 + 2\phi)d\eta^2 + 2B_{,i}d\eta dx^i + \{(1 - 2\psi)\delta_{ij} + 2E_{,ij}\} dx^i dx^j \right],\tag{4.1.14}$$

the components of  $g_{\mu\nu}$  is written as

$$\delta g_{00} = -2a^2\phi,\tag{4.1.15}$$

$$\delta g_{0i} = a^2 B_{,i},\tag{4.1.16}$$

$$\delta g_{ij} = a^2 (-2\psi\delta_{ij} + 2E_{,ij}),\tag{4.1.17}$$

and thus the transformations for  $\phi, B, E, \psi$  are

$$\phi \rightarrow \tilde{\phi} = \phi - \frac{1}{a} (a\xi^0)', \quad (4.1.18)$$

$$B \rightarrow \tilde{B} = B + \xi_s' - \xi^0, \quad (4.1.19)$$

$$E \rightarrow \tilde{E} = E + \xi_s, \quad (4.1.20)$$

$$\psi \rightarrow \tilde{\psi} = \psi + \mathcal{H}\xi^0. \quad (4.1.21)$$

Now we have 4 degrees of freedom shown by  $\xi^\mu$ , and we can fix a gauge freely. As eq.(4.1.18)-eq.(4.1.21) have 2 of 4 components, however, we can obtain the gauge invariant values without fixing the gauge. Introducing the gauge invariant value  $\Phi$  and  $\Psi$ , we can find

$$\Phi = \phi - \frac{1}{a} [a(B - E')]', \quad (4.1.22)$$

$$\Psi = \psi + \mathcal{H}(B - E'). \quad (4.1.23)$$

In the other case, if we take the metric with vector perturbations

$$ds^2 = a(t)^2 [-d\eta^2 + 2S_i d\eta dx^i + (\delta_{ij} - F_{i,j} - F_{j,i}) dx^i dx^j], \quad (4.1.24)$$

the metric is described as

$$\delta g_{00} = 0, \quad (4.1.25)$$

$$\delta g_{0i} = a^2 S_i, \quad (4.1.26)$$

$$\delta g_{ij} = -a^2 (F_{i,j} + F_{j,i}). \quad (4.1.27)$$

We can find the transformations for  $S_i$  and  $F_i$

$$S_i \rightarrow \tilde{S}_i = S_i - \xi_{\perp i}', \quad (4.1.28)$$

$$F_i \rightarrow \tilde{F}_i = F_i + \xi_{\perp i}. \quad (4.1.29)$$

In this case, we can find the gauge invariant value  $V_i$  as

$$V_i = S_i + F_i', \quad (4.1.30)$$

For the tensor perturbations, we take this metric

$$ds^2 = a(t)^2 [-d\eta^2 + (\delta_{ij} + h_{ij}) dx^i dx^j], \quad (4.1.31)$$

and the metric is given as

$$\delta g_{00} = \delta g_{0i} = 0, \quad (4.1.32)$$

$$\delta g_{ij} = a^2 h_{ij}. \quad (4.1.33)$$

For the transformation of  $h_{ij}$ , we can find

$$h_{ij} \rightarrow \tilde{h}_{ij} = h_{ij}, \quad (4.1.34)$$

and this shows  $h_{ij}$  is gauge invariant.

## 4.2 Matter perturbation

In this subsection, we discuss matter perturbations which we ignored in pre sections. Now we assume the perfect fluid and discuss the perturbations for the matter.

$$T_{\mu\nu} = (\rho + p)u_\mu u_\nu + g_{\mu\nu}p, \quad (4.2.1)$$

Introducing  $\delta T_{\mu\nu}$  as the perturbation for matter, we have

$$T_{\mu\nu} = {}^{(0)}T_{\mu\nu} + \delta T_{\mu\nu}, \quad (4.2.2)$$

Taking the transformation and we define  $\tilde{T}_{\mu\nu}$  as the tensor after transformation for  $T_{\mu\nu}$

$$\begin{aligned} \delta\tilde{T}_{00} &= \delta T_{00} - 2{}^{(0)}T_{00}\xi^{0'} - {}^{(0)}T_{00}'\xi^0 \\ &= \delta T_{00} - 2a^2\rho_0\xi^{0'} - (a^2\rho_0)'\xi^0 \\ &= \delta T_{00} - a^2\rho_0 \left\{ (B - E') - (\tilde{B} - \tilde{E}') \right\}, \end{aligned} \quad (4.2.3)$$

$$\begin{aligned} \delta\tilde{T}_{0i} &= \delta T_{0i} - {}^{(0)}T_{00}\xi'^i - {}^{(0)}T_{ij}\xi^{j'} \\ &= \delta T_{0i} - a^2(\rho_0 + p_0) \left\{ (B - E') - (\tilde{B} - \tilde{E}') \right\}_{,i}, \end{aligned} \quad (4.2.4)$$

$$\begin{aligned} \delta\tilde{T}_{ij} &= \delta T_{ij} - {}^{(0)}T_{ki}\xi_s^k{}_{,j} - {}^{(0)}T_{kj}\xi_s^k{}_{,i} - {}^{(0)}T_{ij}'\xi^0 \\ &= \delta T_{ij} - a^2\delta_{ij}p'_0 \left\{ (B - E') - (\tilde{B} - \tilde{E}') \right\}, \end{aligned} \quad (4.2.5)$$

These equations suggest us

$$\delta\bar{T}_{00} = \delta T_{00} - a^2\rho_0'(B - E'), \quad (4.2.6)$$

$$\delta\bar{T}_{0i} = \delta T_{0i} - a^2(\rho_0 + p_0)(B - E')_{,i}, \quad (4.2.7)$$

$$\delta\bar{T}_{ij} = \delta T_{ij} - a^2\delta_{ij}p_0'(B - E'). \quad (4.2.8)$$

As the components of the energy momentum tensor  $T_{\mu\nu}$  have the energy density  $\rho$ , the pressure  $p$  and the 4-velocity  $u_\mu$

$$\rho = \rho_0 + \delta\rho, \quad (4.2.9)$$

$$p = p_0 + \delta p, \quad (4.2.10)$$

$$u_\mu = u_{0\mu} + \delta u_\mu, \quad (4.2.11)$$

we can obtain from above equations

$$\delta\bar{\rho} = \delta\rho - \rho'_0(B - E'), \quad (4.2.12)$$

$$\delta\bar{p} = \delta p - p'_0(B - E'), \quad (4.2.13)$$

$$\delta\bar{u}_0 = \delta u_0 - \{a(B - E')\}', \quad (4.2.14)$$

$$\delta\bar{u}_i = \delta u_i - a(B - E')_{,i}, \quad (4.2.15)$$

$$\delta T_{\mu\nu} = (\delta\rho + \delta p)u_\mu u_\nu + (\rho + p)(\delta u_\mu u_\nu + u_\mu \delta u_\nu) + g_{\mu\nu}\delta p + \delta g_{\mu\nu}p, \quad (4.2.16)$$

Thus we obtain the components of perturbations of the energy momentum tensor as

$$\delta \bar{T}_{00} = a^2 \delta \bar{\rho}, \quad (4.2.17)$$

$$\delta \bar{T}_{0i} = a(\rho_0 + p_0)\delta \bar{u}_i, \quad (4.2.18)$$

$$\delta \bar{T}_{ij} = a^2 \delta \bar{p}. \quad (4.2.19)$$

### 4.3 Gauge

We have discussed the perturbations, and we find there are some degrees of freedom. Thus we can fix the gauge, and there are some ways to fix them. In this subsection, we introduce some gauges.

#### 4.3.1 Conformal Newtonian gauge

First, we introduce conformal Newtonian gauge (or longitudinal gauge, conformal gauge). In this gauge, we take the condition as

$$B = E = 0, \quad (4.3.1)$$

and thus we obtain

$$ds^2 = a^2(\eta) [-(1 + 2\Phi)d\eta^2 + (1 - 2\Psi)\delta_{ij}dx^i dx^j]. \quad (4.3.2)$$

#### 4.3.2 Comoving gauge

For the comoving gauge, we take the rule for perturbation of energy momentum tensor as

$$\delta T_i^0 = 0. \quad (4.3.3)$$

In this case, contravariant vector for velocity becomes

$$\delta u^i = -\frac{1}{a}B_i + \frac{1}{a^2}\delta u_i. \quad (4.3.4)$$

As the gauge transformation for  $\delta u_i$  and  $B$  is

$$\delta \tilde{u}_i = \delta u_i - a\xi_{,i}^0, \quad (4.3.5)$$

$$\tilde{B} = B + \zeta'_s - \xi^0, \quad (4.3.6)$$

we can find we have to fix  $\zeta' = 0$ .

## 4.4 Cosmological perturbations in General Relativity

Applying the components of metric, we discussed before into the Einstein equation

$$\delta G_{\mu\nu} = 8\pi G\delta T_{\mu\nu}, \quad (4.4.1)$$

we can obtain the equations for perturbations.

### 4.4.1 Scalar perturbation

For scalar perturbation, we obtain the equations with scalar part of the energy momentum tensor  $\delta T_{\mu\nu}^{(S)}$  as follows

$$\Delta\psi - 3\mathcal{H}(\psi' + \mathcal{H}\phi) = 4\pi G\delta T_{00}^{(S)}, \quad (4.4.2)$$

$$(\psi + \mathcal{H}\phi)_{,i} = 4\pi G\delta T_{0i}^{(S)}, \quad (4.4.3)$$

$$\begin{aligned} \delta_{ij} \{ 2\psi'' + \Delta(\phi - \psi) + 2\mathcal{H}(2\psi + \phi)' + 2\mathcal{H}^2(\phi - 2\psi) \\ + 2\mathcal{H}'(\phi + \psi) \} + (\psi - \phi)_{,ij} = 8\pi G\delta T_{ij}^{(S)}. \end{aligned} \quad (4.4.4)$$

Focusing on eq.(4.4.4), if we assume  $\delta T_{ij} \propto \delta_{ij}$ , we can find  $\psi - \phi = 0$ . Therefore eq.(4.4.4) becomes

$$\phi'' + 3\mathcal{H}\phi + (2\mathcal{H}' - \mathcal{H}^2)\phi = 4\pi G\delta T_{ij}^{(S)}. \quad (4.4.5)$$

### 4.4.2 Vector perturbation

For vector perturbation, the equations with vector part of the energy momentum tensor  $\delta T_{\mu\nu}^{(V)}$  is

$$\Delta V_i = -16\pi G\delta T_{0i}^{(V)}, \quad (4.4.6)$$

$$(V_{i,j} + V_{j,i})' + 2\mathcal{H}(V_{i,j} + V_{j,i}) = -16\pi G\delta T_{ij}^{(V)}, \quad (4.4.7)$$

From eq.(4.4.7) we find the vector mode is always decaying.

### 4.4.3 Tensor perturbation

For tensor perturbations, the equation with tensor part of the energy momentum tensor  $\delta T_{ij}^{(T)}$  is

$$h''_{ij} + 2\mathcal{H}h'_{ij} - \Delta h_{ij} = 16\pi G\delta T_{ij}^{(T)}. \quad (4.4.8)$$

## 4.5 Cosmological perturbations in Horndeski Theory

In this way, we derived the equations for the cosmological perturbations from the equation of motion. However, there is another approach where we derive the equations from the variation of quadratic action. In this thesis, we consider the model written by the scalar field and the gravitational field. Let us consider the equations for Horndeski theory in this section. This is the review of [15]. The action and background equations have been already shown in sec.3.5. Then in this section, let us see the perturbations in FRLW metric and unitary gauge in ADM formalism in the unitary gauge.

$$ds^2 = -N^2 dt^2 + \gamma_{ij}(dx^i + N^i dt)(dx^j + N^j dt). \quad (4.5.1)$$

### 4.5.1 Unitary gauge

When we consider the case that the Lagrangian is written by the scalar field and the gravitational field, we can use the unitary gauge defined as follows. In the unitary gauge, we set that the scalar field depends on only time

$$\phi = \phi(t). \quad (4.5.2)$$

From eq.(2.3.2), we find

$$X = -\frac{\dot{\phi}^2}{2N^2}. \quad (4.5.3)$$

Thus the kinetic term of scalar field  $\phi$  is the function of  $t$  and  $N$ , and the arbitrary functions in eq.(3.6.4) are written as the function of  $t$  and  $N$ .

### 4.5.2 The quadratic action in Horndeski theory

The Friedmann equation eq.(3.5.8) and the evolution equation eq.(3.5.13) are derived from the variation of  $\delta a$  and  $\delta N$ . The quadratic Lagrangian for tensor perturbations is

$$\mathcal{S}_T = \frac{1}{8} \int dt d^3 x a^3 \left[ \mathcal{G}_T h_{ij}^2 - \frac{\mathcal{F}_T}{a^2} (\nabla h_{ij})^2 \right], \quad (4.5.4)$$

where

$$\mathcal{G}_T := 2 \left[ G_4 - 2XG_{4X} - X \left( H\dot{\phi}G_{5X} - G_{5\phi} \right) \right], \quad (4.5.5)$$

$$\mathcal{F}_T := 2 \left[ G_4 - X \left( \ddot{\phi}G_{5X} + G_{5\phi} \right) \right]. \quad (4.5.6)$$

The quadratic Lagrangian for scalar perturbation in unitary gauge is

$$\mathcal{S}_S = \int dt d^3 x a^3 \left[ \mathcal{G}_S \dot{\zeta}^2 - \frac{\mathcal{F}_S}{a^2} (\nabla \zeta)^2 \right], \quad (4.5.7)$$

where

$$\mathcal{F}_S := \frac{1}{a} \frac{d}{dt} \left( \frac{a}{\Theta} \mathcal{G}_T^2 \right) - \mathcal{F}_T, \quad (4.5.8)$$

$$\mathcal{G}_S := \frac{\Sigma}{\Theta^2} \mathcal{G}_T^2 + 3\mathcal{G}_T, \quad (4.5.9)$$

$$\begin{aligned} \Sigma &:= XG_{2X} + 2X^2G_{2XX} + 12H\dot{\phi}XG_{3X} \\ &\quad + 6H\dot{\phi}X^2G_{3XX} - 2XG_{3\phi} - 2X^2G_{3\phi X} - 6H^2G_4 \\ &\quad + 6 \left[ H^2 (7XG_{4X} + 16X^2G_{4XX} + 4X^3G_{4XXX}) \right. \\ &\quad \left. - H\dot{\phi} (G_{4\phi} + 5XG_{4\phi X} + 2X^2G_{4\phi XX}) \right] \\ &\quad + 30H^3\dot{\phi}XG_{5X} + 26H^3\dot{\phi}X^2G_{5XX} \\ &\quad + 4H^3\dot{\phi}X^3G_{5XXX} - 6H^2X (6G_{5\phi} + 9XG_{5\phi X} + 2X^2G_{5\phi XX}) \\ &= X \sum_{i=2}^5 \frac{\partial \mathcal{E}_i}{\partial X} + \frac{1}{2} \sum_{i=2}^5 \frac{\partial \mathcal{E}_i}{\partial H}, \end{aligned} \quad (4.5.10)$$

$$\begin{aligned} \Theta &:= -\dot{\phi}XG_{3X} + 2HG_4 - 8HXG_{4X} - 8HX^2G_{4XX} + \dot{\phi}G_{4\phi} + 2X\dot{\phi}G_{4\phi X} \\ &\quad - H^2\dot{\phi} (5XG_{5X} + 2X^2G_{5XX}) + 2HX (3G_{5\phi} + 2XG_{5\phi X}) \\ &= -\frac{1}{6} \sum_{i=2}^5 \frac{\partial \mathcal{E}_i}{\partial H}. \end{aligned} \quad (4.5.11)$$

The definition of  $\mathcal{E}_i$  ( $i = 2, 3, 4, 5$ ) is written in eq.(3.5.8). The propagation speed for tensor perturbations  $c_T$  and the scalar perturbation  $c_S$  are described as

$$c_T^2 = \frac{\mathcal{F}_T}{\mathcal{G}_T}, \quad (4.5.12)$$

$$c_S^2 = \frac{\mathcal{F}_S}{\mathcal{G}_S}. \quad (4.5.13)$$

## 4.6 Power spectrum

When we want to distinguish between the models of early universe, we discuss the observation of the cosmological perturbations. In this subsection, we discuss how we can see the perturbation from observation. First what we review is the power spectrum, which is very useful value for distinguishing between the models. When we calculate this, we need to solve the equation for perturbation and take the initial condition. Thus we will review the Bunch-Davies vacuum which is usually used [29].

### 4.6.1 Initial state

We can choose how define the initial state. Now we introduce Bunch-Davies vacuum There is an argument how we take the vacuum depends on the physical value. Now we assume



the action for the inflaton  $\phi$  as

$$\begin{aligned} S_\phi &= \frac{1}{2} \int \sqrt{-g} d^4x [-g^{\mu\nu} \phi_\alpha \phi_\beta - m^2 \phi^2] \\ &= \frac{1}{2} \int \sqrt{-g} d^4x [\dot{\phi}^2 + (\nabla\phi)^2 - m^2 \phi^2], \end{aligned} \quad (4.6.1)$$

for simplification, we introduce  $\chi$  as

$$\chi = a(\eta)\phi, \quad (4.6.2)$$

and thus the action eq.(4.6.1) can be rewritten for the action of  $\chi(\mathbf{x}, \eta)$  as

$$S_\chi = \frac{1}{2} \int d^3x d\eta \left[ \dot{\chi}^2 - (\nabla\chi)^2 - \left( m^2 a^2 - \frac{a''}{a} \right) \chi^2 \right]. \quad (4.6.3)$$

Using the Fourier transformation for  $\chi(\mathbf{x}, \eta)$

$$\chi(\mathbf{x}, \eta) = \int \frac{d^3\mathbf{k}}{(2\pi)^{\frac{3}{2}}} \chi_k(\eta) e^{i\mathbf{k}\cdot\mathbf{x}}, \quad (4.6.4)$$

we can obtain the equation for  $\chi_k(\eta)$

$$\chi_k'' + \omega_k^2(\eta) \chi_k = 0, \quad (4.6.5)$$

where  $\omega_k^2(\eta)$  is defined as

$$\omega_k^2(\eta) \equiv k^2 + m^2 a^2 - \frac{a''}{a}. \quad (4.6.6)$$

Introducing the canonically conjugate momentum  $\pi$

$$\pi \equiv \frac{\partial \mathcal{L}}{\partial v'} = v', \quad (4.6.7)$$

from eq.(4.6.3) by defining  $m_{eff}^2 = \left( m^2 a^2 - \frac{a''}{a} \right)$  we can find the Hamiltonian for  $\chi$

$$\mathcal{H}_\chi(\eta) = \frac{1}{2} \int d^3\mathbf{x} \left[ \pi^2 + (\nabla\chi)^2 + m_{eff}^2 \chi^2 \right], \quad (4.6.8)$$

and the commutation relation between  $\pi$  and  $\chi$  are

$$[\pi(\mathbf{x}, \eta), \pi(\mathbf{y}, \eta)] = [\chi(\mathbf{x}, \eta), \chi(\mathbf{y}, \eta)] = 0, \quad (4.6.9)$$

$$[\chi(\mathbf{x}, \eta), \pi(\mathbf{y}, \eta)] = i\delta(\mathbf{x} - \mathbf{y}). \quad (4.6.10)$$

The solution of  $\chi$  explaining by mode function  $v_k(\eta)$

$$\chi_k(\eta) = \frac{1}{\sqrt{2}} [a_k^- v_k^*(\eta) + a_{-k}^+ v_k(\eta)]. \quad (4.6.11)$$

$a_k^-$  and  $a_k^+$  are the operator,

$$a_k^- = \sqrt{2} \frac{W[v_k, \chi_k]}{W[v_k, v_k^*]}, \quad a_k^+ = (a_k^-), \quad (4.6.12)$$

where  $W$  is the Wronskian. Thus we have

$$\chi(\mathbf{x}, \eta) = \frac{1}{\sqrt{2}} \int \frac{d^3 \mathbf{k}}{(2\pi)^{\frac{3}{2}}} [e^{i\mathbf{k} \cdot \mathbf{x}} a_k^- v_k^* + e^{-i\mathbf{k} \cdot \mathbf{x}} a_{-k}^+ v_k]. \quad (4.6.13)$$

Applying the solution for eq.(4.6.8), we obtain

$$\begin{aligned} \mathcal{H}_\chi(\eta) = & \frac{1}{4} \int d^3 \mathbf{k} [a_k^- a_{-k}^- (v_k'^2 + \omega_k^2 v_k^2)^* + a_k^+ a_{-k}^+ (v_k'^2 + \omega_k^2 v_k^2) \\ & + (2a_k^+ a_k^- + \delta^3(0)) (|v_k'|^2 + \omega_k^2 |v_k|^2)]. \end{aligned} \quad (4.6.14)$$

Taking account of  $a_k^- |0\rangle = 0$ , the expectation is given as

$$\langle 0 | \mathcal{H}_\chi | 0 \rangle = \frac{1}{4} \int d^3 \mathbf{k} \delta^3(0) (|v_k'|^2 + \omega_k^2 |v_k|^2), \quad (4.6.15)$$

and thus

$$E = |v_k'|^2 + \omega_k^2 |v_k|^2. \quad (4.6.16)$$

where  $v_k', v_k$  and  $v_k^*, v_k^*$  have the relation

$$[v_k', v_k] = v_k' v_k^* - v_k v_k^{*'} = 2i, \quad (4.6.17)$$

Assuming  $v_k$  as

$$v_k = r_k e^{i\alpha}, \quad (4.6.18)$$

we have

$$r_k^2 \alpha_k' = 1. \quad (4.6.19)$$

Therefore, eq.(4.6.16) is explained as

$$E = \frac{1}{4} \left( r_k'^2 + \omega_k^2 r_k^2 + \frac{1}{r_k^2} \right). \quad (4.6.20)$$

If the energy is minimal, we obtain

$$r_k' = 0, \quad (4.6.21)$$

$$r_k = \omega_k^{-\frac{1}{2}}, \quad (4.6.22)$$

and thus  $v_k, v_k'$  and  $\alpha_k$  as the initial state of the perturbation

$$\begin{aligned} v_k &= \frac{1}{\sqrt{\omega_k}} e^{-i\alpha_k}, \\ v_k' &= i\sqrt{\omega_k} e^{-i\alpha_k}, \\ \alpha_k' &= \omega_k. \end{aligned} \quad (4.6.23)$$

In the following subsection, we use this initial state for scalar and tensor perturbations.

#### 4.6.2 Definition of power spectrum

Let us introduce the definition of the power spectrum, which is defined by the two-point correlation for the function at the vacuum state. Now we consider the wave function  $f(k)$  and the definition of the power spectrum is

$$\langle 0|f(k)f(k')|0 \rangle \equiv \frac{2\pi^2}{k^3} \delta^{(3)}(k+k') \mathcal{P}(k). \quad (4.6.24)$$

##### ▷ Scalar perturbation

We have reviewed the quadratic action for scalar and tensor perturbations and the initial condition for the perturbations. To calculate the power spectrum, we have to solve the equation for the perturbation. Now we consider the quadratic action for scalar perturbation which can be written as

$$S_\zeta^{(2)} = \int dt d^3x \left[ C_1 (-t)^{2p} \dot{\zeta}^2 - C_2 (-t)^{2q} (\vec{\nabla}\zeta)^2 \right], \quad (4.6.25)$$

where  $C_1$  and  $C_2$  are constant,  $p$  and  $q$  are the constant parameters. Then we take as a variable

$$-y := \frac{C_2^{1/2} (-t)^{1-p+q}}{C_1^{1/2} (1-p+q)}, \quad (4.6.26)$$

and we introduce  $u$  related to  $\zeta$  as

$$u := \sqrt{2}(C_1 C_2)^{1/4} (-t)^{(p+q)/2} \zeta, \quad (4.6.27)$$

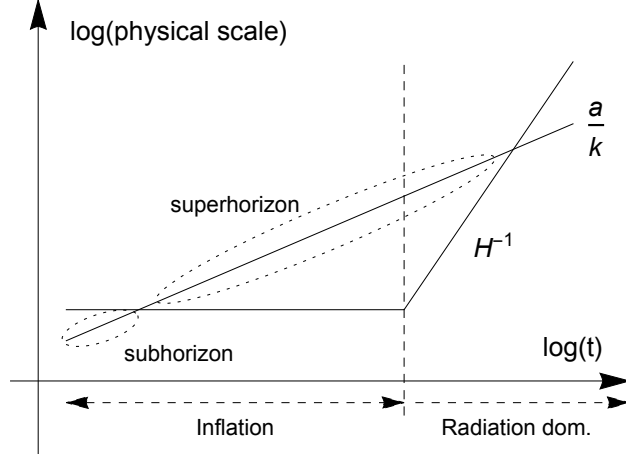


Figure 4.1: Schematic picture of the relation for the evolution of  $H^{-1}$  and  $a/k$ . We call  $H^{-1} \ll a/k$  superhorizon and  $a/k \ll H^{-1}$  subhorizon. On superhorizon scale, the perturbation do not perturb.

Thus we can find

$$S^{(2)} = \frac{1}{2} \int dy d^3x \left[ \left( \frac{\partial u}{\partial y} \right)^2 - (\vec{\nabla} u)^2 + \frac{\nu^2 - 1/4}{y^2} u^2 \right], \quad (4.6.28)$$

where

$$\nu := \frac{1 - 2p}{2(1 - p + q)}. \quad (4.6.29)$$

By using the Fourier transformation, the solution  $u$  is given as

$$u_k = \frac{\sqrt{\pi}}{2} \sqrt{-y} H_\nu^{(1)}(-ky). \quad (4.6.30)$$

As we can see from this formula or in fig.4.1, the behavior of wave depends on  $|ky|$ . Once the wavelength becomes larger than Hubble scale, the wave quit perturbation. Now we discuss the waves for early universe, thus we take the sub horizon limit  $|ky| \ll 1$ . The solution of  $\zeta$  is

$$\begin{aligned} |\zeta_k| &\simeq \frac{2^{|\nu|-3/2}}{\pi} \frac{\sqrt{\pi}}{(C_1 C_2)^{1/4}} \left[ (1 - p + q) \frac{C_1^{1/2}}{C_2^{1/2}} (-y) \right]^{\nu-1/2} k^{-|\nu|} (-y)^{1/2-|\nu|} \\ &\propto k^{-|\nu|} |y|^{\nu-|\nu|}. \end{aligned} \quad (4.6.31)$$

Therefore we obtain

$$\mathcal{P}_\zeta = \left[ \frac{2^{|\nu|-3/2}\Gamma(|\nu|)}{\Gamma(3/2)} \right]^2 \frac{k^{3-2|\nu|}}{8\pi^2} \frac{C_1^{\nu-1}}{C_2^\nu} (1-p+q)^{2\nu-1} |y|^{2(\nu-|\nu|)}. \quad (4.6.32)$$

▷ **Tensor perturbations**

For the tensor perturbations, we can calculate in the same way to the scalar perturbation. We assume the quadratic action for the tensor perturbations as

$$S_h^{(2)} = \frac{1}{8} \int dt d^3x \left[ C_1 (-t)^{2p} \dot{h}_{ij}^2 - C_2 (-t)^{2q} (\vec{\nabla} h_{ij})^2 \right], \quad (4.6.33)$$

and we obtain

$$\mathcal{P}_h = 16 \left[ \frac{2^{|\nu|-3/2}\Gamma(|\nu|)}{\Gamma(3/2)} \right]^2 \frac{k^{3-2|\nu|}}{8\pi^2} \frac{C_1^{\nu-1}}{C_2^\nu} (1-p+q)^{2\nu-1} |y|^{2(\nu-|\nu|)}. \quad (4.6.34)$$

▷ **G-inflation**

The power spectrum for scalar perturbation in generalized G-inflation [16] is given as follows. First, in the quadratic action of scalar perturbation eq.(4.5.7), we take

$$dy_S = \frac{c_S}{a} dt, \quad (4.6.35)$$

$$z_S = \sqrt{2} (\mathcal{F}_S \mathcal{G}_S)^{1/4}, \quad (4.6.36)$$

$$u = z_S \zeta. \quad (4.6.37)$$

The action becomes

$$S_S^{(2)} = \frac{1}{2} \int dy_S d^3x \left[ (u')^2 - (\vec{\nabla} u)^2 + \frac{z_S''}{z_S} u^2 \right], \quad (4.6.38)$$

where “'” is the derivative of  $y_S$ . On superhorizon scales, we have the solution

$$\zeta = C_1 + C_2 \int \frac{dt'}{a^3 \mathcal{G}_S}. \quad (4.6.39)$$

where  $C_1$  and  $C_2$  are constant and  $\mathcal{G}_S$  is the varying function. Now we define and assume

$$f_S \equiv \frac{\dot{\mathcal{F}}_S}{H \mathcal{F}_S} \simeq \text{const}, \quad (4.6.40)$$

$$g_S \equiv \frac{\dot{\mathcal{G}}_S}{H \mathcal{G}_S} \simeq \text{const}, \quad (4.6.41)$$

and we have

$$\mathcal{P}_s = \frac{\gamma_S \mathcal{G}_s^{1/2} H^2}{2 \mathcal{F}_s^{3/2} 4\pi^2} \Big|_{ky_S=1}, \quad (4.6.42)$$

where

$$\gamma_S = 2^{2\nu_S-3} \left| \frac{\Gamma(\nu_S)}{\Gamma(\frac{3}{2})} \right|^2 \left( 1 - \epsilon_H - \frac{f_S}{2} + \frac{g_S}{2} \right), \quad (4.6.43)$$

$$\nu_T \equiv \frac{3 - \epsilon_H + g_T}{2 - 2\epsilon_H - f_T + g_T}. \quad (4.6.44)$$

In the similar way to the scalar perturbation, we have the power spectrum for the tensor perturbations. From the quadratic action of tensor perturbations eq.(4.5.4), we obtain

$$\mathcal{P}_h = 8\gamma_T \frac{\mathcal{G}_T^{1/2} H^2}{\mathcal{F}_T^{3/2} 4\pi^2} \Big|_{ky_T=1}, \quad (4.6.45)$$

where

$$\gamma_T = 2^{2\nu_T-3} \left| \frac{\Gamma(\nu_T)}{\Gamma(\frac{3}{2})} \right|^2 \left( 1 - \epsilon_H - \frac{f_T}{2} + \frac{g_T}{2} \right), \quad (4.6.46)$$

$$\nu_T \equiv \frac{3 - \epsilon_H + g_T}{2 - 2\epsilon_H - f_T + g_T}, \quad (4.6.47)$$

$$f_T \equiv \frac{\dot{\mathcal{F}}_T}{H\mathcal{F}_T}, \quad g_T \equiv \frac{\dot{\mathcal{G}}_T}{H\mathcal{G}_T}, \quad (4.6.48)$$

$\gamma_S$  and  $\gamma_T$  are constant in inflationary phase, and they take  $\gamma_S, \gamma_T \simeq \mathcal{O}(1)$ .

### ▷ Inflation

In the slow-roll inflation, whose action is described by eq.(2.2.2) and eq.(2.2.3), the arbitrary functions in Horndeski theory are written as

$$G_2(\phi, X) = -\frac{1}{2}g^{\mu\nu}\partial_\mu\phi\partial_\nu\phi + V(\phi) = X + V(\phi), \quad (4.6.49)$$

$$G_3(\phi, X) = 0, \quad (4.6.50)$$

$$G_4(\phi, X) = \frac{1}{16\pi G}, \quad (4.6.51)$$

$$G_5(\phi, X) = 0. \quad (4.6.52)$$

Substituting these functions into the definitions in Horndeski theory, we obtain

$$\mathcal{G}_T = \frac{1}{8\pi G}, \quad \mathcal{F}_T = \frac{1}{8\pi G}, \quad (4.6.53)$$

$$\mathcal{G}_S = \frac{\dot{\phi}^2}{2H^2}, \quad \mathcal{F}_S = \frac{\epsilon_H}{8\pi G}. \quad (4.6.54)$$

and thus

$$g_T = 0, \quad f_T = 0, \quad (4.6.55)$$

$$g_S = 2(\epsilon_H - \eta_H), \quad f_S = 2(\epsilon_H - \eta_H), \quad (4.6.56)$$

As the slow-roll parameters are much smaller than 1 during inflation, we find  $g_S, f_S \simeq 0$  and  $\nu_S, \nu_T \simeq \frac{3}{2}$ . Therefore, in inflation, we can find the power spectrum for scalar and tensor perturbations as

$$\mathcal{P}_s = \frac{16GH_{inf}^2}{\pi^2}, \quad (4.6.57)$$

$$\mathcal{P}_h = \frac{H_{inf}^4}{4\pi^2\dot{\phi}^2}. \quad (4.6.58)$$





## Chapter 5

# Some topics in Modern Cosmology

Above all, we have discussed the standard inflationary scenario and modified gravity theories. After this section, we will discuss the alternative to inflation scenario called Galilean genesis. To compare the scenarios, we discuss some relevant topics in inflation.

### 5.1 Curvaton field

In some cases, we consider the power spectrum is explained by curvaton field  $\chi$  [30]. In this section, we review basic information for the curvaton. As the mass of curvaton is lighter than that of inflaton, Inflation does not contribute to making the power spectrum due to the curvaton field lives longer than the inflaton. Let us consider this mechanism. Definition of the curvature perturbation is written as

$$\zeta \equiv -\psi - \frac{H}{\dot{\rho}} \delta\rho. \quad (5.1.1)$$

If there exists some kind of fields, the total curvature perturbation  $\zeta_{tot}$  is written as

$$\zeta_{tot} \equiv \sum \frac{\dot{\rho}_i}{\dot{\rho}} \zeta_i, \quad (5.1.2)$$

where  $\zeta_i$  is given as

$$\zeta_i \equiv -\psi - \frac{H}{\dot{\rho}_i} \delta\rho_i. \quad (5.1.3)$$

Note that the definition of  $\zeta$  in this section is in the gauge of  $\delta\rho = 0$ . In part 2, we use  $\delta\phi = 0$ . Now we consider inflaton and curvaton. As inflaton changes to radiation before curvaton decay,  $\zeta_{tot}$  can be written as

$$\zeta_{tot} = \frac{4\rho_r \zeta_r + 3\rho_\chi \zeta_\chi}{4\rho_r + 3\rho_\chi}, \quad (5.1.4)$$

where  $\chi$  behaves as the matter, thus the energy density of each field are

$$\rho_r \propto a^{-4}, \quad (5.1.5)$$

$$\rho_\chi \propto a^{-3}, \quad (5.1.6)$$

where we assume that the scalar field behaves as a matter, and thus we take  $w = 0$  for  $\chi$ . Eq.(5.1.4) suggests that the rate of the energy density determines  $\zeta_{tot}$ , and the energy density of radiation decays faster than that of curvaton. Therefore, we can find the curvature perturbation is made from curvaton, and  $\zeta_{tot}$  can be described as

$$\zeta_{tot} \simeq \zeta_\chi. \quad (5.1.7)$$

## 5.2 Reheating of the universe

It is considered the temperature of the universe once grows at the phase transition from inflation to radiation dominant phase. As we usually consider the universe was started from the high energy state, we call this reheating. (The scenario of Galilean Genesis we discuss in chap.2 suggests the low energy initial state.) Various mechanisms are explaining how reheating was caused. We introduce two ways to reheat the universe, from oscillating of the inflaton and energy transformation by gravitation.

We assume the matter generated during reheating phase as  $\chi$ . The Lagrangian of the matter is written as

$$\mathcal{L} = -\frac{1}{2}g^{\mu\nu}\partial_\mu\chi\partial_\nu\chi - \frac{1}{2}m^2X^2, \quad (5.2.1)$$

where  $m$  is the mass of the matter. By deriving the equation for  $\chi$ , using the Fourier transformation, and define  $X$  as

$$\chi_k(\eta) = e^{-\frac{3}{2}\int H d\eta} X(\eta), \quad (5.2.2)$$

we obtain

$$\ddot{X}_k + \omega^2 X_k = 0, \quad (5.2.3)$$

where  $\omega$  is defined as

$$\omega^2 = \frac{k^2}{a^2} + m^2 - \frac{3}{2}\dot{H} - \frac{9}{4}H^2. \quad (5.2.4)$$

### 5.2.1 Reheating from oscillating inflaton

Let us consider the decay of inflaton. We usually assume the scenario that inflaton oscillates on the bottom of its potential and decays with the rate  $\Gamma_\phi$ . In this case, the equations

for the energy density are written as

$$\frac{d\rho_\phi}{dt} + 3H\rho_\phi = -\Gamma_\phi\rho_\phi, \quad (5.2.5)$$

$$\frac{d\rho_r}{dt} + 4H\rho_r = \Gamma_\phi\rho_\phi. \quad (5.2.6)$$

Solving these equations gives us

$$\rho_\phi(t) = \rho_\phi(t_*) \left(\frac{a_*}{a}\right)^3 e^{-\Gamma_\phi(t_*-t)}, \quad (5.2.7)$$

$$\rho_r(t) = \frac{\Gamma_\phi}{a^4(t)} \int_t^{t_*} a^4(t') \rho_\phi dt, \quad (5.2.8)$$

where  $t = t_*$  is the end of inflation. From the relation between energy density  $\rho$  and reheating temperature  $T_R$ ,

$$\rho = \frac{\pi^2}{30} g_* T_R^4, \quad (5.2.9)$$

where  $g_*$  is the effective number of relativistic species of particles, we can find the reheating temperature. Moreover, by using Friedmann equation, the temperature can be shown by Hubble parameter.

### 5.2.2 Bogolybov coefficients

Recalling the action eq.(4.6.1), we have chosen the mode function  $v_k$  and the operators  $\hat{a}_k^\pm$ . However, we can select the different function and operators. Let us consider the function  $u_k$  which satisfies eq.(5.2.3) given as

$$u_k = \alpha_k v_k(\eta) + \beta_k v_k^*(\eta). \quad (5.2.10)$$

This mode function  $u_k$  also satisfy the normalization condition eq.(4.6.17), and thus the relation between  $\alpha$  and  $\beta$  is

$$|\alpha|^2 - |\beta|^2 = 1. \quad (5.2.11)$$

Introducing the operator  $\hat{b}_k^\pm$  corresponding to the mode function  $u_k$  which is described as

$$\begin{aligned} \chi_k(\eta) &= \frac{1}{\sqrt{2}} [a_k^- v_k^*(\eta) + a_{-k}^+ v_k(\eta)] \\ &= \frac{1}{\sqrt{2}} [b_k^- u_k^*(\eta) + b_{-k}^+ u_k(\eta)] \quad , \end{aligned} \quad (5.2.12)$$

we find the relations between the operators  $\hat{a}_k^\pm$  and  $\hat{b}_k^\pm$

$$\begin{aligned}\hat{a}_k^+ &= \alpha_k \hat{b}_k^+ + \beta_k^* \hat{b}_{-k}^-, \\ \hat{a}_k^- &= \alpha_k^* \hat{b}_k^- + \beta_k \hat{b}_{-k}^+, \\ \hat{b}_k^+ &= \alpha_k \hat{a}_k^+ - \beta_k^* \hat{a}_{-k}^-, \\ \hat{b}_k^- &= \alpha_k^* \hat{a}_k^- - \beta_k \hat{a}_{-k}^+.\end{aligned}\tag{5.2.13}$$

These are called Bogolybov transformation and  $\alpha$  and  $\beta$  are called the Bogolybov coefficients, and we can obtain the coefficients is given from the relations as

$$\alpha_k = \frac{W(u_k, v_k^*)}{2i},\tag{5.2.14}$$

$$\beta_k = \frac{W(v_k), u_k}{2i},\tag{5.2.15}$$

where the function  $W$  is the Wronskian. Using this transformation gives us the information of the density for the state of  $b$ . Taking  $\langle 0|$  and  $|0\rangle$  as the vacuum state for  $b$  and  $N_k = \hat{a}_k^+ \hat{a}_k^-$  as the number operator. The particle number is

$$\begin{aligned}\langle 0|N_k|0\rangle &= \langle 0|\hat{a}_k^+ \hat{a}_k^-|0\rangle \\ &= \langle 0|(\alpha_k \hat{b}_k^+ + \beta_k^* \hat{b}_{-k}^-)(\alpha_k^* \hat{b}_k^- + \beta_k \hat{b}_{-k}^+)|0\rangle \\ &= \langle 0|(\beta_k^* \hat{b}_{-k}^-)(\beta_k \hat{b}_{-k}^+)|0\rangle \\ &= |\beta_k|^2 \delta^3(0).\end{aligned}\tag{5.2.16}$$

Therefore we obtain the particle number for wave number  $k$  as

$$n_k = |\beta_k|^2.\tag{5.2.17}$$

Then we can obtain the energy density

$$\rho = \frac{1}{2\pi a^4} \int n_k k^3 dk.\tag{5.2.18}$$

and the temperature from eq.(5.2.9).

### 5.2.3 Gravitational reheating

For the phase transition from inflation to the next phase, we can consider another scenario. In one case, the oscillation of inflaton on the bottom of its potential generates the matter we discussed the last subsection. In the other case, the energy transition generates the matter. In genesis model, we discuss reheating phase caused in the latter case. Let us consider the gravitational reheating in inflation discussed in [31]. This subsection is the

review of [29]. Assuming the Bogolybov coefficients as the function of  $\eta$ , we can show the solution of eq.(4.6.11)

$$X_k(\eta) = \frac{\alpha(\eta)}{\sqrt{2k}} e^{-ik\eta} + \frac{\beta(\eta)}{\sqrt{2k}} e^{ik\eta}, \quad (5.2.19)$$

and applying this into eq.(5.2.3) the equations for  $\alpha$ ,  $\beta$  is shown as

$$\beta'' + 2ik\beta' - \frac{a''}{a}\beta = 0, \quad (5.2.20)$$

$$\alpha'' - 2ik\alpha' - \frac{a''}{a}\alpha = 0. \quad (5.2.21)$$

Then we can find its solution

$$\beta(\eta) = -\frac{i}{2k} \int_{-\infty}^{\infty} e^{2ik\eta} V(\eta) d\eta. \quad (5.2.22)$$

The particle number  $n_k$  and the energy density  $\rho_k$  for generated matter  $\chi$  is written by the coefficients  $\beta$  as

$$n_k = \frac{1}{2\pi^2 a^3} \int_{-\infty}^{\infty} |\beta_k|^2 k^3 dk, \quad (5.2.23)$$

$$\rho_k = \frac{1}{2\pi^2 a^4} \int_{-\infty}^{\infty} |\beta_k|^2 k^3 dk, \quad (5.2.24)$$

and thus the total energy density is given as

$$\rho = -\frac{1}{128\pi^2 a^4} \int_{-\infty}^{\infty} d\eta_1 \int_{-\infty}^{\infty} d\eta_2 \ln(m|\eta_1 - \eta_2|) V'(\eta_1) V'(\eta_2), \quad (5.2.25)$$

and we inserted some arbitrary mass scale  $m$  in  $\ln$  for a dimensional reason, though  $\rho_\chi$  will be dependent only logarithmically on  $m$ . The definition of  $V(\eta)$  in eq.(5.2.25) is

$$V(x) = \frac{f''f - (f')^2}{f^2}, \quad f(\eta) \equiv a^2(\eta), \quad (5.2.26)$$

where  $x = H_{\text{inf}}\eta$ . This shows us the time derivative of  $V(\eta)$  generated the created matter. Now we consider the phase transition from inflation to the radiation dominant phase as an example. The function  $V(x)$  is related to the time derivative of Hubble parameter. Whenever  $f(x)$  in (5.2.26) does not have the formula, we can calculate  $\rho$  with assuming the function as follows

$$f(x) = \begin{cases} \frac{1}{x^2}, & (x < x_0) \\ c_0 + c_1x + c_2x^2 + c_3x^3, & (x_0 < x < x_1) \\ d_0(x + d_1) & (x_1 < x), \end{cases} \quad (5.2.27)$$

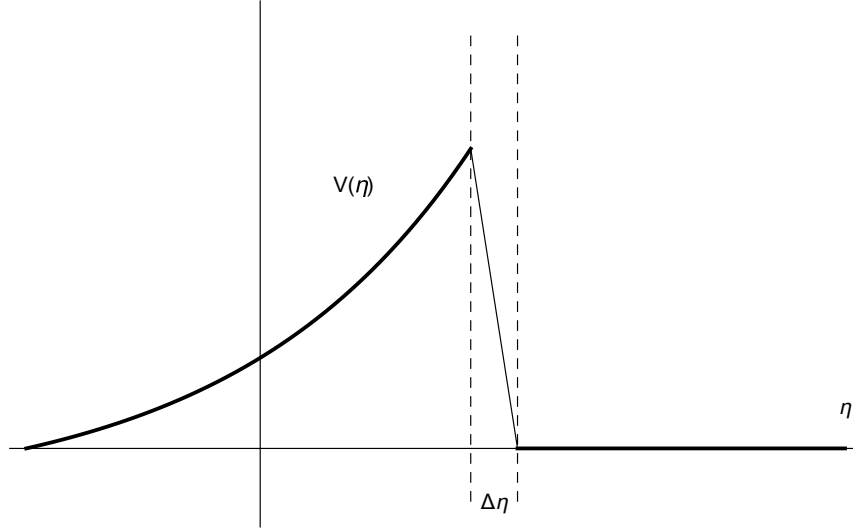


Figure 5.1: The schematic picture of the evolution of Hubble parameter during the phase transition from inflationary phase to radiation dominant phase.  $\Delta\eta$  which we assume very short is the phase transition era.

where  $x_0$  is the end of inflation and  $x_1$  is the beginning of the radiation dominant phase. Finding each coefficients in eq.(5.2.27), we can find the function  $V(\eta)$ . This method is available when  $\Delta\eta$  is very small, and  $V$  during  $\Delta\eta$  is approximately a line like fig.(5.1). Therefore in eq.(5.2.25), we can find  $\rho$  by calculating during only  $\Delta\eta$ , and we obtain the reheating temperature from eq.(5.2.9).

### 5.3 Alternative scenarios to inflation

In the later section, we discuss one of the alternative scenarios to inflation. There are many models which explain the behave of early universe, thus in this section, we review the feature of alternative scenarios and some scenarios such as bouncing cosmology and string gas cosmology.

#### 5.3.1 Null energy condition

In the study of the model of the early universe, we have to discuss some stability conditions. The null energy condition (NEC) is one of that stability. This condition appears in the basic field equation, and let us derive it. The review of this topic is written in [32]. The

NEC is given by

$$T_{\mu\nu}k^\alpha k^\beta > 0, \quad (5.3.1)$$

where  $T_{\mu\nu}$  is the energy momentum tensor and  $k^\alpha$  is the null vector. The component of the energy momentum tensor is shown in eq.(1.4.3), and thus

$$\rho + p > 0, \quad (5.3.2)$$

Let us applying this condition into the cosmological context. The Friedmann equation and evolution equation gives

$$\dot{H} = -4\pi G(\rho + p). \quad (5.3.3)$$

Thus when NEC is violated, Hubble parameter satisfy

$$\dot{H} > 0. \quad (5.3.4)$$

In the cosmological context, we call the null energy condition as this equation. Let us see some examples of this condition. In standard inflationary scenario, we can obtain

$$\rho + p = \dot{\phi}^2 > 0, \quad (5.3.5)$$

and this says NEC is satisfied. In the K-inflation scenario, NEC is violated if

$$\rho + p = 2XK_X < 0. \quad (5.3.6)$$

In alternative scenarios of early universe, it is known that NEC is violated without generating instabilities.

### 5.3.2 Bouncing cosmology

In inflationary model, we have reviewed the scale factor always grows, and it may have the singularity. To avoid this problem, we can consider the scale factor grows after contraction as we can see in fig.5.2. Such scenarios are called bouncing scenario, and there are many models of the bouncing universe (see the review [33, 34]). The feature of this scenario is the Hubble parameter takes  $H = 0$  at the turning point in bouncing phase. As an example. let us see the models of the two field matter bouncing universe [35]. In this model, we consider two scalar fields, and the action is given like

$$\mathcal{L} = K(\phi, X) - G(\phi, X)\square\phi + P(\psi, Y), \quad (5.3.7)$$

$$Y = -\frac{1}{2}g^{\mu\nu}\partial_\mu\psi\partial_\nu\psi, \quad (5.3.8)$$

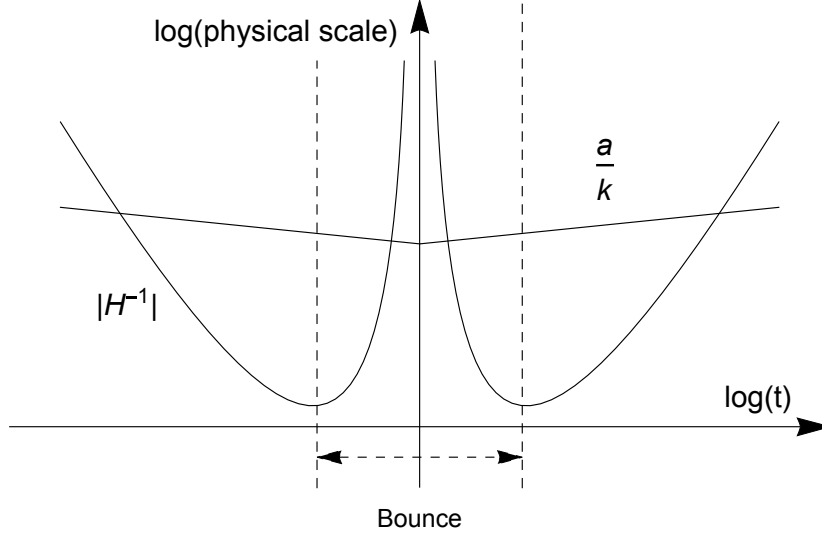


Figure 5.2: The schematic picture in the bouncing scenario.

where

$$K(\phi, X) = M_{\text{Pl}}[1 - g(\phi)]X + \beta X^2 - V(\phi) \quad (5.3.9)$$

$$G(\phi, X) = \gamma X, \quad (5.3.10)$$

where  $P(\psi, Y)$  is the function of the scalar field  $\psi$  and its kinetic term,  $V(\phi)$  is the potential of the scalar field  $\phi$ , and  $\beta, \gamma$  are the positive constant parameters.

$$g(\phi) = \frac{2g_0}{e^{-\sqrt{2/p}\phi} + e^{b_g\sqrt{2/q}\phi}}, \quad (5.3.11)$$

$$V(\phi) = -\frac{2V_0}{e^{-\sqrt{2/p}\phi} + e^{b_v\sqrt{2/q}\phi}}, \quad (5.3.12)$$

where  $b_g, b_v$  are the constants. In  $-\sqrt{p/2}\ln(2g_0) < \phi < \sqrt{p/2}\ln(2g_0)/b_g$ , we can obtain the solutions of the bouncing phase as

$$H \sim \Upsilon t, \quad (5.3.13)$$

$$a(t) \sim a_B e^{\frac{1}{2}\Upsilon t^2}, \quad (5.3.14)$$

where  $a_B$  is the scale factor at the beginning of the bouncing phase.

### 5.3.3 Galilean genesis

The Galilean genesis is proposed by P. Creminelli, A. Nicolis and E. Trincherini [1]. The schematic picture of this scenario is described in fig.5.3. Now let us review the original



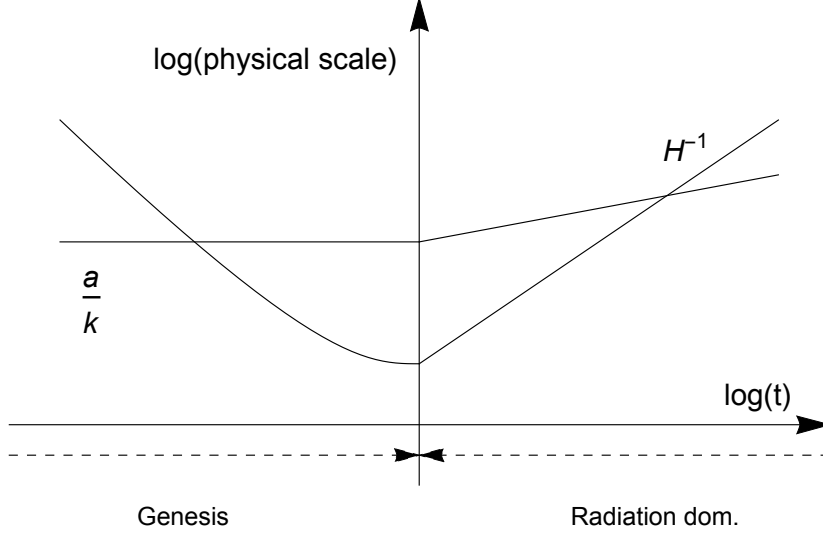


Figure 5.3: The schematic picture in the genesis scenario.

model of Galilean genesis constructed by using the Lagrangian of the form [1, 36]

$$\mathcal{L} = \frac{1}{16\pi G}R + 2f^2\lambda^2 e^{2\lambda\phi} X + \frac{2f^3\lambda^4}{\Lambda^3} X^2 + \frac{2f^3\lambda^3}{\Lambda^3} X \square\phi, \quad (5.3.15)$$

where  $f$ ,  $\lambda$  and  $\Lambda$  are constants. For this Lagrangian at  $t \rightarrow -\infty$ , we consider the Hubble parameter takes  $H \rightarrow 0$  and  $e^{\lambda\phi}$  behaves like the de-Sitter solution as

$$e^{\lambda\phi} = -\frac{1}{H_0 t}, \quad (5.3.16)$$

$$H_0 = \frac{2\Lambda^3}{3f}. \quad (5.3.17)$$

Then, we obtain the energy density and the pressure from the Lagrangian,

$$\begin{aligned} \rho &= -f^2\lambda^2 \left[ e^{2\lambda\phi} \dot{\phi}^2 - \frac{1}{H_0^2} (\lambda^2 \dot{\phi}^4 + 4\lambda H \dot{\phi}^3) \right] \\ &\simeq -f^2\lambda^2 \left[ e^{2\lambda\phi} \dot{\phi}^2 - \frac{1}{H_0^2} \lambda^2 \dot{\phi}^4 \right], \end{aligned} \quad (5.3.18)$$

$$p = -f^2\lambda^2 \left[ e^{2\lambda\phi} \dot{\phi}^2 - \frac{1}{3H_0^2} (\lambda^2 \dot{\phi}^4 - \frac{4\lambda}{3} \partial_t \dot{\phi}^3) \right]. \quad (5.3.19)$$

We can confirm NEC is violated in genesis solution by applying eq.(5.3.16) to  $\rho$  and  $p$ . Recalling the Friedmann equation eq.(2.0.2), we find neglecting the terms of  $H$  in  $\rho$  leads

$p \gg \rho$ . Thus,  $\dot{H}$  is described as

$$\dot{H} \simeq -4\pi G p, \quad (5.3.20)$$

and thus we obtain

$$H(t) \simeq \frac{8\pi G f^2}{3} \frac{1}{H_0^2 (-t)^3} \quad (-\infty < t < 0), \quad (5.3.21)$$

$$a(t) \simeq a_0 \left[ 1 + \frac{4\pi G f^2}{3} \frac{1}{H_0^2 (-t)^2} \right], \quad (5.3.22)$$

where we take  $a(t)|_{t \rightarrow -\infty} = a_0$ . The solution of the scale factor describes the universe that starts expanding from singularity-free Minkowski in the asymptotic past. The same genesis solution can also be obtained from the DBI conformal galileons [37, 38]. There is the other scenario in which the evolution of scale factor starts from  $a(t) \simeq \text{const.}$ . The string gas cosmology motivated by superstring theory was investigated by Robert Brandenberger [39] also suggests the universe started from Minkowski space-time.

In this way, there are some alternative scenarios which can avoid the singularity. If these scenarios do not have the other theoretical problems, how can we distinguish between the models of the early universe? As the tool for distinction, we can see the difference in the spectrum of perturbations. Especially, in chapter 2, we focus on the gravitational waves. We have discussed the spectrum of gravitational waves in inflation is approximately flat, however, it is known that the spectrum of alternative scenarios is blue.

The discovery of detect of gravitational waves may be fresh in our mind, however, it takes more time to obtain the information of primordial universe. In chapter 2, let us discuss the distinction of the spectrum of gravitational waves with looking forward the success of detecting the information in the future. The main topic of chapter 2 is the growth of the gravitational waves and extending the model for generating various spectrum, so we will conclude these discussions at the conclusions.

**Part II**

**Galilean Genesis**



## Chapter 6

# Generalized Galilean genesis

It is fair to say that inflation [40, 7, 41] followed by a hot Big Bang is a standard scenario of modern cosmology. Inflation is attractive because the period of quasi-de Sitter expansion in the early universe resolves several problems that would otherwise indicate the need for fine-tuning. Moreover, curvature perturbations are naturally generated from quantum fluctuations during inflation, which seed large-scale structure of the universe [42]. The basic prediction of inflation is that the primordial curvature perturbations are nearly scale-invariant, adiabatic, and Gaussian. This is in agreement with observations of CMB anisotropies [43, 44, 45]. Inflationary models also predict the quantum mechanical production of gravitational waves [40], the detection of which would be the evidence for inflation.

Despite the success of inflation, it would be reasonable to ask whether only inflation can be a consistent scenario compatible with observations. It should also be noted that an inflationary universe is past geodesically incomplete [46] and so the problem of an initial singularity still persists. From this viewpoint, various alternative scenarios have been proposed so far, such as bouncing models. Although such models can eliminate the initial singularity, many of them are unfortunately plagued by instabilities originated from the violation of the null energy condition (NEC), the growth of shear, and primordial perturbations incompatible with observations [47].

In the context of cosmology, the violation of the NEC implies that

$$\frac{dH}{dt} > 0, \tag{6.0.1}$$

where  $H$  is the Hubble rate and  $t$  is cosmic time. This signals ghost instabilities in general relativity. Recently, however, it was noticed that in noncanonical galileon-type scalar-field theories the NEC can be violated *stably*,<sup>1</sup> and based on this idea, Creminelli *et al.* proposed a novel, stable alternative to inflation named galilean genesis [1]. (See also

---

<sup>1</sup>The NEC can be violated stably at least within linear perturbation analysis. However, at nonlinear order, it is not clear whether there are no instabilities [48].

Ref. [49].) In the galilean genesis scenario, the universe is asymptotically Minkowski in the past and starts expanding from this low energy state. As such, this scenario is devoid of the horizon and flatness problems. Aspects of galilean genesis have been studied in Refs. [50, 51, 52, 53, 54] and the original model has been extended in Refs. [36, 37, 38] to possess improved properties. See also Refs. [22, 15, 55, 56, 57, 58, 59, 60, 61] for other interesting NEC violating cosmologies in galileon-type theories and Ref. [32] for a related review.

In this chapter, we introduce a unified treatment of the galilean genesis models and give a generic Lagrangian admitting the genesis solutions. This is done by using the Horndeski theory [17], which is the most general scalar-tensor theory with second-order field equations. Our generalized galilean genesis (GGG) Lagrangian contains four functional degrees of freedom and a constant parameter denoted  $\alpha$ . This parameter determines the behavior of the Hubble rate. For specific choices of those functions and  $\alpha = 1$ , our Lagrangian reproduces the previous models explored in Refs. [1, 36, 37, 38]. As is often the case with inflation alternatives, it turns out that the galilean genesis models in general fail to produce nearly scale-invariant curvature perturbations. We show, however, that with an appropriate tuning of  $\alpha$  it is possible to have a slightly tilted spectrum consistent with observations.

## 6.1 Generalized genesis solutions

In Ref. [62] it was noticed that the genesis solution (5.3.21) is obtained generically in the subclass of the Horndeski theory with

$$\begin{aligned} G_2 &= e^{4\lambda\phi} g_2(Y), & G_3 &= e^{2\lambda\phi} g_3(Y), \\ G_4 &= \frac{M_{\text{Pl}}^2}{2} + e^{2\lambda\phi} g_4(Y), & G_5 &= e^{-2\lambda\phi} g_5(Y), \end{aligned} \quad (6.1.1)$$

where each  $g_i$  ( $i = 2, 3, 4, 5$ ) is an arbitrary function of

$$Y := e^{-2\lambda\phi} X. \quad (6.1.2)$$

This extends the Lagrangian given in Ref. [52] to include the Horndeski functions  $G_4$  and  $G_5$ . The Lagrangian (5.3.15) and the DBI conformal galileon theory are included in the general framework defined by (6.1.1) as specific cases.

In this chapter, we further generalize (6.1.1) and consider

$$\begin{aligned} G_2 &= e^{2(\alpha+1)\lambda\phi} g_2(Y), & G_3 &= e^{2\alpha\lambda\phi} g_3(Y), \\ G_4 &= \frac{M_{\text{Pl}}^2}{2} + e^{2\alpha\lambda\phi} g_4(Y), & G_5 &= e^{-2\lambda\phi} g_5(Y), \end{aligned} \quad (6.1.3)$$

where  $\alpha$  ( $> 0$ ) is a new dimensionless parameter. The four functions,  $g_2$ ,  $g_3$ ,  $g_4$ , and  $g_5$ , are arbitrary as long as several conditions presented in this section and in Sec. 6.3 are

satisfied. We assume, however, that  $g_4(0) = 0$ , so that  $G_4 \rightarrow M_{\text{Pl}}^2/2$  as  $Y \rightarrow 0$ . The Horndeski theory with (6.1.3) admits the following *generalized galilean genesis* solution:

$$e^{\lambda\phi} \simeq \frac{1}{\lambda\sqrt{2Y_0}} \frac{1}{(-t)}, \quad H \simeq \frac{h_0}{(-t)^{2\alpha+1}} \quad (-\infty < t < 0), \quad (6.1.4)$$

for large  $|t|$ , where  $Y_0$  and  $h_0$  are positive constants. We see that  $Y \simeq Y_0$  for this background. The parameter  $\alpha$  in the Lagrangian results in controlling the evolution of the Hubble rate. The scale factor is given by

$$a \simeq 1 + \frac{1}{2\alpha} \frac{h_0}{(-t)^{2\alpha}}, \quad (6.1.5)$$

and hence the solution describes the universe that starts expanding from Minkowski in the asymptotic past, similarly to the original galilean genesis solution which corresponds to the case of  $\alpha = 1$ . The “slow-expansion” model considered in Ref. [63] is reproduced by taking the particular functions  $g_i$  with  $\alpha = 2$ . We thus obtain a one-parameter family of the generalized genesis solutions as an alternative to inflation. Note that, although the evolution of the scale factor is very different from quasi-de Sitter, the universe in this scenario is also *accelerating*:  $\partial_t(aH) > 0$ , and hence fluctuation modes will leave the horizon during the genesis phase.

Substituting Eq. (8.1.10) to the background equations (3.5.4)–(3.5.13) and picking up the dominant terms at large  $|t|$ , we have

$$\mathcal{E} \simeq e^{2(\alpha+1)\lambda\phi} \hat{\rho}(Y_0) \simeq 0, \quad (6.1.6)$$

$$\mathcal{P} \simeq 2\mathcal{G}(Y_0)\dot{H} + e^{2(\alpha+1)\lambda\phi} \hat{\rho}(Y_0) \simeq 0, \quad (6.1.7)$$

where

$$\hat{\rho}(Y) := 2Y g_2' - g_2 - 4\lambda Y (\alpha g_3 - Y g_3'), \quad (6.1.8)$$

$$\hat{\rho}(Y) := g_2 - 4\alpha\lambda Y g_3 + 8(2\alpha + 1)\lambda^2 Y (\alpha g_4 - Y g_4'), \quad (6.1.9)$$

$$\mathcal{G}(Y) := M_{\text{Pl}}^2 - 4\lambda Y (g_5 + Y g_5'), \quad (6.1.10)$$

an overdot stands for differentiation with respect to  $t$ , and a prime for differentiation with respect to  $Y$ . The constant  $Y_0$  is determined as a root of

$$\hat{\rho}(Y_0) = 0, \quad (6.1.11)$$

and then  $h_0$  is determined from Eq. (8.1.13) as

$$h_0 = -\frac{1}{2(2\alpha + 1)(2\lambda^2 Y_0)^{\alpha+1}} \frac{\hat{\rho}(Y_0)}{\mathcal{G}(Y_0)}. \quad (6.1.12)$$

As will be seen shortly, this background is stable for  $\mathcal{G}(Y_0) > 0$ . Therefore, the above NEC violating solution is possible provided that

$$\hat{p}(Y_0) < 0. \quad (6.1.13)$$

As will be demonstrated in the next section, the generalized genesis solution will develop a singularity  $H \rightarrow \infty$  at some  $t = t_{\text{sing}}$ , as in the original genesis model. We therefore assume that the genesis phase is matched onto the standard radiation-dominated universe before  $t = t_{\text{sing}}$ , ignoring for the moment the detail of the reheating process. In conventional general relativity, matching two different phases can be done by imposing that the Hubble parameter is continuous across the two phases. However, the matching conditions are modified in general scalar-tensor theories as second-derivatives of the metric and the scalar field are mixed in the field equations. The modified matching condition [62] reads

$$\begin{aligned} M_{\text{Pl}}^2 H_{\text{rad}} &= \mathcal{G}(Y_0)H - \frac{e^{(2\alpha+1)\lambda\phi}}{2} \int_0^{Y_0} \sqrt{2y} g_3'(y) dy \\ &\quad + 2\lambda\dot{\phi}e^{2\alpha\lambda\phi} (\alpha g_4 - Y_0 g_4'), \end{aligned} \quad (6.1.14)$$

and we require that the subsequent radiation-dominated universe is expanding:  $H_{\text{rad}} > 0$ . This condition translates to

$$-g_2 - 2\lambda Y_0 g_3 + (2\alpha + 1)\lambda\sqrt{Y_0} \int_0^{Y_0} \frac{g_3}{\sqrt{y}} dy > 0. \quad (6.1.15)$$

It is easy to see that in the case of  $\alpha = 1$  all the expressions presented above reproduce the previous results [62].

Before closing this section, let us emphasize that (generalized) galilean genesis has the Minkowski phase only in the asymptotic past. The true Minkowski spacetime solution corresponds to the special case of  $Y = 0$ , i.e.,  $\phi = \text{const}$ . The  $Y = 0$  solution is found only if  $g_2(0) = 0$ . One may wonder if the true Minkowski vacuum ( $Y = 0$ ) in our neighborhood begins to expand to form a genesis universe ( $Y = Y_0 > 0$ ). This is forbidden because the two different stable solutions cannot be interpolated, as argued in Ref. [52]. (See, however, Ref. [53].)

## 6.2 Background evolution

To see whether or not the generalized genesis solution presented in the previous section is an attractor, we trace the background evolution starting from generic initial conditions.

### 6.2.1 Analytic argument

Let us begin with a simplified discussion neglecting gravity, i.e., the effect of the cosmic expansion [52]. It is convenient to introduce a new variable

$$\psi := e^{-\lambda\phi} (> 0). \quad (6.2.1)$$



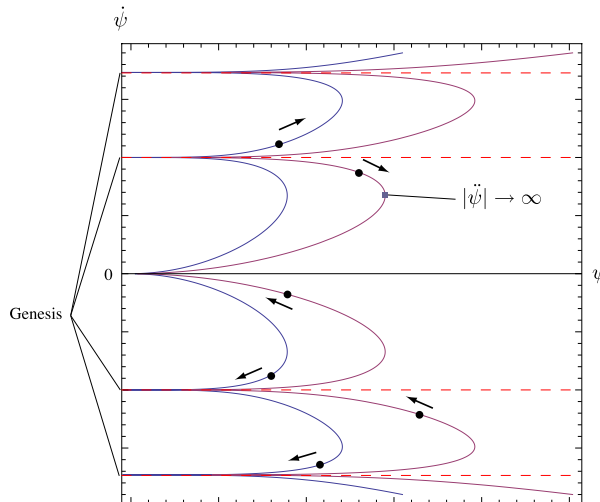


Figure 6.1: Examples of the curves defined by Eq. (6.2.3). Horizontal dashed lines correspond to the genesis solutions.

In terms of  $\psi$  we have  $Y = \dot{\psi}^2/(2\lambda^2)$ . For any homogeneous solutions the scalar-field equation of motion (3.5.14) with the functions (6.1.3) can be written as

$$\frac{d}{dt} \left[ \psi^{-2(\alpha+1)} \hat{\rho}(Y) \right] = 0. \quad (6.2.2)$$

Integrating this, we obtain

$$\hat{\rho}(Y) = C\psi^{2(\alpha+1)}, \quad (6.2.3)$$

where  $C$  is an integration constant. Equation (6.2.3) defines a curve in the  $(\psi, \dot{\psi})$  space for each  $C$ , as shown in Fig. 6.1. With an initial condition  $(\psi_i, \dot{\psi}_i)$  away from the genesis solution, the integration constant is determined as  $C = \dot{\psi}_i^{-2(\alpha+1)} \hat{\rho}(\dot{\psi}_i^2/2\lambda^2)$ . If  $\dot{\psi} < 0$  initially, the scalar field rolls along the curve toward  $\psi \rightarrow 0$ , i.e.,  $\hat{\rho} \rightarrow 0$ . Hence, this solution approach to one of the genesis solutions which are denoted as horizontal lines ( $\dot{\psi} = \text{const}$ ) in the  $(\psi, \dot{\psi})$  plane. If  $\dot{\psi} > 0$  initially, the scalar field rolls the opposite way along the curve and goes further away from the genesis solutions. This is the time reversal of the  $\dot{\psi} < 0$  solutions.

The above analytic argument implies that the genesis solution is the attractor for initial conditions such that  $\dot{\psi} < 0$  ( $\Leftrightarrow (e^{\lambda\phi})' > 0$ ). In the next subsection we perform numerical calculations to show that this is basically true even if one takes into account of the effect of gravity. The numerical analysis also allows us to see the final fate of the genesis solutions for which the effect of the cosmic expansion cannot be ignored.

### 6.2.2 Full numerical analysis

In the Horndeski theory with (6.1.3) the Friedmann equation can be written as

$$\begin{aligned}\mathcal{E} &= e^{2(\alpha+1)\lambda\phi}\hat{\rho}(Y) + 6H\dot{\phi}e^{2\alpha\lambda\phi}c_1(Y) \\ &\quad - 3H^2\left[c_2(Y) + e^{2\alpha\lambda\phi}d_2(Y)\right] + 2H^3\dot{\phi}e^{-2\lambda\phi}c_3(Y) \\ &= 0,\end{aligned}\tag{6.2.4}$$

where

$$c_1 = Yg'_3 - 2\alpha\lambda g_4 + 2(3 - 2\alpha)\lambda Yg'_4 + 4\lambda Y^2g''_4,\tag{6.2.5}$$

$$c_2 = M_{\text{Pl}}^2 - 12\lambda Yg_5 - 28\lambda Y^2g'_5 - 8\lambda Y^3g''_5,\tag{6.2.6}$$

$$c_3 = 5Yg'_5 + 2Y^2g''_5,\tag{6.2.7}$$

$$d_2 = 2g_4 - 8Yg'_4 - 8Y^2g''_4.\tag{6.2.8}$$

Equation (6.2.4) is exact and hence can be used even if the background evolution is away from the genesis solution. Similarly, one can substitute Eq. (6.1.3) to the evolution equation  $\mathcal{P} = 0$  and the scalar-field equation of motion to write straightforwardly the exact equations for the background. The resultant equations are integrated numerically, giving the background evolution starting from generic initial conditions.

Given the initial conditions  $(\phi(t_0), \dot{\phi}(t_0))$ , the initial value for  $H$  is determined from the Friedmann equation (6.2.4). Therefore, the initial values  $(\phi(t_0), \dot{\phi}(t_0))$  must be chosen in such a way that Eq. (6.2.4) admits a real root  $H$ . Equation (6.2.4) is quadratic in  $H$  if  $g_5 = 0$  and cubic if  $g_5 \neq 0$ . In both cases, the discriminant  $\mathcal{D}$  for  $e^{\lambda\phi} \ll 1$  is given by

$$\mathcal{D} = e^{2(\alpha+1)\lambda\phi}c_2(Y)\hat{\rho}(Y) + \mathcal{O}(e^{2(2\alpha+1)\lambda\phi}).\tag{6.2.9}$$

In the  $g_5 = 0$  case, the initial data  $(\phi(t_0), \dot{\phi}(t_0))$  must lie in the region where  $\mathcal{D} \geq 0$  is satisfied. In the  $g_5 \neq 0$  case, the Friedmann equation has at least one real root for any  $(\phi(t_0), \dot{\phi}(t_0))$ .

Concrete numerical examples are presented in Figs. 6.2–6.4. In Figs. 6.2 and 6.3 we show the cases where the Friedmann equation is quadratic in  $H$ . The shaded regions ( $\mathcal{D} < 0$ ) cannot be accessed because  $H$  would be imaginary there. In Fig. 6.2 we have one genesis solution, while we have two in Fig. 6.3. In both cases, generalized galilean genesis is the attractor for  $\dot{\psi} < 0$ . At late times where  $\psi \ll 1$ , the numerical solutions are no longer approximated by Eq. (8.1.10), and within a finite time the Hubble rate  $H$  diverges. As the Friedmann equation is quadratic in  $H$ , we have two branches of the solutions, one of which may be contracting initially ( $H < 0$ ). The cosmological evolution nevertheless approaches the same genesis solution and the trajectories in the  $(\psi, \dot{\psi})$  space are almost indistinguishable.

The behavior of the models with  $g_5 \neq 0$  is more complicated, as illustrated in Fig. 6.4. In the white region, we have  $\mathcal{D} > 0$  and so there are three possible choices for the initial

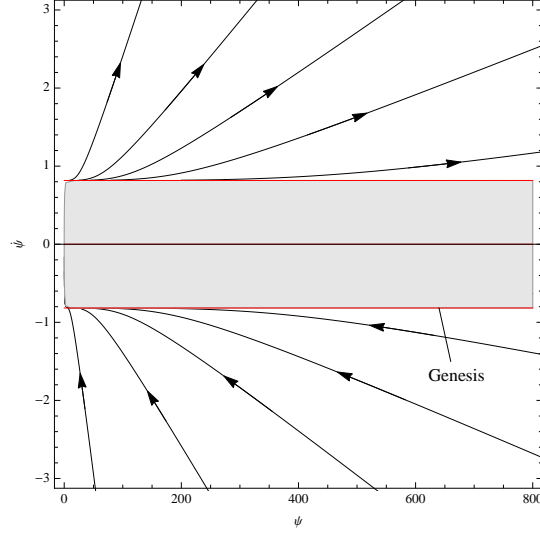


Figure 6.2: Numerical results of the background evolution for the model with  $g_2 = -Y + Y^2$ ,  $g_3 = Y$ , and  $g_4 = g_5 = 0$ . The parameters are given by  $M_{\text{Pl}} = 1$ ,  $\lambda = 1$ , and  $\alpha = 1$ .

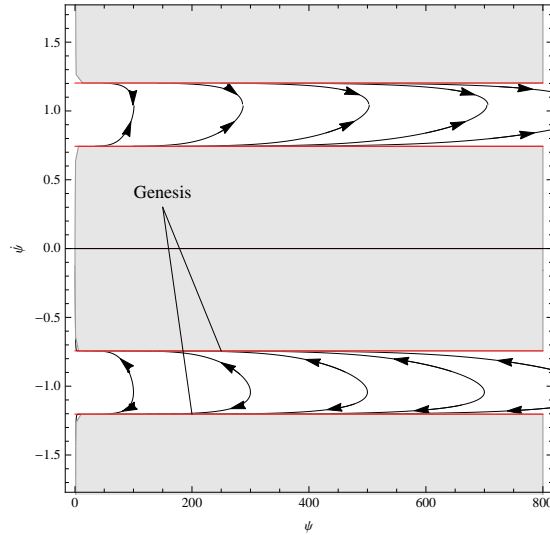


Figure 6.3: Numerical results of the background evolution for the model  $g_2 = -Y + 3Y^2 - Y^3$ ,  $g_3 = Y$ , and  $g_4 = g_5 = 0$ . The parameters are given by  $M_{\text{Pl}} = 1$ ,  $\lambda = 1$ , and  $\alpha = 2$ .

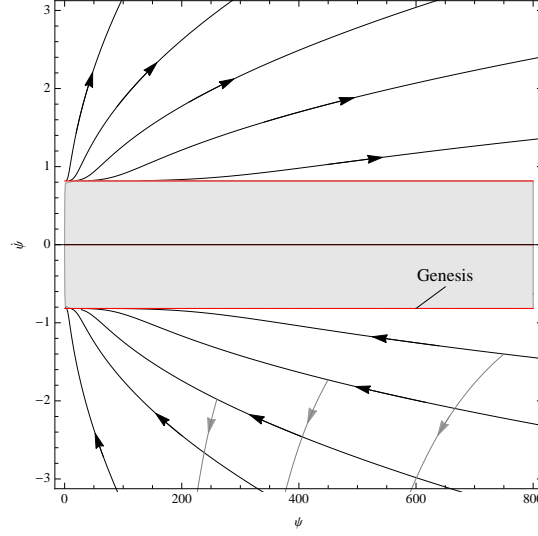


Figure 6.4: Numerical results of the background evolution for  $g_2 = -Y + Y^2$ ,  $g_3 = Y$ ,  $g_4 = 0$ , and  $g_5 = -Y$ . The parameters are given by  $M_{\text{Pl}} = 1$ ,  $\lambda = 1$ , and  $\alpha = 1$ .

value of  $H$ . Two of the three branches converge to the genesis solution similarly to the  $g_5 = 0$  case, as shown as the black lines in Fig. 6.4. Also in this case we find  $H \rightarrow \infty$  within a finite time. However, the remaining one branch never converges to the genesis solution. The corresponding examples are shown as the gray lines in Fig. 6.4. In the shaded region, we have  $\mathcal{D} < 0$  and there is only one possible initial value for  $H$  at each point, which corresponds to the latter branch. Therefore, the generalized galilean genesis solution can be a dynamical attractor for the initial data in the white ( $\mathcal{D} > 0$ ) region.

We thus conclude that the galilean genesis solution is the attractor provided that  $\dot{\psi} < 0$  ( $\Leftrightarrow (e^{\lambda\phi})' > 0$ ) initially, though the situation in the presence of  $g_5$  is involved. In the inflationary scenario, usually it does not matter which direction the scalar field rolls initially, but the universe must be expanding initially. In contrast to the case of inflation, the galilean genesis scenario allows both for expanding and contracting universes at the initial moment, while the scalar field must roll in a particular direction initially. As far as we have investigated numerically, all the solutions develop a singularity  $H \rightarrow \infty$  at some time  $t = t_{\text{sing}}$  in the future. In passing, we have checked that the numerical examples in Figs. 6.2 and 6.4 satisfy the stability conditions presented in the next section.

### 6.2.3 Spatial curvature

We have so far neglected the spatial curvature. In this subsection, let us justify this assumption by showing that the spatial curvature does not interfere with the evolution

of the genesis background. We will use the cosmological background equations with the spatial curvature  $K$  in the Horndeski theory.

Let us take an initial condition such that  $H$  is sufficiently small in the equation of motion for  $\phi$  and  $(e^{\lambda\phi})' > 0$ . Then, in a universe with  $K \neq 0$  the equation of motion for  $\phi$  can be written as

$$\frac{d}{dt} \left[ e^{2(\alpha+1)\lambda\phi} \hat{\rho}(Y) - e^{2\alpha\lambda\phi} \frac{\mathcal{K}_4(Y)}{a^2} - \frac{\mathcal{K}_5(Y)}{a^2} \right] = 0, \quad (6.2.10)$$

where

$$\mathcal{K}_4(Y) := 6(g_4 - 2Yg_4') K, \quad (6.2.11)$$

$$\mathcal{K}_5(Y) := -12\lambda Y(g_5 + Yg_5') K. \quad (6.2.12)$$

Even if  $e^{2(\alpha+1)\lambda\phi} \hat{\rho} \sim e^{2\alpha\lambda\phi} \mathcal{K}_4, \mathcal{K}_5$  at the initial moment, the curvature terms become smaller relative to the  $\hat{\rho}$  term as the scalar field rolls. Thus, we have the same attractor solution  $Y = Y_0$  satisfying  $\hat{\rho}(Y_0) = 0$ , i.e.,  $e^{\lambda\phi} \sim (-t)^{-1}$ . Along this attractor, the evolution equation reads

$$2\mathcal{G}(Y_0)\dot{H} + e^{2(\alpha+1)\lambda\phi} \hat{p}(Y_0) + [M_{\text{Pl}}^2 + 4\lambda Y_0 g_5(Y_0)] \frac{K}{a^2} \simeq 0, \quad (6.2.13)$$

where we assumed that  $\dot{H} \gg H^2$ . Equation (6.2.13) implies that the curvature term becomes subdominant as the scalar field rolls, and as a result  $\dot{H}$  is determined by the  $\hat{p}$  term, recovering the evolution of the genesis background. Thus, the flatness problem is resolved in the genesis model.

#### 6.2.4 Anisotropy

In conventional cosmology, an initial anisotropy is wiped out during inflation [64]. However, in alternative scenarios such as bouncing cosmology, it is often problematic that the initial anisotropy grows in a contracting phase [65, 66, 67] (see however [58]). In this subsection we will show that adding the initial anisotropy on the generalized Galilean genesis solution does not destabilize the background evolution.

We consider the Kasner metric

$$ds^2 = -dt^2 + a^2 \left[ e^{2\theta_1(t)} dx^2 + e^{2\theta_2(t)} dy^2 + e^{2\theta_3(t)} dz^2 \right], \quad (6.2.14)$$

where it is convenient to write

$$\theta_1 = \beta_+ + \sqrt{3}\beta_-, \quad \theta_2 = \beta_+ - \sqrt{3}\beta_-, \quad \theta_3 = -2\beta_+. \quad (6.2.15)$$

In Horndeski theory, the equations for anisotropy is given as

$$\frac{d}{dt} \left\{ a^3 \left[ \mathcal{G}_T \dot{\beta}_+ - 2X \dot{\phi} G_{5X} \left( \dot{\beta}_+^2 - \dot{\beta}_-^2 \right) \right] \right\} = 0, \quad (6.2.16)$$

$$\frac{d}{dt} \left\{ a^3 \left[ \mathcal{G}_T \dot{\beta}_- + 4X \dot{\phi} G_{5X} \dot{\beta}_+ \dot{\beta}_- \right] \right\} = 0. \quad (6.2.17)$$

If the deviations from the genesis background are not large, it follows from Eqs. (6.2.16) and (6.2.17) that

$$\frac{d}{dt} \left[ \mathcal{G} \dot{\beta}_+ - 2e^{-2\lambda\phi} \dot{\phi} Y_0 g'_5 \left( \dot{\beta}_+^2 - \dot{\beta}_-^2 \right) \right] = 0, \quad (6.2.18)$$

$$\frac{d}{dt} \left[ \mathcal{G} \dot{\beta}_- + 4e^{-2\lambda\phi} \dot{\phi} Y_0 g'_5 \dot{\beta}_+ \dot{\beta}_- \right] = 0. \quad (6.2.19)$$

In the models with  $g'_5 = 0$ , this simply gives

$$\dot{\beta}_+, \dot{\beta}_- \sim \text{const}, \quad (6.2.20)$$

so that the initial anisotropy dilutes as  $\theta_i \sim (-t)$ . In the models with  $g'_5 \neq 0$ , we have the following possibilities:

$$(\dot{\beta}_+, \dot{\beta}_-) = (0, 0), (b, 0), \left(-\frac{1}{2}b, \frac{\sqrt{3}}{2}b\right), \left(-\frac{1}{2}b, -\frac{\sqrt{3}}{2}b\right), \quad (6.2.21)$$

where

$$b := \frac{\mathcal{G}}{2e^{-2\lambda\phi} \dot{\phi} Y_0 g'_5} \sim (-t)^{-1}. \quad (6.2.22)$$

In this case, for nonzero  $\dot{\beta}_\pm$  the initial anisotropy can grow logarithmically:  $\theta_i \sim \ln(-t)$ . However, this should be compared with  $\ln a \sim (-t)^{-2\alpha}$ ; we see that the logarithmic growth of  $\theta_i$  does not spoil the genesis background.

### 6.3 Primordial perturbations

Let us now study the behavior of primordial tensor and scalar perturbations around the generalized genesis background to obtain predictions of our scenario as well as to impose stability conditions. To do so, we utilize the general quadratic action for cosmological perturbations in the Horndeski theory derived in Ref. [16].

### 6.3.1 Tensor perturbations

The quadratic action for tensor perturbations  $h_{ij}$  in the genesis phase is given by

$$S_h^{(2)} = \frac{1}{8} \int dt d^3x a^3 \mathcal{G}(Y_0) \left[ \dot{h}_{ij}^2 - \frac{c_t^2}{a^2} (\nabla h_{ij})^2 \right], \quad (6.3.1)$$

where

$$c_t^2 = \frac{M_{\text{Pl}}^2 + 4\lambda Y_0 g_5(Y_0)}{\mathcal{G}(Y_0)} \quad (6.3.2)$$

and note that  $a \simeq 1$ . It can be seen that stability against tensor perturbations is assured if

$$\mathcal{G}(Y_0) > 0, \quad (6.3.3)$$

$$M_{\text{Pl}}^2 + 4\lambda Y_0 g_5(Y_0) > 0, \quad (6.3.4)$$

are satisfied.

Since both  $\mathcal{G}(Y_0)$  and  $c_t^2$  are constant during the genesis phase, the tensor perturbations are effectively living in Minkowski without regard to  $\alpha$  and the concrete form of  $g_i(Y)$ , and consequently amplification of quantum fluctuations does not occur as opposed to the case of quasi-de Sitter inflation. This means that no detectable primordial gravitational waves are generated from our generic class of the genesis models.

### 6.3.2 Scalar perturbations

The quadratic action for the curvature perturbation  $\zeta$  in the unitary gauge is given by

$$S_\zeta^{(2)} = \int dt d^3x a^3 \mathcal{G}_S \left[ \dot{\zeta}^2 - \frac{c_s^2}{a^2} (\nabla \zeta)^2 \right], \quad (6.3.5)$$

where with some manipulation  $\mathcal{G}_S$  and  $c_s^2$  in the genesis phase are written as

$$\mathcal{G}_S = 2 \left[ \frac{(2\alpha + 1)\lambda \xi^2(Y_0)}{Y_0 \xi'(Y_0)} \right]^2 \hat{\rho}'(Y_0) e^{-2\alpha\lambda\phi}, \quad (6.3.6)$$

$$c_s^2 = \frac{\xi'(Y_0) \hat{p}(Y_0)}{\xi(Y_0) \hat{\rho}'(Y_0)}, \quad (6.3.7)$$

with

$$\xi(Y) := -\frac{Y \mathcal{G}(Y)}{\hat{p}(Y)}. \quad (6.3.8)$$

Equations (6.3.6) and (6.3.7) show that  $\mathcal{G}_S \propto (-t)^{2\alpha}$  and  $c_s^2 = \text{const}$ . It follows from Eqs. (6.1.13) and (6.3.3) that  $\xi(Y_0) > 0$ . We thus find that stability against scalar perturbations is guaranteed if

$$\hat{\rho}'(Y_0) > 0, \quad (6.3.9)$$

$$\xi'(Y_0) < 0, \quad (6.3.10)$$

are fulfilled. We can choose the functional degrees of freedom so that this is possible.

Let us evaluate the power spectrum of  $\zeta$ . To simplify the notation, it is convenient to write  $\mathcal{G}_S = \mathcal{A}(-t)^{2\alpha}$ , where  $\mathcal{A}$  is a constant deduced from Eq. (6.3.6), the value of which depends on the model, i.e.,  $\alpha$  and the concrete form of  $g_i(Y)$ . The equation of motion derived from the action (6.3.5) is given by

$$\ddot{\zeta}_k + \frac{2\alpha}{t}\dot{\zeta}_k + c_s^2 k^2 \zeta_k = 0, \quad (6.3.11)$$

where we moved to the Fourier space. This equation can be solved to give

$$\zeta_k = \frac{1}{2} \sqrt{\frac{\pi}{2\mathcal{A}(Y_0)}} (-t)^\nu H_\nu^{(1)}(-c_s k t), \quad \nu := \frac{1}{2} - \alpha, \quad (6.3.12)$$

where  $H_\nu^{(1)}$  is the Hankel function of the first kind and the positive frequency modes have been chosen. On large scales,  $|c_s k t| \ll 1$ , we have

$$\zeta_k \simeq A_k + B_k (-t)^{1-2\alpha}, \quad (6.3.13)$$

where

$$A_k := -i 2^{\nu-1} \sqrt{\frac{\pi}{2\mathcal{A}}} \frac{\Gamma(\nu)}{\pi} (c_s k)^{-\nu}, \quad (6.3.14)$$

$$B_k := 2^{-\nu-1} \sqrt{\frac{\pi}{2\mathcal{A}}} \left[ \frac{1}{\Gamma(\nu+1)} - \frac{i \cos(\pi\nu) \Gamma(-\nu)}{\pi} \right] \times (c_s k)^\nu. \quad (6.3.15)$$

If  $0 < \alpha < 1/2$ , the second term in Eq. (6.3.13) decays as is common to usual cosmologies, leaving the constant mode at late times. Thus, in this case the power spectrum is given by

$$\mathcal{P}_\zeta(k) = \frac{2^{2\nu-4} c_s^{-2\nu} \Gamma^2(\nu)}{\pi^3 \mathcal{A}} k^{3-2\nu}, \quad (6.3.16)$$

and the spectral index is found to be

$$n_s = 2\alpha + 3, \quad (6.3.17)$$



yielding a blue spectrum incompatible with observations.

The case of  $\alpha > 1/2$  is more subtle, because the second term in Eq. (6.3.13) grows and dominates on large scales. This is what happens in the original galilean genesis model ( $\alpha = 1$ ) [1]. To extract the late-time amplitude of  $\zeta_k$ , let us consider the following situation. Suppose that the genesis phase terminates at  $t = t_{\text{end}}$  and is matched onto some other phase. We assume that the scalar field is homogeneous on the  $t = t_{\text{end}}$  hypersurface. In the subsequent phase, the curvature perturbation on large scales may be written as

$$\zeta_k = C_k - D_k \int_t^\infty \frac{dt'}{a^3(t')\mathcal{G}_S(t')}, \quad (6.3.18)$$

where we do not specify  $\mathcal{G}_S(t)$  for  $t > t_{\text{end}}$ , but assume that Eq. (6.3.18) gives the constant and decaying modes and hence the integral converges. The late-time amplitude is given by  $C_k$ . The matching conditions [62] imply that  $\zeta_k$  and  $\mathcal{G}_S\dot{\zeta}_k$  are continuous across the two phases (cf. [68, 69, 70]). It is then straightforward to obtain  $C_k = A_k + B_k(-t_{\text{end}})^{1-2\alpha}(1 + \mathcal{I}) \simeq B_k(-t_{\text{end}})^{1-2\alpha}(1 + \mathcal{I})$ , where

$$\mathcal{I} := (2\alpha - 1) \int_{t_{\text{end}}}^\infty \frac{a^3(t_{\text{end}})\mathcal{A}(-t_{\text{end}})^{2\alpha}}{a^3(t')\mathcal{G}_S(t')} \frac{dt'}{|t_{\text{end}}|} \quad (6.3.19)$$

is independent of  $k$ . We may thus use the estimate

$$\mathcal{P}_\zeta(k) \sim \mathcal{C} \times \mathcal{P}_\zeta(k)|_{t=t_{\text{end}}}, \quad (6.3.20)$$

with  $\mathcal{C}$  being some  $k$ -independent factor. The power spectrum evaluated at the end of the genesis phase is given by

$$\mathcal{P}_\zeta(k)|_{t=t_{\text{end}}} = \frac{2^{-2\nu-4}c_s^{2\nu}\Gamma^2(-\nu)}{\pi^3\mathcal{A}} |t_{\text{end}}|^{4\nu} k^{3+2\nu}, \quad (6.3.21)$$

so that

$$n_s = 5 - 2\alpha. \quad (6.3.22)$$

Although the overall amplitude depends on the details of the model construction, the spectral index depends only on  $\alpha$  and not on the concrete form of  $g_i(Y)$ . We have an exactly scale-invariant spectrum for  $\alpha = 2$ , and this is in sharp contrast to the original galilean genesis model having  $\alpha = 1$ , which produces a blue-tilted spectrum of curvature perturbations. A particular realization of  $\alpha = 2$  is found in Ref. [63, 71], where the same conclusion is reached. Taking  $\alpha = 2.02$ , one can obtain the nearly scale-invariant, but slightly red-tilted, spectrum with  $n_s \simeq 0.96$ .

## 6.4 Curvaton

In the previous section we have seen that the nearly scale-invariant spectrum for curvature perturbations is possible only in the case of  $\alpha \simeq 2$ . In the other cases we need to consider an alternative mechanism such as the curvaton in order to obtain a scale-invariant spectrum. In this section, we study slightly in more detail the curvaton coupled to a conformal metric, the basic idea of which was proposed earlier in Ref. [1]. A similar mechanism was proposed in Ref. [51].

To make a scale-invariant power spectrum, we introduce a curvaton field  $\sigma$  coupled to the conformal metric,

$$\hat{g}_{\mu\nu} = e^{2\beta\lambda\phi} g_{\mu\nu}, \quad (6.4.1)$$

where  $\beta$  is a constant parameter which is assumed to be close to unity,  $\beta \simeq 1$ . Assuming the simplest potential, we consider the following action for  $\sigma$ :

$$S_\sigma = \int d^4x \sqrt{-\hat{g}} \left[ -\frac{1}{2} \hat{g}^{\mu\nu} \partial_\mu \sigma \partial_\nu \sigma - \frac{1}{2} m^2 \sigma^2 \right]. \quad (6.4.2)$$

The conformal metric (6.4.1) implies that the effective scale factor for the curvaton is  $e^{\beta\lambda\phi} \sim (-t)^{-\beta}$  with  $\beta \simeq 1$ , so that  $\sigma$  lives effectively in a quasi-de Sitter spacetime.

The equations of motion for the homogeneous part  $\sigma = \sigma_0(t)$  is given by

$$\ddot{\sigma}_0 + (2\beta\lambda\dot{\phi} + 3H)\dot{\sigma}_0 + e^{2\beta\lambda\phi} m^2 \sigma_0 = 0. \quad (6.4.3)$$

On the genesis background, one can ignore  $H \sim (-t)^{-(2\alpha+1)}$  relative to  $\lambda\dot{\phi} \sim (-t)^{-1}$ , leading to

$$\ddot{\sigma}_0 - \frac{2\beta}{t} \dot{\sigma}_0 + \frac{m^2}{[\lambda\sqrt{2Y_0}(-t)]^{2\beta}} \sigma_0 = 0. \quad (6.4.4)$$

The effective Hubble rate for the curvaton is  $\sim \lambda\sqrt{2Y_0}$ . For the ‘‘light’’ curvaton with

$$m^2 \ll \lambda^2 Y_0, \quad (6.4.5)$$

we thus have  $\sigma_0 \simeq \text{const}$  and the other independent solution decays quickly.

The energy density and pressure of  $\sigma$  are given by

$$\rho_\sigma = \frac{1}{2} e^{2\beta\lambda\phi} \dot{\sigma}_0^2 + \frac{1}{2} e^{4\beta\lambda\phi} m^2 \sigma_0^2 \sim (-t)^{-4\beta}, \quad (6.4.6)$$

$$p_\sigma = \frac{1}{2} e^{2\beta\lambda\phi} \dot{\sigma}_0^2 - \frac{1}{2} e^{4\beta\lambda\phi} m^2 \sigma_0^2 \sim (-t)^{-4\beta}. \quad (6.4.7)$$

Equations (8.1.12) and (8.1.13) imply that the dominant part of the cosmological background equations grows as  $\sim (-t)^{-2(\alpha+1)}$ . Thus, in order for the (initially subdominant) curvaton not to spoil the genesis background as time proceeds, we require that

$$\alpha + 1 \geq 2\beta. \quad (6.4.8)$$

The fluctuation of the curvaton,  $\delta\sigma(t, \mathbf{x})$ , obeys

$$\delta\ddot{\sigma} - \frac{2\beta}{t}\delta\dot{\sigma} - \nabla^2\delta\sigma + \frac{m^2}{[\lambda\sqrt{2Y_0}(-t)]^{2\beta}}\delta\sigma = 0. \quad (6.4.9)$$

Neglecting the mass term, this can be solved in the Fourier space to give

$$\delta\sigma_k = \frac{\sqrt{\pi}}{2} \left(\lambda\sqrt{2Y_0}\right)^\beta (-t)^{\beta+1/2} H_{\beta+1/2}^{(1)}(-kt), \quad (6.4.10)$$

where the positive frequency modes have been chosen. Thus, the power spectrum of the curvaton fluctuations is

$$\mathcal{P}_{\delta\sigma}(k) = \frac{2^{3\beta-2}\lambda^{2\beta}Y_0^\beta\Gamma^2(\beta+1/2)}{\pi^3}k^{2-2\beta}, \quad (6.4.11)$$

and we find

$$n_s = 3 - 2\beta. \quad (6.4.12)$$

In the case of  $\beta = 1$ , the effective scale factor for the curvaton is that of exact de Sitter, and hence the power spectrum is exactly scale-invariant, as is expected. Taking  $\beta = 1.04$  we obtain  $n_s = 0.96$ . The curvaton fluctuations can be converted into adiabatic ones after the genesis phase, where  $\sigma$  behaves as a conventional scalar field in a true expanding universe, in the same way as the usual curvaton field in the inflationary scenarios. Note, however, that due to the restriction (6.4.8) the present curvaton mechanism works only for the models with  $\alpha \geq 2 - n_s (> 1)$ .

## 6.5 Conclusions in this chapter

In this chapter, we have extended the galilean genesis models [1, 36, 37, 38] and constructed a generic Lagrangian from the Horndeski theory that admits the *generalized galilean genesis* solution. In generalized galilean genesis, the universe starts expanding from Minkowski in a singularity free manner with the increasing Hubble rate  $H \sim (-t)^{-(2\alpha+1)}$ , where  $\alpha (> 0)$  is a new constant parameter in the Lagrangian. We have investigated the background evolution and shown that the generalized galilean genesis solution is the attractor for a wide range of initial conditions. In particular, we have seen that the spatial curvature and an initial anisotropy do not hinder the evolution of the genesis phase.

We have then studied the primordial perturbations from the generalized galilean genesis models. From the quadratic actions for cosmological perturbations we have imposed several stability conditions on the functions in our generic Lagrangian. In contrast to the case of quasi-de Sitter inflation, tensor fluctuations are not amplified in the genesis phase in all the galilean genesis models we have constructed, and hence no detectable primordial

gravitational waves are expected. The evolution of the curvature perturbation  $\zeta$  depends on the parameter  $\alpha$  and has turned out to be more interesting. In the case of  $\alpha > 1/2$ ,  $\zeta$  grows on large scales, as in the original galilean genesis model ( $\alpha = 1$ ) [1]. The tilt of the power spectrum at the end of the genesis phase is given by  $n_s = 5 - 2\alpha$ , irrespective of the other details of the model. Thus, we have a slightly red-tilted spectrum for  $\alpha \gtrsim 2$ . In the case of  $\alpha < 1/2$ , the constant mode dominates on large scales as in conventional cosmology. In this case, the power spectrum has been shown to be always blue-tilted. We have also discussed the possibility of the curvaton mechanism in the generalized galilean genesis scenario.

We have ignored the reheating process in our scenario. It would be interesting to explore how the universe reheats and how matter is created at the end of generalized galilean genesis. Since the Lagrangian defined by (6.1.3) excludes a cosmological constant, it is not clear how the genesis phase is connected finally to the late-time universe described by the  $\Lambda$ CDM model. These are the open questions.

## Chapter 7

# Reheating and primordial gravitational waves in GGG

Inflation [7, 41] is now the standard model of the early universe, solving the problems that Big Bang cosmology faces and explaining the origin of large scale structure in the way consistent with observations. However, the inflationary universe still suffers from the problem of initial singularity [72] as long as the null energy condition (NEC) is satisfied. To circumvent the singularity, alternative scenarios such as the bouncing models [73, 74, 75, 76] have been proposed so far, but a majority of the alternative models are unstable due to the violation of the NEC. Recently, an interesting class of scalar field theories called the Galileon has been constructed [23] and various aspects of the Galileon theory have been explored extensively in the literature. One of the most intriguing nature of this theory is that the null energy condition can be violated stably<sup>1</sup>. Thus, the Galileon opens up a new possibility of stable, singularity-free models alternative to inflation [55, 56, 57, 58, 59, 60], as well as stable NEC violating models of dark energy [22] and inflation [15].

In this chapter, we consider an initial phase of NEC violating quasi-Minkowski expansion driven by the Galileon field as an alternative to inflation. The scenario is called the Galilean genesis [1], and different versions of genesis models can be found in Refs. [63, 36, 37, 38]. The purpose of this chapter is to address how the genesis phase is connected to the subsequent hot universe through the reheating stage. In the case of inflation, reheating usually proceeds with coherent oscillation of the scalar field at the minimum of the potential and its decay. However, the scalar field that drives Galilean genesis does not have the potential. The situation here is similar to that in kinetically driven inflation models such as k- [14] and G-inflation [15]. We therefore consider reheating through gravitational particle production [77]. Reheating after Galilean genesis has also been discussed in Ref. [50]. See also Refs. [54, 61, 78, 79] for the other aspects of genesis models.

The exit from k- and G-inflation is accompanied by the kination phase, *i.e.*, the phase

---

<sup>1</sup>See Ref. [48] for a subtle point beyond linear perturbations.

where the kinetic energy of the scalar field is dominant. Similarly, the kination phase can also be incorporated at the end of Galilean genesis as we will do in this chapter. The primordial gravitational waves that re-enter the horizon during this kination era have a blue spectrum, giving enhanced amplitudes at high frequencies [80]. In addition to this, the primordial spectrum of gravitational waves is expected to be blue due to NEC violating quasi-Minkowski expansion in the earliest stage of the universe. The combined effect will therefore give rise to strongly blue gravitational waves. In the second part of this chapter we evaluate the spectrum of gravitational waves generated from Galilean genesis and explore the possibility of testing this alternative scenario *e.g.*, with the advanced LIGO detector.

In the previous chapter [4], we have developed a general framework unifying the original genesis model [1] and its extensions [63, 36, 37, 38], using which we have derived the stability conditions and primordial power spectra of scalar and tensor perturbations. The framework is based on the Horndeski theory [17, 18, 16], the most general second-order scalar-tensor theory in four dimensions. We use this general framework also in this chapter.

The plan of this chapter is as follows. In the next section, we review the Galilean genesis solution and its generalization. In Sec. III, we investigate the creation of massless scalar particles after Galilean genesis and compute the reheating temperature. Using the result of Sec. III, we then evaluate the power spectrum of gravitational waves in Sec. IV. We present some concrete examples and discuss the detectability of the primordial gravitational waves in Sec. V. Finally, we conclude in Sec. VI.

## 7.1 Gravitational particle production

In this chapter, we consider the generalized Galilean genesis shown in chapter 6 and now we redefine the scale factor

$$a \simeq a_G \left[ 1 + \frac{1}{2\alpha} \frac{h_0}{(-t)^{2\alpha}} \right], \quad (7.1.1)$$

where  $a_G$  is the constant value. This means the scale factor approaches to  $a_G$  as  $t \rightarrow -\infty$ . The genesis solution is the approximate one valid for

$$\frac{h_0}{(-t)^{2\alpha}} \ll 1. \quad (7.1.2)$$

The background evolution begins to deviate from the above solution when  $h_0/(-t)^{2\alpha} \sim 1$ , and one need to invoke a numerical calculation for a later epoch. To make the calculations tractable analytically, in this chapter we impose the technical assumption that the genesis phase terminates before Eq. (7.1.2) is violated. Denoting the Hubble parameter at the end of genesis by  $H_*$ , the condition (7.1.2) can be written as

$$H_* \ll h_0^{-1/2\alpha}, \quad (7.1.3)$$

or, equivalently,

$$H_*(-t_*) \ll 1, \quad (7.1.4)$$

where  $t_*$  is the proper time at the end of the genesis phase. This inequality defines the range of validity of our computation.

The universe must eventually be connected to a radiation dominated phase. In standard inflationary cosmology, the inflaton field oscillates about the minimum of the potential and reheat the universe. The radiation dominated universe follows after this reheating stage. However, the Lagrangian for generalized Galilean genesis does not have the potential term and hence conventional reheating would not be suitable for the genesis scenario. This is also the case for k-inflation [14]. In this chapter, we therefore explore the possibility of gravitational reheating after the genesis phase, *i.e.*, reheating via gravitational particle production at the transition to the intermediate phase where the kinetic energy of the scalar field is dominant (the kination phase). See [50] for preheating after Galilean genesis via a direct coupling between the scalar field and the other fields. Note in passing that we have another possibility that the genesis phase is followed by inflation [61, 78, 79]. The inflationary stage is then naturally described by k- or G-inflation [15], so that also in this case we employ gravitational reheating. In this chapter, we do not consider this latter possibility and focus on the scenario in which the genesis phase is followed by the intermediate kination phase and then by the radiation dominated phase. To realize the background evolution suitable to this reheating mechanism, we assume that the Lagrangian of the form (6.1.3) is only valid until  $\phi$  (which is increasing during the genesis phase) reaches some value,  $\phi_*$ , and for  $\phi > \phi_*$  the Lagrangian is such that the kinetic energy of  $\phi$  decreases quickly to make only the standard kinetic term  $X$  relevant in the Lagrangian:  $\mathcal{L} \simeq (M_{\text{Pl}}^2/2)R + X$ . The genesis phase thus terminates and is followed by the kination phase where  $3M_{\text{Pl}}^2 H^2 = \rho_\phi \propto a^{-6}$ .<sup>2</sup> The basic scenario here is essentially the same as those at the end of k- and G-inflation [14, 15] described in some detail in [31]. We do not provide a concrete model realizing this because it is reasonable to presume that this is indeed possible by using the functional degrees of freedom in the Horndeski theory,<sup>3</sup> and also because particle creation is only sensitive to the evolution of the scale factor but not to an underlying concrete model of generalized Galilean genesis. Note that in many cases it is likely that perturbations become unstable at the transition between the two phases. Even if this occurs we can solve the issue by using the idea in Ref. [79], though one must go beyond the Horndeski theory to do so.

Let us consider the creation of massless, minimally coupled scalar particles at the transition from the genesis phase to kination. The created particle is denoted by  $\chi$ , whose

---

<sup>2</sup>The necessary requirement here is that the energy density of  $\phi$  dilutes more rapidly than that of radiation. We assume the kination phase just for simplicity.

<sup>3</sup>We assume the particular form of the Lagrangian (6.1.3) only during the genesis phase. At the very end of genesis, the Lagrangian may be away from the form (6.1.3).

the Lagrangian is given by

$$\mathcal{L}_\chi = -\frac{1}{2}g^{\mu\nu}\partial_\mu\chi\partial_\nu\chi. \quad (7.1.5)$$

Its Fourier component,  $\chi_k$ , obeys

$$\frac{1}{a}(a\chi_k)'' + \left(k^2 - \frac{a''}{a}\right)\chi_k = 0, \quad (7.1.6)$$

where a dash stands for differentiation with respect to the conformal time  $\eta$ . Since  $a \simeq a_G = \text{const}$  in the genesis phase, we have  $\eta \simeq t/a_G$  and hence  $\eta = -\infty$  corresponds to the asymptotic past. We write the solution using the Bogoliubov coefficients as

$$a\chi_k = \frac{\alpha_k(\eta)}{\sqrt{2k}}e^{-ik\eta} + \frac{\beta_k(\eta)}{\sqrt{2k}}e^{ik\eta}, \quad (7.1.7)$$

and impose the boundary conditions that  $\alpha_k \rightarrow 1$  and  $\beta_k \rightarrow 0$  as  $\eta \rightarrow -\infty$ . For  $k^2 \gg |a''/a|$ , we have [81, 82, 83, 84]

$$\beta_k(\eta) = -\frac{i}{2k} \int_{-\infty}^{\eta} e^{-2iks} \frac{a''}{a} ds. \quad (7.1.8)$$

The energy density of the created particles can be computed as

$$\rho_\chi = \frac{1}{2\pi^2 a^4} \int_0^\infty k^3 |\beta_k(\infty)|^2 dk, \quad (7.1.9)$$

and this can be described as eq.(5.2.25) and eq.(5.2.26).

In the genesis phase, we have

$$f(\eta) \simeq a_G^2 \left[ 1 + \frac{h_0}{\alpha} \frac{1}{(-a_G\eta)^{2\alpha}} \right] \quad (\eta < \eta_*), \quad (7.1.10)$$

with  $\eta_* := t_*/a_G$ , while in the subsequent kination phase  $a \propto (\eta + \text{const})^{1/2}$  and hence  $f$  is of the form

$$f(\eta) = c_0 \frac{\eta}{-\eta_*} + c_1, \quad (7.1.11)$$

where  $c_0$  and  $c_1$  are to be determined by requiring that  $f$  and  $f'$  are continuous at  $\eta = \eta_*$ . Under this ‘‘sudden transition’’ approximation,  $f''$  is discontinuous and consequently  $V$  is also discontinuous at  $\eta = \eta_*$ . Due to this discontinuity, the integral (5.2.25) diverges, which is unphysical. To avoid divergence, we insert a short stage having a time scale  $\Delta\eta$  between the genesis and kination phases, and join the two phases smoothly. The idea here is also employed in connecting inflation to the radiation/kination phase smoothly [77, 31].



Thus, we make the ansatz

$$f(\eta) = \begin{cases} b_0 + b_1\eta + b_2\eta^2 + b_3\eta^3 & (\eta_* < \eta < \eta_* + \Delta\eta) \\ c_0\eta/(-\eta_*) + c_1 & (\eta_* + \Delta\eta < \eta) \end{cases}, \quad (7.1.12)$$

after the end of genesis, and determine the six coefficients by requiring that  $f$ ,  $f'$ , and  $f''$  are continuous at  $\eta = \eta_*$  and  $\eta = \eta_* + \Delta\eta$ . This allows us to obtain continuous  $V$  and hence finite  $\rho_\chi$ . For the current purpose we do not have to write  $b_0$ ,  $b_1$ ,  $b_2$ , and  $b_3$  explicitly, but we only need

$$c_0 = \frac{2a_G^2 h_0}{(-t_*)^{2\alpha}} \left[ 1 + \mathcal{O}\left(\frac{\Delta\eta}{-\eta_*}\right) \right], \quad (7.1.13)$$

$$c_1 = a_G^2 \left\{ 1 + \frac{(2\alpha+1)h_0}{\alpha(-t_*)^{2\alpha}} \left[ 1 + \mathcal{O}\left(\frac{\Delta\eta}{-\eta_*}\right) \right] \right\}. \quad (7.1.14)$$

Now we have

$$V(\eta) \simeq 2a_G^2(2\alpha+1)h_0(-a_G\eta)^{-2(\alpha+1)} \quad (\eta < \eta_*), \quad (7.1.15)$$

and  $|V| \ll V(\eta_*)$  for  $\eta > \eta_* + \Delta\eta$ . To evaluate the integral (5.2.25), it is sufficient to approximate  $V$  as a straight line for  $\eta_* < \eta < \eta_* + \Delta\eta$ . Thus,

$$V \simeq a_G^2 \frac{2(2\alpha+1)h_0}{(-t_*)^{2(\alpha+1)}\Delta\eta} (-\eta + \eta_* + \Delta\eta) \quad (\eta_* < \eta < \eta_* + \Delta\eta).$$

The main contribution to the integral (5.2.25) comes from the region  $\eta_* < \eta < \eta_* + \Delta\eta$  where  $V'$  gets much larger than in the genesis and kination phases. Performing the integral in this domain, we obtain

$$\rho_\chi = \frac{(2\alpha+1)^2}{32\pi^2} \ln\left(\frac{1}{a_G H_* \Delta\eta}\right) \frac{h_0^2}{(-t_*)^{4(\alpha+1)}} \left(\frac{a_G}{a}\right)^4. \quad (7.1.16)$$

A logarithmic divergence is now manifest in the sudden transition limit,  $\Delta\eta \rightarrow 0$ . In the case of the smooth transition, however, we may take  $\ln(1/a_G H_* \Delta\eta) = \mathcal{O}(1)$ , leading to a finite energy density of relativistic particles. Now since  $h_0$  has the dimension of  $[\text{mass}]^{-2\alpha}$ , it is convenient to introduce the dimensionless quantity  $\tilde{h}_0$  defined as

$$\tilde{h}_0 := M_{\text{Pl}}^{2\alpha} h_0. \quad (7.1.17)$$

Then, to make Eq. (7.1.16) more suggestive, we rewrite the equation in different ways by using  $-t_* = h_0^{1/(2\alpha+1)} H_*^{-1/(2\alpha+1)}$  and Eq. (7.1.17). First, we have

$$\rho_\chi = \frac{A}{32\pi^2} \tilde{h}_0^{-\frac{2}{2\alpha+1}} \left(\frac{H_*}{M_{\text{Pl}}}\right)^{-\frac{4\alpha}{2\alpha+1}} H_*^4 \left(\frac{a_G}{a}\right)^4, \quad (7.1.18)$$

where

$$A := (2\alpha + 1)^2 \ln \left( \frac{1}{a_G H_* \Delta \eta} \right) \quad (7.1.19)$$

is a number of  $\mathcal{O}(1)$ . This result is in contrast to that in the inflationary scenario, where the energy density of the created particles is simply given by  $\rho_\chi \sim H_{\text{inf}}^4/a^4$ , with  $H_{\text{inf}}$  being the inflationary energy scale. We may also write  $\rho_\chi$  as

$$\rho_\chi = \frac{A}{128\pi^2\alpha^2} \frac{H_*^4}{\delta_*^2} \left( \frac{a_G}{a} \right)^4, \quad (7.1.20)$$

where  $\delta_*$  is defined as

$$\delta_* := \frac{a(\eta_*)}{a_G} - 1 (\ll 1). \quad (7.1.21)$$

This second expression shows that actual  $\rho_\chi$  is much larger than the naive estimate deduced from the case of inflation,  $\rho_\chi \sim H_*^4(a_G/a)^4$ .

The reheating temperature  $T_R$  is determined from  $\rho_\chi = \rho_\phi$ , where  $\rho_\phi$  is the energy density of the scalar field after the end of genesis,

$$\rho_\phi = 3M_{\text{Pl}}^2 H_*^2 \left( \frac{a_G}{a} \right)^6. \quad (7.1.22)$$

The scale factor at the time when  $\rho_\chi = \rho_\phi$  occurs,  $a_R$ , is given by

$$\frac{a_R}{a_G} = \sqrt{\frac{96\pi^2}{A}} \left( \frac{H_*}{M_{\text{Pl}}} \right)^{-\frac{1}{2\alpha+1}} \tilde{h}_0^{\frac{1}{2\alpha+1}}. \quad (7.1.23)$$

Since  $a_R > a_G$ , we have the condition

$$\frac{H_*}{M_{\text{Pl}}} < \left( \frac{96\pi^2}{A} \right)^{(2\alpha+1)/2} \tilde{h}_0. \quad (7.1.24)$$

Equating the radiation energy density at  $a = a_R$  to  $(\pi^2 g_*/30)T_R^4$ , where  $g_*$  is the effective number of relativistic species of particles, we obtain

$$\frac{T_R}{M_{\text{Pl}}} = \left( \frac{30}{\pi^2 g_*} \right)^{1/4} \frac{A^{3/4}}{\sqrt{3}(32\pi^2)^{3/4}} \tilde{h}_0^{-\frac{3}{2(2\alpha+1)}} \left( \frac{H_*}{M_{\text{Pl}}} \right)^{\frac{\alpha+2}{2\alpha+1}}. \quad (7.1.25)$$

This result is again in contrast to that in the inflationary scenario, where  $T_R \sim H_{\text{inf}}^2/M_{\text{Pl}}$ . One can also write  $T_R$  as

$$T_R = \left( \frac{30}{\pi^2 g_*} \right)^{1/4} \frac{A^{3/4}}{\sqrt{3}(32\pi^2)^{3/4} (2\alpha)^{3/2}} \frac{H_*^2}{M_{\text{Pl}} \delta_*^{3/2}}. \quad (7.1.26)$$

From this one can clearly see that the reheating temperature is much higher than the naive estimate deduced from inflation,  $T_R \sim H_*^2/M_{\text{Pl}}$ . In other words, for a fixed reheating temperature, the Hubble parameter at the end of genesis is smaller than the corresponding inflationary value.

## 7.2 The spectrum of primordial gravitational waves

Having obtained the background evolution in the previous section, let us discuss the spectrum of primordial gravitational waves from generalized Galilean genesis. As expected from the null energy condition violating nature of the scenario, generated gravitational waves exhibit a blue spectrum and hence are relevant only at high frequencies.

The quadratic action for the gravitational waves in generalized Galilean genesis is [4]

$$S_h^{(2)} = \frac{1}{8} \int dt d^3x a^3 \mathcal{G}(Y_0) \left[ \dot{h}_{ij}^2 - \frac{c_t^2}{a^2} (\partial_k h_{ij})^2 \right], \quad (7.2.1)$$

where  $c_t^2 := [M_{\text{Pl}}^2 + 4\lambda Y_0 g_5(Y_0)]/\mathcal{G}(Y_0)$ . Note that the coefficients  $\mathcal{G}(Y_0)$  and  $c_t^2$  are constant during the genesis phase. The equation of motion for each Fourier mode of two polarization states,  $h_k^\lambda$  ( $\lambda = +, \times$ ), reads

$$\frac{1}{a} (ah_k)'' + \left( c_t^2 k^2 - \frac{a''}{a} \right) h_k = 0, \quad (7.2.2)$$

where

$$\frac{a''}{a} \simeq \frac{h_0}{(-a_G \eta)^{2\alpha}} \cdot \frac{2\alpha + 1}{\eta^2} \quad (7.2.3)$$

and  $\lambda$  is omitted here and hereafter. From Eq. (7.2.3) it can be seen that the gravitational waves freeze not at  $|c_t k \eta| \sim 1$  but at later times,  $|c_t k \eta| \sim \sqrt{h_0/(-a_G \eta)^{2\alpha}} \ll 1$ . The WKB solution for the subhorizon modes is given by

$$h_k = \frac{1}{a} \sqrt{\frac{2}{\mathcal{G} c_t k}} e^{-i c_t k \eta}. \quad (7.2.4)$$

Since  $a \simeq a_G$ , the power spectrum is already constant at early times,

$$\frac{k^3}{\pi^2} |h_k|^2 = \frac{2k^2}{\pi^2 \mathcal{G} c_t a_G^2}. \quad (7.2.5)$$

After each mode exits the ‘‘horizon’’ and ceases to oscillate, this amplitude is retained, as illustrated by the numerical example in Fig. 7.1. Thus, the power spectrum of the primordial gravitational waves evaluated at the end of the genesis phase is given by

$$\mathcal{P}_h^{(p)}(k) = \frac{2k^2}{\pi^2 \mathcal{G} c_t a_G^2}. \quad (7.2.6)$$

In contrast to the gravitational waves from inflation, the primordial spectrum is blue, and hence gravitational waves could be relevant observationally only at high frequencies.

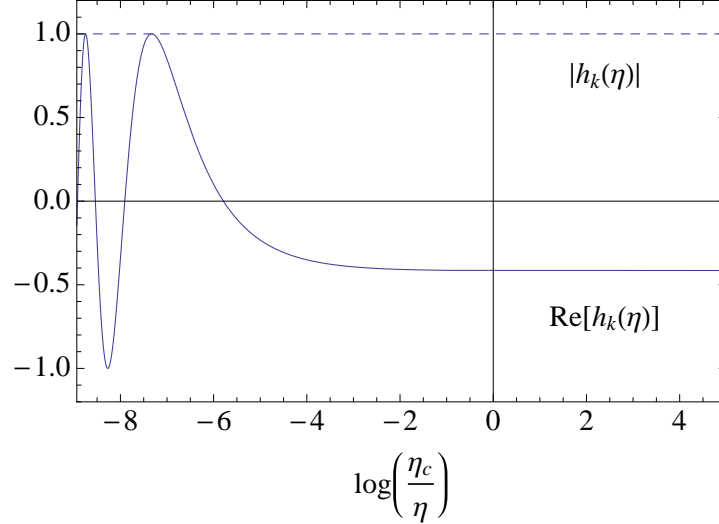


Figure 7.1: The numerical evolution of gravitational waves during generalized Galilean genesis with  $\alpha = 1$ .  $\eta_c$  denotes the horizon-crossing time.

The density parameter for the gravitational waves per log frequency interval,  $\Omega_{\text{gw}}$ , evaluated at the present epoch is given by

$$\Omega_{\text{gw}} = \frac{k^2}{12H_0^2} \mathcal{P}_h(k), \quad (7.2.7)$$

where  $H_0$  is the present value of the Hubble parameter and the power spectrum  $\mathcal{P}_h$  characterizes the present amplitude of the gravitational waves. Since  $h_k = \text{const}$  on superhorizon scales and  $h_k \propto a^{-1}$  after horizon re-entry, we have

$$\mathcal{P}_h(k) = \mathcal{P}_h^{(p)}(k) \left( \frac{a_k}{a_0} \right)^2, \quad (7.2.8)$$

where  $a_k$  is the scale factor at horizon re-entry and  $a_0 (= 1)$  is the scale factor at present.

Suppose that a mode with wavenumber  $k$  re-enters the horizon at the epoch characterized by the equation-of-state parameter  $w$ . Since  $k = a_k H_k$ , where the Hubble parameter at horizon re-entry obeys  $H_k \propto a_k^{-3(1+w)/2}$ , we find

$$a_k \propto k^{-2/(1+3w)}. \quad (7.2.9)$$

In our scenario we have the kination phase ( $w = 1$ ) after the end of genesis and subse-

quently the conventional radiation and matter dominated phases. Thus, we obtain

$$\Omega_{\text{gw}} = \Omega_{\text{gw}}^{(p)}(k) \times \begin{cases} \frac{k_R}{k} \frac{k_{\text{eq}}^2}{k_R^2} \frac{k_0^4}{k_{\text{eq}}^4} & (k_R < k < k_*) \\ \frac{k_{\text{eq}}^2}{k^2} \frac{k_0^4}{k_{\text{eq}}^4} & (k_{\text{eq}} < k < k_R) \\ \frac{k_0^4}{k^4} & (k_0 < k < k_{\text{eq}}), \end{cases} \quad (7.2.10)$$

where we write

$$\Omega_{\text{gw}}^{(p)}(k) = \frac{k^2}{12H_0^2} \mathcal{P}_h^{(p)} = \frac{k^4}{6\pi^2 H_0^2 \mathcal{G} c_t a_G^2}. \quad (7.2.11)$$

Here, the wavenumbers  $k_*$ ,  $k_R$ ,  $k_{\text{eq}}$ , and  $k_0$  correspond to the modes that re-enter the horizon at the end of genesis, at the reheating time, at the epoch of matter-radiation equality, and at the present epoch. Explicitly, we have

$$k_0 = a_0 H_0 = 2.235 \times 10^{-4} \left( \frac{h}{0.67} \right) \text{Mpc}^{-1}, \quad (7.2.12)$$

$$k_{\text{eq}} = a_{\text{eq}} H_{\text{eq}} = 1.028 \times 10^{-2} \left( \frac{\Omega_m h^2}{0.141} \right) \text{Mpc}^{-1}. \quad (7.2.13)$$

It is also useful to write

$$\begin{aligned} \frac{k_*}{k_R} &= \left( \frac{a_R}{a_G} \right)^2 \\ &= 3^{\frac{1+\alpha}{2+\alpha}} \left( \frac{32\pi^2}{A} \right)^{\frac{1+2\alpha}{2(2+\alpha)}} \left( \frac{\pi^2 g_*}{30} \right)^{-\frac{1}{2(2+\alpha)}} \tilde{h}_0^{\frac{1}{2+\alpha}} \left( \frac{T_R}{M_{\text{Pl}}} \right)^{-\frac{2}{2+\alpha}}, \end{aligned} \quad (7.2.14)$$

where we used the fact that the Hubble parameter at the reheating time,  $H_R$ , follows from  $H_R = H_*(a_G/a_R)^3$ . In terms of the frequency,  $k_R$  corresponds to

$$f_R \simeq 0.026 \left( \frac{g_*}{106.75} \right)^{1/6} \left( \frac{T_R}{10^6 \text{ GeV}} \right) \text{Hz}. \quad (7.2.15)$$

Using (7.2.14) one can also write  $f_*$ . A schematic picture of  $\Omega_{\text{gw}}$  as a function of the frequency  $f$  is shown in Fig. 7.2. This should be compared with the standard prediction from inflation, where one has a flat spectrum for  $f_{\text{eq}} < f < f_R$  [85].

To see the possibility of detecting the gravitational waves from generalized Galilean genesis, let us evaluate  $\Omega_{\text{gw}}$  at  $k = k_R$  and  $k = k_*$ . For simplicity, we assume that  $\mathcal{G} = M_{\text{Pl}}^2$  and  $c_t = 1$ . This is exact for  $g_5 = 0$  models, and extending the following estimate to the

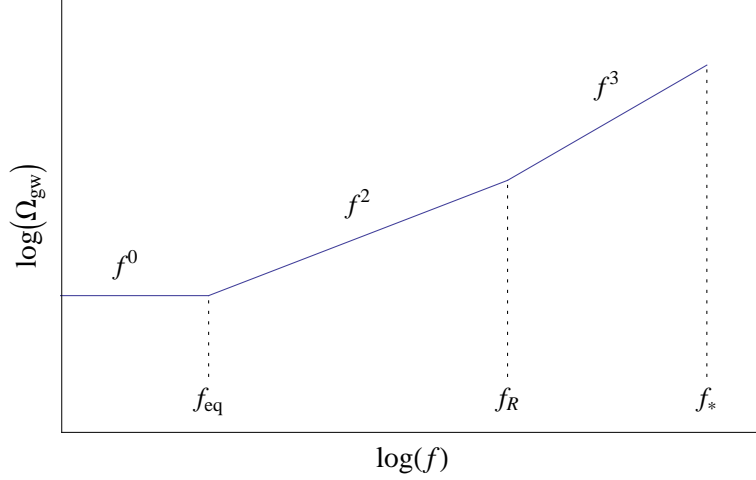


Figure 7.2: Schematic shape of the power spectrum of gravitational waves in generalized Galilean genesis.

$g_5 \neq 0$  case is straightforward. Then, it can be seen from Eq. (7.2.10) that

$$\begin{aligned} \Omega_{\text{gw}}(k_R) &= \frac{1}{6\pi^2 M_{\text{Pl}}^2 H_0^2 a_G^2} \frac{k_R^2 k_0^4}{k_{\text{eq}}^2} \\ &\simeq 10^{-5} \times \left( \frac{H_*}{M_{\text{Pl}}} \right)^2 \left( \frac{a_R}{a_G} \right)^{-4}, \end{aligned} \quad (7.2.16)$$

$$\begin{aligned} \Omega_{\text{gw}}(k_*) &= \Omega_{\text{gw}}(k_R) \times \frac{k_*^3}{k_R^3} \\ &\simeq 10^{-5} \times \left( \frac{H_*}{M_{\text{Pl}}} \right)^2 \left( \frac{a_R}{a_G} \right)^2, \end{aligned} \quad (7.2.17)$$

where we used  $k_0 = H_0$ . The ratio  $a_R/a_G (> 1)$  itself depends on  $H_*$  and model parameters through Eq. (7.1.23). At this stage it is instructive to compare those results with the flat spectrum in the inflationary scenario,

$$\Omega_{\text{gw}}^{\text{inf}} \simeq 10^{-5} \times \left( \frac{H_{\text{inf}}}{M_{\text{Pl}}} \right)^2. \quad (7.2.18)$$

For fixed  $T_R$ , it follows from Eq. (7.1.26) that  $H_* < H_{\text{inf}}$ . This shows that  $\Omega_{\text{gw}}(k_R)$  in generalized Galilean genesis is smaller than the inflationary prediction for fixed  $T_R$ . However, this does not hold true for  $\Omega_{\text{gw}}(k_*)$ .

Now, by the use of Eqs. (7.1.23) and (7.1.25) we obtain

$$\Omega_{\text{gw}}(k_R) = 10^{-5} \cdot 3^{-\frac{1}{2+\alpha}} \left( \frac{32\pi^2}{A} \right)^{\frac{1+2\alpha}{2(2+\alpha)}} \left( \frac{\pi^2 g_*}{30} \right)^{\frac{3+2\alpha}{2(2+\alpha)}} \tilde{h}_0^{\frac{1}{2+\alpha}} \left( \frac{T_R}{M_{\text{Pl}}} \right)^{\frac{2(3+2\alpha)}{2+\alpha}}, \quad (7.2.19)$$

and

$$\Omega_{\text{gw}}(k_*) = 10^{-5} \cdot 3^{\frac{2+3\alpha}{2+\alpha}} \left( \frac{32\pi^2}{A} \right)^{\frac{2(1+2\alpha)}{2+\alpha}} \left( \frac{\pi^2 g_*}{30} \right)^{\frac{\alpha}{2+\alpha}} \tilde{h}_0^{\frac{4}{2+\alpha}} \left( \frac{T_R}{M_{\text{Pl}}} \right)^{\frac{4\alpha}{2+\alpha}}. \quad (7.2.20)$$

In the frequency range  $f_R < f < f_*$ , we have

$$\Omega_{\text{gw}}(f) = 10^{-31} \cdot 3^{-\frac{1}{2+\alpha}} \left( \frac{32\pi^2}{A} \right)^{\frac{1+2\alpha}{2(2+\alpha)}} \left( \frac{\pi^2 g_*}{30} \right)^{\frac{1+\alpha}{2(2+\alpha)}} \tilde{h}_0^{\frac{1}{2+\alpha}} \left( \frac{T_R}{M_{\text{Pl}}} \right)^{\frac{\alpha}{2+\alpha}} \left( \frac{f}{100 \text{ Hz}} \right)^3. \quad (7.2.21)$$

One could enhance  $\Omega_{\text{gw}}$  by taking large  $\tilde{h}_0$ , but too large  $\tilde{h}_0$  would violate Eq. (7.1.3), indicating the breaking of the approximation  $a \simeq a_G [1 + h_0/2\alpha(-t)^{2\alpha}]$ . Using Eqs. (7.1.3) and (7.1.25) we have, for  $f_R < f < f_*$ ,

$$\Omega_{\text{gw}}(f) \lesssim 10^{-30} A^{-1/4} \left( \frac{g_*}{106.75} \right)^{1/4} \left( \frac{f}{100 \text{ Hz}} \right)^3. \quad (7.2.22)$$

Note that the right hand side is independent of  $\alpha$  and the reheating temperature. To generate a higher amplitude of the gravitational waves, one would relax the limitation imposed by Eq. (7.1.3).

In the above argument we have assumed  $c_t = 1$  for simplicity, but it is worth noting that we can enhance the amplitude of the gravitational waves by assuming that  $c_t < 1$ .

## 7.3 Examples

To be more specific, let us move to the discussion of concrete examples in the this section.

### 7.3.1 The original model of Galilean genesis

First, we apply the above results to the original model of Galilean genesis [1], which corresponds to the  $\alpha = 1$  case. The original model is given by choosing the arbitrary functions and parameters in (6.1.3) as

$$\begin{aligned} g_2 &= -2\mu^2 Y + \frac{2\mu^3}{\Lambda^3} Y^2, & g_3 &= \frac{2\mu^3}{\Lambda^3} Y, \\ g_4 &= g_5 = 0, & \lambda &= 1, \quad \alpha = 1, \end{aligned} \quad (7.3.1)$$

where  $\mu$  and  $\Lambda$  are the parameters having the dimension of mass. Note that  $\phi$  is taken to be dimensionless and so  $[Y] = \text{mass}^2$ . It is easy to verify that the model satisfies the stability conditions for scalar and tensor perturbations. From Eqs. (8.1.12) and (6.1.12) we find

$$Y_0 = \frac{\Lambda^3}{3\mu}, \quad h_0 = \frac{\mu^3}{2M_{\text{Pl}}^2 \Lambda^3}. \quad (7.3.2)$$

Assuming that  $A = \mathcal{O}(1)$ , the reheating temperature can be written as

$$T_R \simeq 10^{-3} \left( \frac{g_*}{106.75} \right)^{-1/4} \left( \frac{\Lambda}{\mu} \right)^{3/2} H_*. \quad (7.3.3)$$

The condition that the analytic approximation for the genesis background solution is valid, Eq. (7.1.3), translates to

$$\frac{\mu}{\Lambda} < 10^2 \left( \frac{T_R}{10^{10} \text{GeV}} \right)^{-1/3} \left( \frac{g_*}{106.75} \right)^{-1/12}, \quad (7.3.4)$$

while  $a_R/a_G > 1$  yields

$$\frac{\mu}{\Lambda} > 10^{-7} \left( \frac{T_R}{10^{10} \text{GeV}} \right)^{2/3} \left( \frac{g_*}{106.75} \right)^{1/6}. \quad (7.3.5)$$

The density parameters at  $k = k_R$  and  $k = k_*$  are given respectively by

$$\Omega_{\text{gw}}(k_R) \simeq 10^{-31} \left( \frac{g_*}{106.75} \right)^{5/6} \left( \frac{\mu}{\Lambda} \right) \left( \frac{T_R}{10^{10} \text{GeV}} \right)^{10/3}, \quad (7.3.6)$$

and

$$\Omega_{\text{gw}}(k_*) \simeq 10^{-10} \left( \frac{g_*}{106.75} \right)^{1/3} \left( \frac{\mu}{\Lambda} \right)^4 \left( \frac{T_R}{10^{10} \text{GeV}} \right)^{4/3}, \quad (7.3.7)$$

where the corresponding frequency is

$$f_* = 10^9 \left( \frac{\mu}{\Lambda} \right) \left( \frac{T_R}{10^{10} \text{GeV}} \right)^{1/3} \text{Hz}. \quad (7.3.8)$$

In the frequency range  $f_R < f < f_*$  we have

$$\Omega_{\text{gw}}(f) \simeq 10^{-32} \left( \frac{g_*}{106.75} \right)^{1/3} \left( \frac{\mu}{\Lambda} \right) \left( \frac{T_R}{10^{10} \text{GeV}} \right)^{1/3} \left( \frac{f}{100 \text{Hz}} \right)^3. \quad (7.3.9)$$

Figure 7.3 shows the examples of the power spectra compared with the anticipated sensitivity of the advanced LIGO. We consider two different reheating temperatures. One



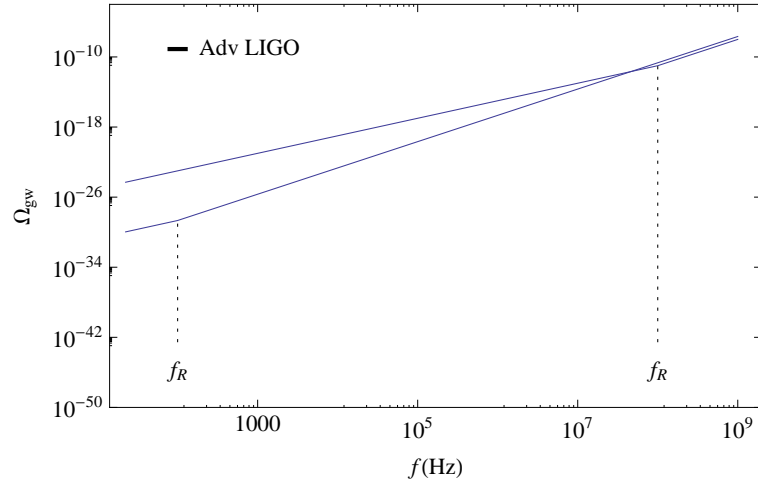


Figure 7.3: The density parameters  $\Omega_{\text{gw}}(f)$  for different reheating temperatures in the original model of Galilean genesis. The two plots correspond to  $T_R \sim 10^{10}$  GeV ( $f_R = 100$  Hz) with  $\mu/\Lambda = 10^2$  and  $T_R \sim 10^{16}$  GeV ( $f_R = 10^8$  Hz) with  $\mu/\Lambda = 1$ . Here  $\mu/\Lambda$  is taken to be the largest value allowed by Eq. (7.3.4). The anticipated sensitivity of the advanced LIGO is also marked.

is  $T_R \sim 10^{10}$  GeV and it follows from Eq. (7.2.15) that the corresponding frequency is given by  $f_R = 100$  Hz. In this case, the amplitude is too small to be detected by the advanced LIGO. The other is as high as  $T_R \sim 10^{16}$  GeV, giving  $f_R = 100$  MHz. Also in this case it is unlikely to be able to detect the primordial gravitational waves at  $f = 100$  Hz. In both cases we have  $\Omega_{\text{gw}} \sim 10^{-12}$  at  $f = 100$  MHz, as can be seen directly from Eq. (7.2.22). The gravitational reheating stage after Galilean genesis could therefore be probed by the gravitational waves at very high frequencies.

### 7.3.2 A model generating the scale invariant curvature perturbation

As a second example, let us consider the case of  $\alpha = 2$ . This class of models is of particular interest because it gives rise to a scale-invariant spectrum of the curvature perturbation [63, 4]. The Lagrangian is given in a similar form to the previous example by

$$\begin{aligned} g_2 &= -2\mu^2 Y + \frac{2\mu^3}{\Lambda^3} Y^2, & g_3 &= \frac{\mu^3}{\Lambda^3} Y, \\ g_4 &= g_5 = 0, & \lambda &= 1, \end{aligned} \quad (7.3.10)$$

but now  $\alpha = 2$ . It follows from Eqs. (8.1.12) and (6.1.12) that

$$Y_0 = \frac{\Lambda^3}{\mu}, \quad h_0 = \frac{\mu^4}{10M_{\text{Pl}}^2 \Lambda^6}. \quad (7.3.11)$$

The reheating temperature is obtained as

$$T_R \simeq 10^{-2} \left( \frac{g_*}{106.75} \right)^{-1/4} \frac{\Lambda^{9/5} H_*^{4/5}}{M_{\text{Pl}}^{2/5} \mu^{6/5}}. \quad (7.3.12)$$

Equation (7.1.3) in this case reduces to

$$\frac{M_{\text{Pl}} \mu^2}{\Lambda^3} < 10^6 \left( \frac{T_R}{10^{10} \text{GeV}} \right)^{-1} \left( \frac{g_*}{106.75} \right)^{-1/4}, \quad (7.3.13)$$

while  $a_R/a_G > 1$  gives

$$\frac{M_{\text{Pl}} \mu^2}{\Lambda^3} > 10^{-11} \left( \frac{T_R}{10^{10} \text{GeV}} \right) \left( \frac{g_*}{106.75} \right)^{1/4}. \quad (7.3.14)$$

The density parameters at  $k = k_R$  and  $k = k_*$  are computed respectively as

$$\Omega_{\text{gw}}(k_R) \simeq 10^{-32} \left( \frac{g_*}{106.75} \right)^{7/8} \left( \frac{M_{\text{Pl}} \mu^2}{\Lambda^3} \right)^{1/2} \left( \frac{T_R}{10^{10} \text{GeV}} \right)^{7/2}, \quad (7.3.15)$$

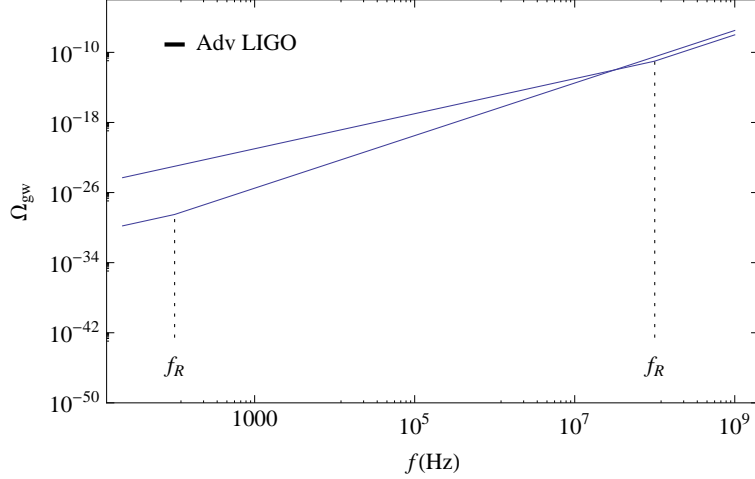


Figure 7.4: The density parameters  $\Omega_{\text{gw}}(f)$  for different reheating temperatures in the  $\alpha = 2$  model, in comparison with the anticipated sensitivity of the advanced LIGO. The parameter  $M_{\text{Pl}}\mu^2/\Lambda^3$  is taken to be the possible largest values:  $M_{\text{Pl}}\mu^2/\Lambda^3 = 10^6$  for  $T_R \sim 10^{10}$  GeV ( $f_R = 100$  Hz) and  $M_{\text{Pl}}\mu^2/\Lambda^3 = 1$  for  $T_R \sim 10^{16}$  GeV ( $f_R = 10^8$  Hz).

and

$$\Omega_{\text{gw}}(k_*) \simeq 10^{-15} \left( \frac{g_*}{106.75} \right)^{1/2} \left( \frac{M_{\text{Pl}}\mu^2}{\Lambda^3} \right)^2 \left( \frac{T_R}{10^{10} \text{ GeV}} \right)^2, \quad (7.3.16)$$

with the corresponding frequency

$$f_* = 10^8 \left( \frac{g_*}{106.75} \right)^{1/24} \left( \frac{M_{\text{Pl}}\mu^2}{\Lambda^3} \right)^{1/2} \left( \frac{T_R}{10^{10} \text{ GeV}} \right)^{1/2} \text{ Hz}. \quad (7.3.17)$$

In the range  $f_R < f < f_*$ , we find

$$\Omega_{\text{gw}}(f) \simeq 10^{-33} \left( \frac{g_*}{106.75} \right)^{3/8} \left( \frac{M_{\text{Pl}}\mu^2}{\Lambda^3} \right)^{1/2} \left( \frac{T_R}{10^{10} \text{ GeV}} \right)^{1/2} \left( \frac{f}{100 \text{ Hz}} \right)^3. \quad (7.3.18)$$

The basic conclusions for the  $\alpha = 2$  model is the same as those for  $\alpha = 1$ , as presented in Fig. 7.4. Though detectable gravitational waves are not expected in the sensitive bands of, say, the LIGO detector,  $\Omega_{\text{gw}}$  is enhanced at high frequencies up to the model independent value as shown in Eq. (7.2.22) and  $\Omega_{\text{gw}} \sim 10^{-12}$  at  $f = 100$  MHz under the optimistic choice of the parameters.

Since the  $\alpha = 2$  model can generate scale-invariant curvature perturbations, let us now consider consistency between the above optimistic estimate of  $\Omega_{\text{gw}}$  and the prediction

for the curvature perturbations. The power spectrum of the curvature perturbation  $\zeta$  evaluated at the end of Galilean genesis is given by [4]

$$\mathcal{P}_\zeta|_{t=t_*} = \frac{\Gamma^2(-3/2)}{2\pi^3 c_s^3 \mathcal{A}} (-t_*)^{-6}, \quad (7.3.19)$$

where in the present model it is found that  $c_s = \sqrt{3}$  and  $\mathcal{A} = (100/9)(M_{\text{Pl}}\mu^2/\Lambda^3)^2$ . For simplicity we assume that the evolution of  $\zeta$  in the post-genesis phase is negligible. We can write  $t_*$  in terms of  $T_R$  to obtain

$$\mathcal{P}_\zeta \simeq 10^{-11} \left(\frac{g_*}{106.75}\right)^{3/8} \left(\frac{M_{\text{Pl}}\mu^2}{\Lambda^3}\right)^{1/2} \left(\frac{T_R}{10^{10} \text{ GeV}}\right)^{3/2}. \quad (7.3.20)$$

Using  $\mathcal{P}_\zeta \sim 10^{-9}$ , the parameters are fixed as

$$\frac{M_{\text{Pl}}\mu^2}{\Lambda^3} \sim 10^4 \left(\frac{T_R}{10^{10} \text{ GeV}}\right)^{-3}. \quad (7.3.21)$$

This gives smaller values of  $M_{\text{Pl}}\mu^2/\Lambda^3$  than the most optimistic ones used in Fig. 7.4. For  $T_R \sim 10^{10} \text{ GeV}$  we have  $\Omega_{\text{gw}} \sim 10^{-13}$  at  $f = 100 \text{ MHz}$ . If one would use the curvaton mechanism to produce the observed spectrum of the curvature perturbation even in the case of  $\alpha = 2$ , one has  $\mathcal{P}_\zeta < 10^{-9}$  but then  $M_{\text{Pl}}\mu^2/\Lambda^3 < 10^4 (T_R/100 \text{ GeV})^{-3}$ .

## 7.4 Conclusions in this chapter

In this chapter, we have studied the reheating stage after the initial quasi-Minkowski expanding phase and its consequences on the primordial gravitational waves. The initial stage was described in a unified manner as *generalized Galilean genesis* [4] in terms of the Horndeski scalar-tensor theory. Since the scalar field does not have a potential in which it oscillates, we have considered reheating through the gravitational production of massless scalar particles at the transition from the genesis phase to the kination phase. To avoid an unphysical diverging result which would come from a sudden transition approximation, we have followed the previous works [77, 31] and considered a smooth matching of the two phases. We have computed in that way the energy density of created particles and the reheating temperature. In the case of gravitational reheating after inflation, it is known that the created energy density is given by  $\sim H_{\text{inf}}^4$ , where  $H_{\text{inf}}$  is the inflationary Hubble parameter [77]. We have shown that the energy density of massless scalar particles created after Galilean genesis is not simply given by the naive replacement,  $\sim H_*^4$ , where  $H_*$  is the Hubble parameter at the end of the genesis phase, but rather by a more involved form which depends on the model parameters as well as  $H_*$ . In particular, it has been found that for the same reheating temperature the Hubble parameter at the end of genesis is smaller compared with the corresponding value in the inflation scenario.

We have then discussed the spectrum of the primordial gravitational waves from generalized Galilean genesis. The combined effects of the quasi-Minkowski expanding background and the kination phase give rise to the blue gravitational waves,  $\Omega_{\text{gw}} \propto f^3$ , at high frequencies, while their amplitude is highly suppressed at low frequencies in contrast with the inflationary gravitational waves. Unfortunately, the expected amplitude is too small to be detected in the sensitive bands of the advanced LIGO detector. However, it is possible to have  $\Omega_{\text{gw}} \sim 10^{-12}$  at  $f \sim 100$  MHz. Thus, the primordial gravitational waves having a spectrum  $\Omega_{\text{gw}} \propto f^3$  at  $f \gtrsim 100$  MHz and the lack thereof at low frequencies would offer an interesting test of Galilean genesis in future experiments.

Finally, let us comment that the equations of motion for a massless scalar field and gravitational waves are practically the same, though we have discussed the particle production of the former on subhorizon scales while the latter cross the horizon. This implies that the gravitons can also be generated on subhorizon scales at the transition between the two phases in the same way as the massless scalar field, and this concern must be taken care of in the gravitational reheating scenario.



## Chapter 8

# Scale-invariant perturbations

It is no exaggeration to say that inflation [40, 7, 41] is now a part of the “standard model” of the Universe. Not only homogeneity, isotropy, and flatness of space, but also the inhomogeneous structure of the Universe originated from tiny primordial fluctuations [42], can be elegantly explained by a phase of quasi-de Sitter expansion in the early Universe. However, even the inflationary scenario cannot resolve the initial singularity problem [46], which raises the motivation for debating the possibilities of alternatives to inflation (for a review, see, e.g., Refs. [73, 34]). In order to be convinced that the epoch of quasi-de Sitter expansion did exist in the early Universe, one must rule out such alternatives.

A typical feature of singularity-free alternative scenarios is that the Hubble parameter  $H$  is an *increasing* function of time in the early universe. The null energy condition requires that for all null vectors  $k^\mu$  the energy-momentum tensor satisfies  $T_{\mu\nu}k^\mu k^\nu \geq 0$ , which, upon using the Einstein equations, translates to the condition for the Ricci tensor,  $R_{\mu\nu}k^\mu k^\nu \geq 0$ . In a cosmological setup this reads  $\dot{H} \leq 0$ , and hence the NEC<sup>1</sup> is violated in such alternative scenarios. Unfortunately, in many cases the violation of the NEC implies that the system under consideration is unstable. Earlier NEC-violating models are indeed precluded by this instability issue [47]. Recently, however, it was noticed that scalar-field theories with second-derivative Lagrangians admit stable NEC-violating solutions [1, 22, 15], which revitalizes singularity-free alternatives to inflation [55, 56, 57, 58, 59, 60, 78, 32]. One can avoid the initial singularity also in emergent universe cosmology [86, 87, 88, 89] and in string gas cosmology [39, 90].

The future detection of primordial gravitational waves (tensor perturbations) is supposed to give us valuable information of the early Universe. It is folklore that a nearly scale-invariant red spectrum of primordial gravitational waves is the “smoking gun” of inflation. The reason that this is believed to be so is the following. The amplitude of each gravitational wave mode is determined solely by the value of the Hubble parameter

---

<sup>1</sup>In this chapter, we use the terminology NEC when referring to  $R_{\mu\nu}k^\mu k^\nu \geq 0$ , which is, more properly, the null convergence condition.

evaluated at horizon crossing. During inflation  $H$  is a slowly decreasing function of time, while in alternative scenarios the time evolution of  $H$  is very different. This folklore is not true, however, even in the context of inflation, because some extended models of inflation can violate the NEC stably and thereby the Hubble parameter slowly increases, giving rise to nearly scale-invariant *blue* tensor spectra [15]. Then, does the detection of nearly scale-invariant tensor perturbations indicate a phase of quasi-de Sitter expansion? Naively, the gross violation of the NEC in alternative models implies strongly blue tensor spectra, and by this feature one would be able to discriminate inflation from alternatives. In this chapter, we show that this expectation is not true: nearly scale-invariant scalar and tensor perturbations can be generated from quantum fluctuations on a NEC-violating background.<sup>2</sup> Thus, it is possible that the individual spectrum has no difference from that of inflation, though the consistency relation turns out to be different.

The model we present in this chapter is a variant of Galilean Genesis [1], in which the universe starts expanding from Minkowski by violating the NEC stably. The earlier proposal of Galilean Genesis [1, 36, 37, 38] fails to produce scale-invariant curvature perturbations (without invoking the curvaton), but it was shown in [4, 63, 71] that it is possible if one generalizes the original models. In all those models, the tensor perturbations have strongly blue spectra and hence the amplitudes are too small to be detected at low frequencies [2]. In our new models of Galilean Genesis, however, the primordial tensor spectrum can be red, blue, or scale invariant, depending on the parameters of the model, and the curvature perturbation can have a nearly scale-invariant spectrum. We work in the Horndeski theory [17, 18, 16], the most general scalar-tensor theory with second-order field equations, to construct a general Lagrangian admitting the new Genesis solution with the above-mentioned properties. As a specific case our Lagrangian includes the Genesis model recently obtained by Cai and Piao [93], which yields scale-invariant tensor perturbations and *strongly red* scalar perturbations.

The plan of this chapter is as follows. In Sec. II, we introduce the general Lagrangian for our new variant of Galilean Genesis, and study the background evolution to discuss whether homogeneity, isotropy, and flatness of space can be explained in the present scenario. Then, in Sec. III, we calculate primordial scalar and tensor spectra. We give a concrete example yielding scale-invariant scalar and tensor perturbations in Sec. IV. In Sec. V we draw our conclusions.

## 8.1 A new Lagrangian for Galilean Genesis

Now let us present a new variant of generalized Galilean Genesis that enjoys a similar background evolution but exhibits a novel behavior of perturbations compared to the

---

<sup>2</sup>It has been known that in string gas cosmology scale-invariant scalar and tensor perturbations are generated from thermal string fluctuations [73, 34]. Nearly scale-invariant tensor perturbations can also be sourced by gauge fields in bouncing [91] and ekpyrotic [92] scenarios.



existing Genesis models. As the arbitrary functions  $G_i(\phi, X)$  in the Horndeski theory we choose

$$\begin{aligned} G_2 &= e^{2(\alpha+1)\lambda\phi} g_2(Y) + e^{-2(\beta-1)\lambda\phi} a_2(Y) + e^{-2(\alpha+2\beta-1)\lambda\phi} b_2(Y), \\ G_3 &= e^{2\alpha\lambda\phi} g_3(Y) + e^{-2\beta\lambda\phi} a_3(Y) + e^{-2(\alpha+2\beta)\lambda\phi} b_3(Y), \\ G_4 &= e^{-2\beta\lambda\phi} a_4(Y) + e^{-2(\alpha+2\beta)\lambda\phi} b_4(Y), \\ G_5 &= e^{-2(\alpha+2\beta+1)\lambda\phi} b_5(Y), \end{aligned} \quad (8.1.1)$$

where  $g_2$  and  $g_3$  are arbitrary functions of  $Y$ , but  $a_i(Y)$  and  $b_i(Y)$  are such that

$$a_2(Y) = 8\lambda^2 Y (Y \partial_Y + \beta)^2 A(Y), \quad (8.1.2)$$

$$a_3(Y) = -2\lambda(2Y \partial_Y + 1)(Y \partial_Y + \beta)A(Y), \quad (8.1.3)$$

$$a_4(Y) = Y \partial_Y A(Y), \quad (8.1.4)$$

$$b_2(Y) = 16\lambda^3 Y^2 (Y \partial_Y + \alpha + 2\beta + 1)^3 B(Y), \quad (8.1.5)$$

$$b_3(Y) = -4\lambda^2 Y (2Y \partial_Y + 3)(Y \partial_Y + \alpha + 2\beta + 1)^2 B(Y), \quad (8.1.6)$$

$$b_4(Y) = 2\lambda Y (Y \partial_Y + 1)(Y \partial_Y + \alpha + 2\beta + 1)B(Y), \quad (8.1.7)$$

$$b_5(Y) = -(2Y \partial_Y + 1)(Y \partial_Y + 1)B(Y), \quad (8.1.8)$$

with arbitrary functions  $A(Y)$  and  $B(Y)$ . We thus have four functional degrees of freedom, as well as two constant parameters  $\alpha$  and  $\beta$  in this setup. We assume that

$$\alpha + \beta > 0 \quad (8.1.9)$$

in order to obtain the background evolution which we will present shortly. However, at this stage we do *not* impose that  $\alpha > 0$  and  $\beta > 0$ .

We assume the ansatz,

$$Y \simeq Y_0 = \text{const}, \quad H \simeq \frac{h_0}{(-t)^{2\alpha+2\beta+1}}, \quad (8.1.10)$$

and substitute this into the field equations to see that eq. (8.1.10) indeed gives a consistent solution for a large  $|t|$ . (The range of  $t$  is  $-\infty < t < 0$ .) The scale factor for a large  $|t|$  is given by

$$a \simeq 1 + \frac{1}{2(\alpha + \beta)} \frac{h_0}{(-t)^{2(\alpha+\beta)}}. \quad (8.1.11)$$

The (00) and ( $ij$ ) components of the gravitational field equations read, respectively,

$$\hat{\rho}(Y_0) + \mathcal{O}(|t|^{-2(\alpha+\beta)}) = 0, \quad (8.1.12)$$

$$2\mathcal{G}_T \dot{H} + e^{2(\alpha+1)\lambda\phi} \hat{p}(Y_0) + \mathcal{O}(|t|^{-2(2\alpha+\beta+1)}) = 0, \quad (8.1.13)$$

where

$$\begin{aligned} \mathcal{G}_T \simeq & -2e^{-2\beta\lambda\phi}Y_0(A' + 2YA'') \\ & + 2e^{-2(\alpha+2\beta+1)\lambda\phi}H\dot{\phi}Y_0(6B' + 9YB'' + 2Y^2B'''). \end{aligned} \quad (8.1.14)$$

Note that

$$\mathcal{G}_T \propto (-t)^{2\beta}, \quad (8.1.15)$$

and hence  $\mathcal{G}_T\dot{H} = \mathcal{O}(|t|^{-2(\alpha+1)})$ . Equation (8.1.12) fixes  $Y_0$  as a root of

$$\hat{\rho}(Y_0) = 0, \quad (8.1.16)$$

and then eq. (8.1.13) is used to determine  $h_0$ . Since there is  $H$  in  $\mathcal{G}_T$ , eq. (8.1.13) reduces to a quadratic equation in  $h_0$  in general. We have sensible NEC-violating cosmology only for  $h_0 > 0$ . Since it will turn out that the condition

$$\mathcal{G}_T > 0 \quad (8.1.17)$$

is required from the stability of tensor perturbations, one must impose

$$\hat{p}(Y_0) < 0, \quad (8.1.18)$$

though this is not a sufficient condition for  $h_0 > 0$ .

A particular case of this class of Genesis models can be found in [93], which corresponds to  $A \propto Y^{-2}$ ,  $B = 0$  with  $\alpha = \beta = 2$ .

We have thus found that the Horndeski theory with (8.1.1) admits the Genesis solution (8.1.10), which is similar to previous ones [4]. However, we will show in the next section that the evolution of tensor perturbations is quite different: they can even grow on superhorizon scales and can give rise to a variety of values of the spectral index  $n_t$ . Before seeing this, let us address more about the background evolution.

## 8.2 Problems

### 8.2.1 Flatness Problem

Now let us move on to discuss the problems which inflation solves. In the inflationary universe, the curvature term in the Friedmann equation is diluted exponentially relative to the other terms, and thus the flatness problem in standard Big Bang cosmology is resolved. Since cosmic expansion is very slow in Galilean Genesis,  $a \simeq 1$ , one may wonder if the flatness problem is solved as well in this scenario. We have shown in the previous chapter [4] that the curvature term is eventually diluted away in all existing Galilean Genesis models. We now check this point in our new variant of Galilean Genesis.

The background equations in the presence of the spatial curvature  $K$  are given by [4]

$$e^{2(\alpha+1)\lambda\phi}\hat{\rho}(Y_0) - \frac{3\mathcal{G}_T K}{a^2} \simeq 0, \quad (8.2.1)$$

$$2\mathcal{G}_T \dot{H} + e^{2(\alpha+1)\lambda\phi}\hat{p}(Y_0) + \frac{\mathcal{F}_T K}{a^2} \simeq 0, \quad (8.2.2)$$

where

$$\begin{aligned} \mathcal{F}_T &\simeq 2e^{-2\beta\lambda\phi}Y_0 A' \\ &\quad - 4e^{-2(\alpha+2\beta)\lambda\phi}(1 + 2\alpha + 4\beta)\lambda Y_0^2(2B' + YB''). \end{aligned} \quad (8.2.3)$$

We have

$$\mathcal{F}_T \propto \begin{cases} (-t)^{2\beta} & (2B' + Y_0 B'' = 0) \\ (-t)^{2(\alpha+2\beta)} & (2B' + Y_0 B'' \neq 0) \end{cases}. \quad (8.2.4)$$

In order for the flatness problem to be resolved, the curvature term has to be negligible compared to the other terms. In eq. (8.2.1) the ratio of the curvature term to the first term is  $\sim (-t)^{2(\alpha+\beta)+1}$ , and due to the condition  $\alpha + \beta > 0$  the curvature term becomes negligible as time proceeds. It can be seen using eq. (8.2.4) that the same is true in eq. (8.2.2). We have thus confirmed that the flatness problem can be solved as well in our new variant of Galilean Genesis.

### 8.2.2 Anisotropy

Given the large-scale isotropy of the Universe, let us consider the evolution of anisotropies in the Genesis phase and check whether the universe can safely be isotropized. In standard cosmology, the shear term in the Friedmann equation is diluted rapidly as  $\propto a^{-6}$ . However, the situation is subtle in Galilean Genesis.

We describe an anisotropic universe using the Kasner-type metric. From the equations of motion for  $\beta_+$  and  $\beta_-$  with  $a \simeq 1$ , we obtain [4]

$$\frac{d}{dt} \left[ \mathcal{G}_T \dot{\beta}_+ - 2X \dot{\phi} G_{5X} \left( \dot{\beta}_+^2 - \dot{\beta}_-^2 \right) \right] = 0, \quad (8.2.5)$$

$$\frac{d}{dt} \left[ \mathcal{G}_T \dot{\beta}_- + 4X \dot{\phi} G_{5X} \dot{\beta}_+ \dot{\beta}_- \right] = 0, \quad (8.2.6)$$

where  $\mathcal{G}_T \propto (-t)^{2\beta}$  and

$$\begin{aligned} X \dot{\phi} G_{5X} &= \dot{\phi} e^{-2(\alpha+2\beta+1)\lambda\phi} Y_0 b'_5(Y_0) \\ &\propto (-t)^{2\alpha+4\beta+1}. \end{aligned} \quad (8.2.7)$$

In the  $b'_5(Y_0) = 0$  case, it is easy to see that  $\dot{\beta}_\pm \propto (-t)^{-2\beta}$ , and hence

$$\frac{\dot{\beta}_\pm}{H} \propto (-t)^{2\alpha+1}. \quad (8.2.8)$$

This implies that if  $\alpha > -1/2$ , the universe is isotropized as it expands.

To see what happens in the general case of  $b'_5(Y_0) \neq 0$ , it is convenient to define

$$b := \frac{\mathcal{G}_T}{2X\dot{\phi}G_{5X}} \sim H \propto (-t)^{-2(\alpha+\beta)-1}. \quad (8.2.9)$$

One can integrate eqs. (8.2.5) and (8.2.6) to obtain

$$\left(\frac{\dot{\beta}_+}{b}\right) - \left(\frac{\dot{\beta}_+}{b}\right)^2 + \left(\frac{\dot{\beta}_-}{b}\right)^2 = \text{const} \times (-t)^{2\alpha+1}, \quad (8.2.10)$$

$$\left(\frac{\dot{\beta}_-}{b}\right) + 2\left(\frac{\dot{\beta}_+}{b}\right)\left(\frac{\dot{\beta}_-}{b}\right) = \text{const} \times (-t)^{2\alpha+1}. \quad (8.2.11)$$

If  $\alpha < -1/2$ , the right hand sides grow as the universe expands, leading to the growth of  $\dot{\beta}_\pm/b$ , i.e., the growth of  $\dot{\beta}_\pm/H$ . Therefore, this case is not acceptable. If  $\alpha > -1/2$  and the initial anisotropies are sufficiently smaller than  $b$  ( $\sim H$ ), the quadratic terms in eqs. (8.2.10) and (8.2.11) can be ignored and we have  $\dot{\beta}_\pm/b \propto (-t)^{2\alpha+1}$ , i.e.,

$$\frac{\dot{\beta}_\pm}{H} \propto (-t)^{2\alpha+1}, \quad (8.2.12)$$

implying that the universe is isotropized. However, if  $\alpha > -1/2$  and the initial anisotropies are as large as  $\dot{\beta}_\pm = \mathcal{O}(b)$ , it is possible that the solution approaches one of the attractors shown in eq.(6.2.21). In this case, the anisotropies remain,

$$\frac{\dot{\beta}_\pm}{H} = \text{const}, \quad (8.2.13)$$

which is not acceptable. In light of the above result, it is required that

$$\alpha > -\frac{1}{2} \quad (8.2.14)$$

to avoid a highly anisotropic universe. We also assume in the general case of  $b_5(Y_0) \neq 0$  that the initial anisotropies  $\dot{\beta}_\pm$  are not as large as  $b$  ( $\sim H$ ).

## 8.3 Power Spectra

In the previous section we have seen that the Horndeski theory with (8.1.1) offers a variant of generalized Galilean Genesis, which has a similar background solution to the previous Genesis models. A significant point of this variant is found in the dynamics of scalar and tensor perturbations. In this section, let us discuss the evolution of the cosmological perturbations and their power spectra. As we will see, the quadratic Lagrangian for the curvature perturbation  $\zeta$  is of the form

$$\mathcal{L} \sim C_1(-t)^{2p}\dot{\zeta}^2 - C_2(-t)^{2q}(\vec{\nabla}\zeta)^2, \quad (8.3.1)$$

where  $C_1$ ,  $C_2$ ,  $p$ , and  $q$  are constants satisfying  $C_1, C_2 > 0$  and  $1 - p + q > 0$ . The Lagrangian for the tensor perturbations  $h_{ij}$  is of the same form.

### 8.3.1 Tensor Perturbations

The quadratic action for tensor perturbations in the Horndeski theory is given in eq.(4.5.4), where  $\mathcal{G}_T$  and  $\mathcal{F}_T$  were already defined in eqs. (8.1.14) and (8.2.3). In the previous models of generalized Galilean Genesis, as well as in conventional models of inflation (in Einstein gravity), we have  $\mathcal{G}_T, \mathcal{F}_T \simeq \text{const}$ , giving

$$h_{ij} \sim \text{const} \quad \text{and} \quad \text{decaying solution}, \quad (8.3.2)$$

on superhorizon scales. The amplitude of the dominant constant mode is proportional to  $H$  at horizon crossing, leading to a slightly red spectrum in the case of inflation and a strongly blue spectrum in NEC-violating cosmologies such as Galilean Genesis.

In our new models of Galilean Genesis, we still have  $a \simeq 1$ . However, now  $\mathcal{G}_T$  and  $\mathcal{F}_T$  are strongly time-dependent, as shown in eqs. (8.1.15) and (8.2.4). Noting that  $\mathcal{G}_T \propto (-t)^{2\beta}$ , we obtain two independent solutions on superhorizon scales,

$$h_{ij} \sim \text{const} \quad \text{and} \quad \int^t \frac{dt'}{a^3 \mathcal{G}_T} \sim (-t)^{1-2\beta}. \quad (8.3.3)$$

This indicates that, while we have constant and decaying solutions as usual for  $\beta < 1/2$ , for  $\beta > 1/2$  the would-be decaying mode *grows* on superhorizon scales. This is in sharp contrast to the previous Genesis models.

This peculiar evolution of the tensor perturbations for  $\beta > 1/2$  can be explained in a transparent manner by moving to the ‘‘Einstein frame’’ for the gravitons. Performing a disformal (and conformal) transformation,<sup>3</sup>

$$\tilde{a} = M_{\text{Pl}}^{-2} \mathcal{F}_T^{1/4} \mathcal{G}_T^{1/4} a, \quad (8.3.4)$$

$$d\tilde{t} = M_{\text{Pl}}^{-2} \mathcal{F}_T^{3/4} \mathcal{G}_T^{-1/4} dt, \quad (8.3.5)$$

<sup>3</sup>It was shown in Ref. [94] that in cosmology a pure disformal transformation is equivalent to rescaling the time coordinate.

the action (7.2.1) can be recast into the standard form [95],

$$S_{hE}^{(2)} = \frac{M_{\text{Pl}}^2}{8} \int d\tilde{t} d^3x \tilde{a}^3 \left[ (\partial_{\tilde{t}} h_{ij})^2 - \tilde{a}^{-2} (\vec{\nabla} h_{ij})^2 \right], \quad (8.3.6)$$

where the scale factor in this ‘‘Einstein frame’’ reads

$$\tilde{a} \sim (-\tilde{t})^{(n+1)/3} \quad (-\infty < \tilde{t} < 0) \quad (8.3.7)$$

with  $n > 0$  for  $\beta > 1/2$ . Clearly, this is the scale factor of a contracting universe where the tensor perturbations are effectively living. This is the reason for the superhorizon growth of  $h_{ij}$ . It is worth emphasizing that the frame we have moved to is the Einstein frame only for the gravitons. This frame is not convenient for studying and interpreting the background dynamics and the evolution of the curvature perturbation; it was introduced just to understand the evolution of the tensor perturbations.

Growing tensor perturbations on superhorizon scales imply that the anisotropic shear also grows. Indeed, it can be seen that  $\dot{\beta}_{\pm}$  in Sec. 8.2.2 and  $\dot{h}_{ij}$  share the same time dependence,  $\propto (-t)^{-2\beta}$ . Nevertheless, this does not spoil the Genesis scenario because the Hubble rate grows faster provided that  $\alpha > -1/2$ , as discussed in Sec. 8.2.2.

The power spectrum of the tensor perturbations is dependent not only on  $\mathcal{G}_T$  but also on  $\mathcal{F}_T$ , and from eq. (8.2.4) one finds two distinct cases depending on whether  $2B'(Y_0) + Y_0B''(Y_0)$  vanishes or not. Both cases yield the power spectrum of the form

$$\mathcal{P}_h = A_T k^{n_t}. \quad (8.3.8)$$

Since the explicit expression for  $A_T$  is messy, we do not give it here. Based on a concrete example we will evaluate  $A_T$  in the next section. To see the spectral index, let us first consider the case of  $2B'(Y_0) + Y_0B''(Y_0) = 0$ . In this case, we have  $\mathcal{F}_T = 2e^{-2\beta\lambda\phi} Y_0 A'(Y_0) \propto (-t)^{2\beta}$ . The spectral index is dependent only on the parameter  $\beta$  and is given by

$$n_t = 3 - 2|\nu| \quad \text{with} \quad \nu := \frac{1}{2} - \beta, \quad (8.3.9)$$

where the constant mode is dominant for  $\nu > 0$ , while the would-be decaying mode grows for  $\nu < 0$ . The flat spectrum is obtained for  $\beta = -1, 2$ . In the case of  $2B'(Y_0) + Y_0B''(Y_0) \neq 0$  we have  $\mathcal{F}_T \propto (-t)^{2(\alpha+2\beta)}$ , so that  $n_t$  is determined from the two parameters  $\alpha$  and  $\beta$  as

$$n_t = 3 - 2|\nu| \quad \text{with} \quad \nu := \frac{1 - 2\beta}{2(\alpha + \beta + 1)}. \quad (8.3.10)$$

The flat spectrum is obtained for  $3\alpha + 5\beta + 2 = 0$  and  $3\alpha + \beta + 4 = 0$ , though the latter case is not allowed under the conditions  $\alpha + \beta > 0$  and  $\alpha > -1/2$ .

In the previous study, we typically have blue spectra for tensor perturbations in NEC-violating alternatives to inflation. However, we have confirmed that the spectra can also be flat and red, depending on the parameters, in our variants of Galilean Genesis.

### 8.3.2 Curvature Perturbation

The quadratic action for the curvature perturbation is eq.(4.5.7), where

$$\mathcal{G}_S := \frac{\Sigma \mathcal{G}_T^2}{\Theta^2} + 3\mathcal{G}_T, \quad (8.3.11)$$

$$\mathcal{F}_S := \frac{1}{a} \frac{d}{dt} \left( \frac{a \mathcal{G}_T^2}{\Theta} \right) - \mathcal{F}_T, \quad (8.3.12)$$

and in the present class of Genesis models  $\Sigma$  and  $\Theta$  are given by

$$\Sigma \simeq e^{2(1+\alpha)\lambda\phi} Y_0 \dot{\rho}'(Y_0) \propto (-t)^{-2(\alpha+1)}, \quad (8.3.13)$$

$$\begin{aligned} \Theta &\simeq -e^{2\alpha\lambda\phi} Y_0 \dot{\phi} g_3' \\ &\quad - 2e^{-2\beta\lambda\phi} H Y_0 (3A' + 12Y_0 A'' + 4Y_0^2 A''') \\ &\quad + e^{-2(1+\alpha+2\beta)\lambda\phi} H^2 Y_0 \dot{\phi} (30B' + 75Y_0 B'' + 36Y_0^2 B''' + 4Y_0^3 B^{(4)}) \\ &\propto (-t)^{-(2\alpha+1)}. \end{aligned} \quad (8.3.14)$$

Thus, we have again two distinct cases and if  $\dot{\rho}'(Y_0) = 0$  we find that

$$\mathcal{G}_S \simeq 3\mathcal{G}_T \propto (-t)^{2\beta}, \quad (8.3.15)$$

while if  $\dot{\rho}'(Y_0) \neq 0$  we obtain

$$\mathcal{G}_S \simeq \frac{\Sigma \mathcal{G}_T^2}{\Theta^2} \propto (-t)^{2(\alpha+2\beta)}. \quad (8.3.16)$$

Irrespective of whether  $\mathcal{F}_T \propto (-t)^{2\beta}$  or  $\propto (-t)^{2(\alpha+2\beta)}$ , we have

$$\mathcal{F}_S \simeq \partial_t \left( \frac{\mathcal{G}_T^2}{\Theta} \right) - \mathcal{F}_T \propto (-t)^{2(\alpha+2\beta)}. \quad (8.3.17)$$

It is easy to evaluate the power spectrum of the curvature perturbation,

$$\mathcal{P}_\zeta = A_S k^{n_s-1}. \quad (8.3.18)$$

Again, the explicit expression for  $A_S$  turns out to be messy. Therefore,  $A_S$  will be evaluated through a concrete example in the next section and here we focus only on the spectral index. In the special case of  $\dot{\rho}'(Y_0) = 0$ , we obtain the spectral index

$$n_s - 1 = 3 - 2|\nu| \quad \text{with} \quad \nu := \frac{1 - 2\beta}{2(\alpha + \beta + 1)}, \quad (8.3.19)$$

which shares the same expression as eq. (8.3.10). The spectrum is therefore scale invariant for  $3\alpha + 5\beta + 2 = 0$ . In the general case of  $\dot{\rho}'(Y_0) \neq 0$  we have

$$n_s - 1 = 3 - 2|\nu| \quad \text{with} \quad \nu := \frac{1}{2} - \alpha - 2\beta, \quad (8.3.20)$$

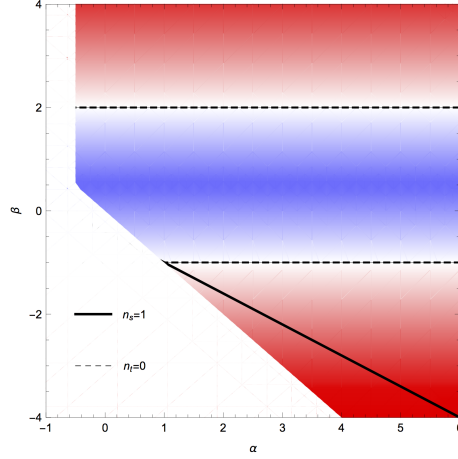


Figure 8.1: Tensor and scalar tilts as functions of  $\alpha$  and  $\beta$  in models with  $2B'(Y_0) + Y_0B''(Y_0) = 0$  and  $\hat{\rho}'(Y_0) = 0$ , plotted in a viable parameter range,  $\alpha + \beta > 0$  and  $\alpha > -1/2$ . The thick solid line shows the parameters giving a scale-invariant spectrum of the curvature perturbation,  $n_s = 1$ . The dashed lines correspond to scale-invariant tensor perturbations,  $n_t = 0$ , and the red (blue) region represents the parameters for which the tensor spectrum is red (blue). For a nearly scale-invariant scalar spectrum,  $n_s \approx 1$ , only a red tensor spectrum is obtained in this class of models.

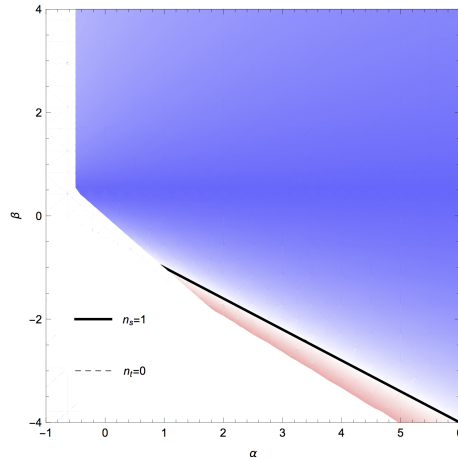


Figure 8.2: Same as Fig. 8.1, but for models with  $2B'(Y_0) + Y_0B''(Y_0) \neq 0$  and  $\hat{\rho}'(Y_0) = 0$ . In this case,  $n_t = n_s - 1$ , and hence the lines giving scale-invariant tensor and scalar spectra coincide. For  $n_s = 0.96$ , the tensor tilt is given by  $n_t = 0.96 - 1 = -0.04$ .



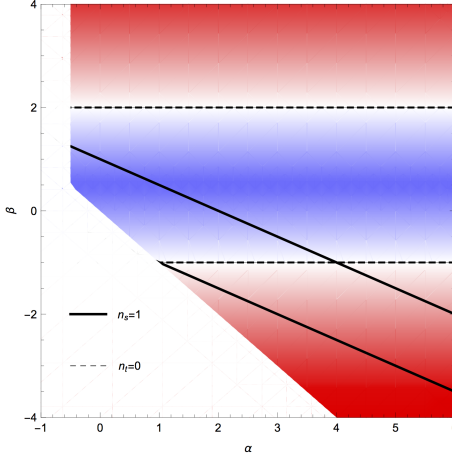


Figure 8.3: Same as Fig. 8.1, but for models with  $2B'(Y_0) + Y_0 B''(Y_0) = 0$  and  $\rho'(Y_0) \neq 0$ . Both tensor and scalar spectra are scale invariant for  $(\alpha, \beta) = (1, -1)$ ,  $(4, -1)$ , though the former is located at the edge of the viable parameter range. For a nearly scale-invariant scalar spectrum,  $n_s \approx 1$ , both red and blue tensor spectra are possible in this class of models.

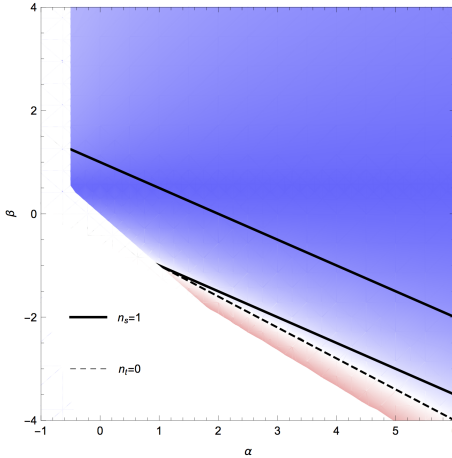


Figure 8.4: Same as Fig. 8.1, but for models with  $2B'(Y_0) + Y_0 B''(Y_0) \neq 0$  and  $\rho'(Y_0) \neq 0$ . For a nearly scale-invariant scalar spectrum,  $n_s \approx 1$ , the tensor spectrum is always blue in this class of models.

and the spectrum is scale invariant for the parameters satisfying  $\alpha + 2\beta + 1 = 0$  or  $\alpha + 2\beta - 2 = 0$ .

Having thus obtained the spectral indices  $n_t$  and  $n_s$ , we summarize the results in Figs. 8.1–8.4. Of particular interest are the cases presented in Figs. 8.2 and 8.3. In the former case both scalar and tensor perturbations have nearly scale-invariant spectra for  $3\alpha + 5\beta + 2 \simeq 0$ , while in the latter case this is possible for  $\alpha \simeq 4$  and  $\beta \simeq -1$ . In the other two cases, i.e., the cases given in Figs. 8.1 and 8.4, the parameters leading to scale-invariant scalar and tensor perturbations are on the boundaries of the viable parameter regions.

Before closing this section, let us comment on the stability of the Genesis solutions. By requiring that  $\mathcal{G}_T, \mathcal{F}_T, \mathcal{G}_S, \mathcal{F}_S > 0$ , one can obtain a stable Genesis phase. However, as shown in [96, 97], non-singular cosmological solutions in the Horndeski theory are plagued with gradient instabilities which occur at some moment in the entire expansion history, provided that the integrals

$$\int_{-\infty}^t a\mathcal{F}_T dt' \quad \text{and} \quad \int_t^{\infty} a\mathcal{F}_T dt' \quad (8.3.21)$$

do not converge. The Genesis models with  $\mathcal{F}_T \sim (-t)^n$  ( $n \geq -1$ ) satisfies the postulates of this no-go theorem, and hence, even though a single genesis phase itself is stable, gradient instability occurs eventually after the Genesis phase. The models with  $\mathcal{F}_T \sim (-t)^n$  ( $n < -1$ ) can evade the no-go theorem [97], but then the universe would be geodesically incomplete for gravitons [98]. If one would prefer a geodesically complete universe for gravitons, some new terms beyond Horndeski must be introduced to avoid gradient instabilities [98, 61, 79, 99].

## 8.4 An example

As a concrete example, let us focus on the case with  $B(Y) = 0$ ,  $\alpha = 4$ , and  $\beta = -1$ , which gives rise to exactly scale-invariant spectra for scalar and tensor perturbations. Our example is given by

$$g_2 = -Y + \frac{Y^2}{\mu^4}, \quad g_3 = \frac{Y}{8\lambda\mu^4}, \quad (8.4.1)$$

and

$$A = M^2 \left[ \frac{Y}{\mu^4} - \left( \frac{Y}{\mu^4} \right)^2 + \frac{2}{5} \left( \frac{Y}{\mu^4} \right)^3 \right], \quad (8.4.2)$$

where  $\mu$  and  $M$  are parameters having dimension of mass, and it follows from eq. (8.4.1) that  $Y_0 = 2\mu^4/3$ .

One can solve the background equations to obtain

$$H = \frac{5\sqrt{3}}{56} \frac{\mu^2}{\lambda M^2} e^{7\lambda\phi} \propto (-t)^{-7}. \quad (8.4.3)$$

It is straightforward to compute

$$\begin{aligned} \mathcal{G}_T &= \frac{4}{9} M^2 e^{2\lambda\phi}, \\ \mathcal{F}_T &= \frac{4}{15} M^2 e^{2\lambda\phi}, \\ \mathcal{G}_S &= \frac{49}{72} \lambda^2 M^4 e^{-4\lambda\phi}, \\ \mathcal{F}_S &= \frac{70}{27} \lambda^2 M^4 e^{-4\lambda\phi}, \end{aligned} \quad (8.4.4)$$

which shows that this model is stable. The primordial power spectra of tensor and curvature perturbations are given, respectively, by

$$\mathcal{P}_h = \sqrt{\frac{5}{3}} \frac{10\lambda^2\mu^4}{\pi^2 M^2} \simeq 1.3 \times \frac{\lambda^2\mu^4}{M^2}, \quad (8.4.5)$$

and

$$\mathcal{P}_\zeta \simeq 0.017 \times (\lambda H_*)^{6/7} \left(\frac{\mu}{M}\right)^{16/7}, \quad (8.4.6)$$

where  $H_*$  is the Hubble parameter at the end of the genesis phase. Note that the curvature perturbation grows on superhorizon scales and hence  $\mathcal{P}_\zeta$  depends on the time when the Genesis phase ends, while tensor perturbations do not. The tensor-to-scalar ratio has a non-standard expression (i.e., it does not depend on  $n_t$  or the slow-roll parameter) and reads

$$r \sim 10^{-2} \times (\lambda H_*)^{-6/7} (\lambda\mu)^{12/7} (\lambda M)^{2/7}, \quad (8.4.7)$$

which can be made sufficiently small by choosing the parameters.

One can improve the above model by introducing slight deviations from  $\alpha = 4$  and  $\beta = -1$  to have  $n_s \simeq 0.96$ . The lesson we learn from this example is that it is rather easy to construct a stable model of Galilean Genesis generating primordial curvature perturbations that are consistent with observations and tensor perturbations that can be hopefully detected by future observations.

## 8.5 Conclusions in this chapter

In this chapter, we have proposed a variant of generalized Galilean Genesis as a possible alternative to inflation. A general Lagrangian for this new class of models has been

constructed within the Horndeski theory. The Lagrangian has four functional degrees of freedom in addition to two constant parameters, and includes the model studied in Ref. [93] as a specific case. We have confirmed that under certain conditions the background evolution of our Genesis models leads to a stable, homogeneous and isotropic universe with flat spatial sections. We have then calculated power spectra of primordial perturbations and shown that a variety of tensor and scalar spectral tilts can be obtained, as summarized in Figs. 8.1–8.4. In some cases, curvature/tensor perturbations grow on superhorizon scales and for this reason the primordial amplitudes depend not only on the functions in the Lagrangian but also on the time when the Genesis phase ends. It should be emphasized that in spite of the gross violation of the null energy condition the tensor spectrum can be (nearly) scale invariant, though the consistency relation is still non-standard.

We have thus seen that in the Galilean Genesis scenario both scalar and tensor power spectra can be nearly scale invariant as in the standard inflationary scenario. It is therefore crucial to evaluate the amount of non-Gaussianities in the primordial curvature perturbations produced during the Genesis phase. This point will be reported elsewhere.

# Conclusions

We have reviewed the history and the fundamental information of cosmology in part 1 and discuss many topics of the generalized Galilean genesis as an alternative scenario to inflation in part 2. These studies aimed to distinguish the models of the early universe, as we have seen in fig.4.1, fig.5.2 and fig.5.3, the evolution of the universe in the model is different each other. However, as a matter of course, we can not see this evolution directly, and thus we have discussed how can we see the difference between the models from observations.

We know the gravitational waves in alternative scenarios shows the blue spectrum so far, however, we have found what kind of genesis models can generate the flat spectrum and other various spectrums. This result suggests we can not reject the alternative scenarios if we detect the flat spectrum in the future, but the consistency relation can distinguish between the models.

The other way to distinguish between the models, we should consider the other cosmological prediction such as non-gaussianity or find the instability in specifically modified gravity theories. For example, in the class of Horndeski theory, the scenario without initial singularity have the instability [97, 100]. This study suggests the genesis model has the instability, and thus we have to consider the genesis scenario in beyond Horndeski theory to avoid this instability. The other remarkable point except for the distinction of the models is the anisotropy from genesis. In part 2, we have discussed the anisotropy and derived the condition not to evolve the anisotropy. This suggests the possibility to construct the model of the anisotropic inflation in the Horndeski theory without vector field.



# Bibliography

- [1] Paolo Creminelli, Alberto Nicolis, and Enrico Trincherini. Galilean Genesis: An Alternative to inflation. *JCAP*, 1011:021, 2010.
- [2] Sakine Nishi and Tsutomu Kobayashi. Reheating and Primordial Gravitational Waves in Generalized Galilean Genesis. *JCAP*, 1604(04):018, 2016.
- [3] Sakine Nishi and Tsutomu Kobayashi. Scale-invariant perturbations from NEC violation: A new variant of Galilean Genesis. *Phys. Rev.*, D95(6):064001, 2017.
- [4] Sakine Nishi and Tsutomu Kobayashi. Generalized Galilean Genesis. *JCAP*, 1503(03):057, 2015.
- [5] Edwin Hubble. A relation between distance and radial velocity among extra-galactic nebulae. *Proc. Nat. Acad. Sci.*, 15:168–173, 1929.
- [6] R. Adam et al. Planck 2015 results. I. Overview of products and scientific results. *Astron. Astrophys.*, 594:A1, 2016.
- [7] Alan H. Guth. The Inflationary Universe: A Possible Solution to the Horizon and Flatness Problems. *Phys. Rev.*, D23:347–356, 1981.
- [8] Steven Weinberg. *Cosmology*. 2008.
- [9] Andrew R. Liddle, Paul Parsons, and John D. Barrow. Formalizing the slow roll approximation in inflation. *Phys. Rev.*, D50:7222–7232, 1994.
- [10] Andrei D. Linde. Chaotic Inflation. *Phys. Lett.*, 129B:177–181, 1983.
- [11] V. Mukhanov. *Physical Foundations of Cosmology*. Cambridge University Press, Oxford, 2005.
- [12] Alexei A. Starobinsky. A New Type of Isotropic Cosmological Models Without Singularity. *Phys. Lett.*, B91:99–102, 1980.
- [13] Takeshi Chiba, Takahiro Okabe, and Masahide Yamaguchi. Kinetically driven quintessence. *Phys. Rev.*, D62:023511, 2000.

- [14] C. Armendariz-Picon, T. Damour, and Viatcheslav F. Mukhanov. k - inflation. *Phys. Lett.*, B458:209–218, 1999.
- [15] Tsutomu Kobayashi, Masahide Yamaguchi, and Jun'ichi Yokoyama. G-inflation: Inflation driven by the Galileon field. *Phys. Rev. Lett.*, 105:231302, 2010.
- [16] Tsutomu Kobayashi, Masahide Yamaguchi, and Jun'ichi Yokoyama. Generalized G-inflation: Inflation with the most general second-order field equations. *Prog. Theor. Phys.*, 126:511–529, 2011.
- [17] Gregory Walter Horndeski. Second-order scalar-tensor field equations in a four-dimensional space. *Int. J. Theor. Phys.*, 10:363–384, 1974.
- [18] C. Deffayet, Xian Gao, D. A. Steer, and G. Zahariade. From k-essence to generalised Galileons. *Phys. Rev.*, D84:064039, 2011.
- [19] Hans A. Buchdahl. Non-linear Lagrangians and cosmological theory. *Mon. Not. Roy. Astron. Soc.*, 150:1, 1970.
- [20] C. Brans and R. H. Dicke. Mach's principle and a relativistic theory of gravitation. *Phys. Rev.*, 124:925–935, 1961.
- [21] Antonio De Felice and Shinji Tsujikawa. f(R) theories. *Living Rev. Rel.*, 13:3, 2010.
- [22] Cedric Deffayet, Oriol Pujolas, Ignacy Sawicki, and Alexander Vikman. Imperfect Dark Energy from Kinetic Gravity Braiding. *JCAP*, 1010:026, 2010.
- [23] Alberto Nicolis, Riccardo Rattazzi, and Enrico Trincherini. The Galileon as a local modification of gravity. *Phys. Rev.*, D79:064036, 2009.
- [24] Nathan Chow and Justin Khoury. Galileon Cosmology. *Phys. Rev.*, D80:024037, 2009.
- [25] C. Deffayet, Gilles Esposito-Farese, and A. Vikman. Covariant Galileon. *Phys. Rev.*, D79:084003, 2009.
- [26] C é dric Deffayet and Dani è le A. Steer. A formal introduction to Horndeski and Galileon theories and their generalizations. *Class. Quant. Grav.*, 30:214006, 2013.
- [27] Jérôme Gleyzes, David Langlois, Federico Piazza, and Filippo Vernizzi. Healthy theories beyond Horndeski. *Phys. Rev. Lett.*, 114(21):211101, 2015.
- [28] Xian Gao. Unifying framework for scalar-tensor theories of gravity. *Phys. Rev.*, D90:081501, 2014.
- [29] Viatcheslav Mukhanov and Sergei Winitzki. *Introduction to quantum effects in gravity*. Cambridge University Press, 2007.



- [30] David H. Lyth, Carlo Ungarelli, and David Wands. The Primordial density perturbation in the curvaton scenario. *Phys. Rev.*, D67:023503, 2003.
- [31] Taro Kunimitsu and Jun'ichi Yokoyama. Higgs condensation as an unwanted curvaton. *Phys. Rev.*, D86:083541, 2012.
- [32] V. A. Rubakov. The Null Energy Condition and its violation. *Phys. Usp.*, 57:128–142, 2014. [Usp. Fiz. Nauk184,no.2,137(2014)].
- [33] M. Novello and S. E. Perez Bergliaffa. Bouncing Cosmologies. *Phys. Rept.*, 463:127–213, 2008.
- [34] Robert Brandenberger and Patrick Peter. Bouncing Cosmologies: Progress and Problems. 2016.
- [35] Yi-Fu Cai, Evan McDonough, Francis Duplessis, and Robert H. Brandenberger. Two Field Matter Bounce Cosmology. *JCAP*, 1310:024, 2013.
- [36] Paolo Creminelli, Kurt Hinterbichler, Justin Khoury, Alberto Nicolis, and Enrico Trincherini. Subluminal Galilean Genesis. *JHEP*, 02:006, 2013.
- [37] Kurt Hinterbichler, Austin Joyce, Justin Khoury, and Godfrey E. J. Miller. DBI Realizations of the Pseudo-Conformal Universe and Galilean Genesis Scenarios. *JCAP*, 1212:030, 2012.
- [38] Kurt Hinterbichler, Austin Joyce, Justin Khoury, and Godfrey E. J. Miller. Dirac-Born-Infeld Genesis: An Improved Violation of the Null Energy Condition. *Phys. Rev. Lett.*, 110(24):241303, 2013.
- [39] Robert H. Brandenberger and C. Vafa. Superstrings in the Early Universe. *Nucl. Phys.*, B316:391–410, 1989.
- [40] Alexei A. Starobinsky. Spectrum of relict gravitational radiation and the early state of the universe. *JETP Lett.*, 30:682–685, 1979. [Pisma Zh. Eksp. Teor. Fiz.30,719(1979)].
- [41] K. Sato. First Order Phase Transition of a Vacuum and Expansion of the Universe. *Mon. Not. Roy. Astron. Soc.*, 195:467–479, 1981.
- [42] Viatcheslav F. Mukhanov and G. V. Chibisov. Quantum Fluctuations and a Nonsingular Universe. *JETP Lett.*, 33:532–535, 1981. [Pisma Zh. Eksp. Teor. Fiz.33,549(1981)].
- [43] D. Larson et al. Seven-Year Wilkinson Microwave Anisotropy Probe (WMAP) Observations: Power Spectra and WMAP-Derived Parameters. *Astrophys. J. Suppl.*, 192:16, 2011.

- [44] P. A. R. Ade et al. Planck 2013 results. XXII. Constraints on inflation. *Astron. Astrophys.*, 571:A22, 2014.
- [45] P. A. R. Ade et al. Planck 2013 results. XVI. Cosmological parameters. *Astron. Astrophys.*, 571:A16, 2014.
- [46] Arvind Borde and Alexander Vilenkin. Singularities in inflationary cosmology: A Review. *Int. J. Mod. Phys.*, D5:813–824, 1996.
- [47] D. Battfeld and Patrick Peter. A Critical Review of Classical Bouncing Cosmologies. *Phys. Rept.*, 571:1–66, 2015.
- [48] Ignacy Sawicki and Alexander Vikman. Hidden Negative Energies in Strongly Accelerated Universes. *Phys. Rev.*, D87(6):067301, 2013.
- [49] Paolo Creminelli, Markus A. Luty, Alberto Nicolis, and Leonardo Senatore. Starting the Universe: Stable Violation of the Null Energy Condition and Non-standard Cosmologies. *JHEP*, 12:080, 2006.
- [50] Laurence Perreault Levasseur, Robert Brandenberger, and Anne-Christine Davis. Defrosting in an Emergent Galileon Cosmology. *Phys. Rev.*, D84:103512, 2011.
- [51] Yi Wang and Robert Brandenberger. Scale-Invariant Fluctuations from Galilean Genesis. *JCAP*, 1210:021, 2012.
- [52] V. A. Rubakov. Consistent NEC-violation: towards creating a universe in the laboratory. *Phys. Rev.*, D88:044015, 2013.
- [53] Benjamin Elder, Austin Joyce, and Justin Khoury. From Satisfying to Violating the Null Energy Condition. *Phys. Rev.*, D89(4):044027, 2014.
- [54] Damien A. Easson, Ignacy Sawicki, and Alexander Vikman. When Matter Matters. *JCAP*, 1307:014, 2013.
- [55] Taotao Qiu, Jarah Evslin, Yi-Fu Cai, Mingzhe Li, and Xinmin Zhang. Bouncing Galileon Cosmologies. *JCAP*, 1110:036, 2011.
- [56] Damien A. Easson, Ignacy Sawicki, and Alexander Vikman. G-Bounce. *JCAP*, 1111:021, 2011.
- [57] Yi-Fu Cai, Damien A. Easson, and Robert Brandenberger. Towards a Nonsingular Bouncing Cosmology. *JCAP*, 1208:020, 2012.
- [58] Yi-Fu Cai, Robert Brandenberger, and Patrick Peter. Anisotropy in a Nonsingular Bounce. *Class. Quant. Grav.*, 30:075019, 2013.

- [59] M. Osipov and V. Rubakov. Galileon bounce after ekpyrotic contraction. *JCAP*, 1311:031, 2013.
- [60] Taotao Qiu, Xian Gao, and Emmanuel N. Saridakis. Towards anisotropy-free and nonsingular bounce cosmology with scale-invariant perturbations. *Phys. Rev.*, D88(4):043525, 2013.
- [61] David Pirtskhalava, Luca Santoni, Enrico Trincherini, and Patipan Uttayarat. Inflation from Minkowski Space. *JHEP*, 12:151, 2014.
- [62] Sakine Nishi, Tsutomu Kobayashi, Norihiro Tanahashi, and Masahide Yamaguchi. Cosmological matching conditions and galilean genesis in Horndeski's theory. *JCAP*, 1403:008, 2014.
- [63] Zhi-Guo Liu, Jun Zhang, and Yun-Song Piao. A Galileon Design of Slow Expansion. *Phys. Rev.*, D84:063508, 2011.
- [64] Robert M. Wald. Asymptotic behavior of homogeneous cosmological models in the presence of a positive cosmological constant. *Phys. Rev.*, D28:2118–2120, 1983.
- [65] Kerstin E. Kunze and Ruth Durrer. Anisotropic 'hairs' in string cosmology. *Class. Quant. Grav.*, 17:2597–2604, 2000.
- [66] Joel K. Erickson, Daniel H. Wesley, Paul J. Steinhardt, and Neil Turok. Kasner and mixmaster behavior in universes with equation of state  $w = 1$ . *Phys. Rev.*, D69:063514, 2004.
- [67] BingKan Xue and Paul J. Steinhardt. Evolution of curvature and anisotropy near a nonsingular bounce. *Phys. Rev.*, D84:083520, 2011.
- [68] Jai-chan Hwang and Ethan T. Vishniac. Gauge-invariant joining conditions for cosmological perturbations. *Astrophys. J.*, 382:363–368, 1991.
- [69] Nathalie Deruelle and Viatcheslav F. Mukhanov. On matching conditions for cosmological perturbations. *Phys. Rev.*, D52:5549–5555, 1995.
- [70] Ruth Durrer and Filippo Vernizzi. Adiabatic perturbations in pre - big bang models: Matching conditions and scale invariance. *Phys. Rev.*, D66:083503, 2002.
- [71] Yun-Song Piao. Adiabatic Spectra During Slowly Evolving. *Phys. Lett.*, B701:526–529, 2011.
- [72] Arvind Borde and Alexander Vilenkin. Eternal inflation and the initial singularity. *Phys. Rev. Lett.*, 72:3305–3309, 1994.

- [73] Robert H. Brandenberger. Alternatives to the inflationary paradigm of structure formation. *Int. J. Mod. Phys. Conf. Ser.*, 01:67–79, 2011.
- [74] Robert H. Brandenberger. Cosmology of the Very Early Universe. *AIP Conf. Proc.*, 1268:3–70, 2010.
- [75] Robert H. Brandenberger. Introduction to Early Universe Cosmology. *PoS, ICFI2010:001*, 2010.
- [76] Jaume de Haro and Yi-Fu Cai. An Extended Matter Bounce Scenario: current status and challenges. *Gen. Rel. Grav.*, 47(8):95, 2015.
- [77] L. H. Ford. Gravitational Particle Creation and Inflation. *Phys. Rev.*, D35:2955, 1987.
- [78] Zhi-Guo Liu, Hong Li, and Yun-Song Piao. Preinflationary genesis with CMB B-mode polarization. *Phys. Rev.*, D90(8):083521, 2014.
- [79] Tsutomu Kobayashi, Masahide Yamaguchi, and Jun’ichi Yokoyama. Galilean Creation of the Inflationary Universe. *JCAP*, 1507(07):017, 2015.
- [80] Hiroyuki Tashiro, Takeshi Chiba, and Misao Sasaki. Reheating after quintessential inflation and gravitational waves. *Class. Quant. Grav.*, 21:1761–1772, 2004.
- [81] N. D. Birrell and P. C. W. Davies. *Quantum Fields in Curved Space*. Cambridge Monographs on Mathematical Physics. Cambridge Univ. Press, Cambridge, UK, 1984.
- [82] Leonard Parker. Quantized fields and particle creation in expanding universes. 1. *Phys. Rev.*, 183:1057–1068, 1969.
- [83] Ya. B. Zeldovich and Alexei A. Starobinsky. Particle production and vacuum polarization in an anisotropic gravitational field. *Sov. Phys. JETP*, 34:1159–1166, 1972. [*Zh. Eksp. Teor. Fiz.*61,2161(1971)].
- [84] Ya. B. Zeldovich and Alexei A. Starobinsky. O skorosti rozhdeniya chastits v gravitatsionnykh polyakh,. *Pisma Zh. Eksp. Toer. Fiz.*, 26:373, 1977. [On the rate of particle production in gravitational fields, *JETP Lett.* 26 (1977) 252].
- [85] Michele Maggiore. Gravitational wave experiments and early universe cosmology. *Phys. Rept.*, 331:283–367, 2000.
- [86] George F. R. Ellis and Roy Maartens. The emergent universe: Inflationary cosmology with no singularity. *Class. Quant. Grav.*, 21:223–232, 2004.

- [87] George F. R. Ellis, Jeff Murugan, and Christos G. Tsagas. The Emergent universe: An Explicit construction. *Class. Quant. Grav.*, 21(1):233–250, 2004.
- [88] Yi-Fu Cai, Mingzhe Li, and Xinmin Zhang. Emergent Universe Scenario via Quintom Matter. *Phys. Lett.*, B718:248–254, 2012.
- [89] Yi-Fu Cai, Youping Wan, and Xinmin Zhang. Cosmology of the Spinor Emergent Universe and Scale-invariant Perturbations. *Phys. Lett.*, B731:217–226, 2014.
- [90] Thorsten Battefeld and Scott Watson. String gas cosmology. *Rev. Mod. Phys.*, 78:435–454, 2006.
- [91] Ido Ben-Dayan. Gravitational Waves in Bouncing Cosmologies from Gauge Field Production. *JCAP*, 1609(09):017, 2016.
- [92] Asuka Ito and Jiro Soda. Primordial Gravitational Waves Induced by Magnetic Fields in Ekpyrotic Scenario. 2016.
- [93] Yong Cai and Yun-Song Piao. The slow expansion with nonminimal derivative coupling and its conformal dual. *JHEP*, 03:134, 2016.
- [94] Guillem Domènech, Atsushi Naruko, and Misao Sasaki. Cosmological disformal invariance. *JCAP*, 1510(10):067, 2015.
- [95] Paolo Creminelli, Jérôme Gleyzes, Jorge Noreña, and Filippo Vernizzi. Resilience of the standard predictions for primordial tensor modes. *Phys. Rev. Lett.*, 113(23):231301, 2014.
- [96] M. Libanov, S. Mironov, and V. Rubakov. Generalized Galileons: instabilities of bouncing and Genesis cosmologies and modified Genesis. *JCAP*, 1608(08):037, 2016.
- [97] Tsutomu Kobayashi. Generic instabilities of nonsingular cosmologies in Horndeski theory: A no-go theorem. *Phys. Rev.*, D94(4):043511, 2016.
- [98] Paolo Creminelli, David Pirtskhalava, Luca Santoni, and Enrico Trincherini. Stability of Geodesically Complete Cosmologies. *JCAP*, 1611(11):047, 2016.
- [99] Yong Cai, Youping Wan, Hai-Guang Li, Taotao Qiu, and Yun-Song Piao. The Effective Field Theory of nonsingular cosmology. *JHEP*, 01:090, 2017.
- [100] Shingo Akama and Tsutomu Kobayashi. Generalized multi-Galileons, covariantized new terms, and the no-go theorem for nonsingular cosmologies. *Phys. Rev.*, D95(6):064011, 2017.